2016

Dynamics of HIV-1 Infection and Therapy In Vivo

Joshua Abraham Horwitz

DYNAMICS OF HIV-1 INFECTION AND THERAPY IN VIVO

A Thesis Presented to the Faculty of

The Rockefeller University

in Partial Fulfillment of the Requirements for

the degree of Doctor of Philosophy

by

Joshua Abraham Horwitz

June 2016

DYNAMICS OF HIV-1 INFECTION AND THERAPY IN VIVO

Joshua Abraham Horwitz, Ph.D.

The Rockefeller University 2016

Human immunodeficiency virus type 1 (HIV-1) is the causative agent of acquired immune deficiency syndrome (AIDS), a disease responsible for extensive morbidity and mortality worldwide. Despite more than thirty years of research since the discovery of HIV-1, no cure or vaccine yet exists. HIV-1 infection, while treatable with suppressive antiretroviral therapy drugs (ART), establishes lifelong persistence in the infected host as a natural consequence of the viral life cycle and the dynamic properties of the human immune cells in which HIV-1 propagates. This persistence is driven by populations of rare, long-lived HIV-1-infected cells, termed latently infected cells (LICs), that are refractory to immune clearance and viral cytopathic effects. Interruption of suppressive therapy – even after years of continuous and effective treatment – rapidly leads to virological rebound, requiring infected persons to remain on ART indefinitely. As the need to maintain lifelong daily ART imposes a substantial compliance burden on those infected, two major goals of HIV-1 research, broadly, concern (1) developing new therapeutic modalities that may alleviate some drawbacks to ART, and (2) identifying means with which to target and eradicate LICs as an approach to curing HIV-1 infection. To these ends, in the first three chapters of my thesis, I discuss my work demonstrating

the utility of highly potent anti-HIV-1 antibodies in a number of therapeutic contexts. As antibody therapy expectedly did not result in cure, I was later motivated to study the nature of LIC formation and persistence. The fourth chapter of this thesis outlines my work to develop new molecular tools to interrogate LICs in a humanized mouse model of HIV-1 infection.

ACKNOWLEDGMENTS

This thesis and the work presented herein would not have been possible without the tremendous support of many individuals.

I am particularly grateful to my advisor, Michel Nussenzweig, not only for his continuous guidance and generosity in directing and supporting my thesis work, but also for his unwavering commitment to the pursuit of truth in science by only the best methods possible. Michel, I have thoroughly enjoyed my time under your mentorship, and I am extremely thankful for your regular willingness to lend significant time and resources to the many high-risk projects I stubbornly undertook during my Ph.D.

I am also grateful to Drs. Charles M. Rice and Alexander Ploss, for whom I had the pleasure of working as a research assistant prior to beginning my Ph.D. A huge part of my scientific technical training took place under their guidance, and they cultivated a deeply motivating and enriching environment in which to learn about and practice virology. They have generously supported me at every step in my pursuit of a career in scientific research. In addition, Charlie has been instrumental in guiding my thesis work through serving on my faculty advisory committee.

I would also like to acknowledge my other faculty advisory committee members, Drs. Paul Bieniasz and Daniel Mucida, upon whose respective expertise in retrovirology and immunology I have relied on numerous occasions. I am additionally grateful to my external thesis advisor, David Margolis, for lending his time and insight to my thesis work and participating in my thesis defense.

I would like to thank all of the members of the Nussenzweig laboratory at The Rockefeller University for their constant support, guidance, friendship, and curiosity. I am particularly grateful to Dr. Ariel Halper-Stromberg, with whom I enjoyed collaborating many times throughout my Ph.D., and whose unfailing tolerance for entertaining my countless unlikely hypotheses I have already come to miss. I am also especially thankful to the many members of the “HIV team” who provided much-needed encouragement while I was struggling to complete the latter portion of my thesis work.

I also thank Drs. Johannes F. Scheid and Marina Caskey for inviting me to help conduct a clinical trial largely of their own design. The preliminary results of that trial (which is still underway at the time of writing) are described in Chapter III of this thesis, and would not have been possible without their tireless efforts and hard work.

I thank Ainsley Lockhart, a first-year Ph.D. student, for dedicating her three-month rotation to helping me develop the reporter virus I describe in Chapter IV of this thesis. Her expertise with flow cytometry and protein biochemistry, and her broad understanding of HIV-1 (particularly with respect to the *nef* gene), were critical to moving that project forward. I additionally thank Yotam Bar-on and Ching-Lan Lu for generously helping me complete my work on validating the HIVivo platform, described in the fourth chapter of this thesis.

I thank my family—my parents, Marcus Horwitz and Helene DesRuisseaux, and my brother Daniel—whose love and support I am never without in all of my pursuits, both personal and professional. I also thank my Dad for stimulating my interest in scientific research from a very early age (despite the fact that he’s a bacteria guy, which

I just couldn’t get into after I discovered viruses), and for generously proofreading this thesis.

Finally, I thank Dr. Caitlin Anne Sengelaub for her love, laughs, and constant encouragement during the years I have worked toward this thesis. Cait, I am daily in awe of how smart, beautiful, hard-working, and capable you are. You have always set an extraordinary example of what it means to chase your dreams and be your best self.

TABLE OF CONTENTS

LIST OF FIGURES viii

LIST OF TABLES xi

INTRODUCTION 1

HIV-1 virus and life cycle 1
Viral genetic material in tissues and cells 2
ART drugs and treatment 2
Human immune response to HIV-1 infection 3
BNAbs in HIV-1 prevention and therapy 4
Animal models of HIV-1 infection 6
Latent HIV-1 infection 8

CHAPTER I: SUPPRESSION OF HIV-1 INFECTION IN VIVO BY COMBINATIONS OF BROADLY NEUTRALIZING ANTIBODIES 11

A humanized mouse model of HIV-1 infection 11
Individual bNAbs rapidly select for viral resistance 15
Combinations of bNAbs can suppress viral loads in hu-mice 21

CHAPTER II: DURABLE CONTROL OF HIV-1 INFECTION BY SINGLE BNABS FOLLOWING SUPPRESSIVE ANTI-RETROVIRAL THERAPY 29

3BNC117 and 45-46W elicit similar profiles of HIV-1_{YU2} resistance 29
An optimized bNAb tri-mix controls viremia and lowers cell-associated HIV-1 DNA 30
An oral ART regimen suppresses viral loads in hu-mice 32
Suppressing viral load reduces the likelihood of viral escape from bNAbs 34
Gene therapy enables durable virological control by individual bNAbs alone 41

CHAPTER III: 3BNC117 DELAYS VIRAL REBOUND IN HIV-1-INFECTED HUMANS DURING TREATMENT INTERRUPTION 49

CHAPTER IV: A REPLICATION-COMPETENT, IN VIVO-ADAPTED HIV-1 REPORTER VIRUS 57

Design of a replication-competent HIV-1 reporter virus 57
HIV-$1_{SV40HSA}$ 57
Improving the fitness of HIV-$1_{SV40HSA}$ 60
HIV-1_{IL16HA} 62
An in vivo-adapted HIV-1_{IL16HA} 64
Most infected cells that do not express Env harbor defective HIV-1 genomes 75
A single-cell viral outgrowth assay to identify bona fide LICs 77

CHAPTER V: DISCUSSION 81

Antibodies as effective therapeutic agents in vivo 81
Reducing viral load improves bNAb effectiveness 84
An optimized bNAb cocktail suppresses viremia and lowers cell-associated DNA 86

BNAb gene therapy durably sustains virological suppression 88
3BNC117 delays viral rebound during ATI 89
Paradigms of bNAb-mediated HIV-1 therapy in vivo 91
A replication-competent reporter virus designed to identify latently infected cells 94
Single-cell assays to facilitate dissection of HIV-1 latency 95
Further proof is required to determine whether HIVivo$_{HA}$ can identify latency 96
REFERENCES 99

LIST OF FIGURES

Figure 0.1: 1st and 2nd generation bNAbs..... 6

Figure 1.1: Hematopoietic reconstitution of hu-mice..... 11

Figure 1.2: Validation of HIV-1 qRT-PCR plasma viral load assay..... 13

Figure 1.3: Viral load and CD4 T-cell depletion in HIV-1_{YU2}-infected hu-mice..... 14

Figure 1.4: Rapid viral diversification after clonal infection..... 15

Figure 1.5: Individual bNAbs transiently lower viral load. 17

Figure 1.6: *env* gp120 sequences reveal amino acid substitutions at antibody contact sites..... 19

Figure 1.7: Amino acid changes found in bNAb contact sites confer bNAb resistance. 20

Figure 1.8: A bNAb tri-mix can durably suppress viremia in some hu-mice. 22

Figure 1.9: Simultaneous bNAb escape mutations arise in tri-mix treated animals..... 23

Figure 1.10: A bNAb penta-mix suppresses viremia in hu-mice. 24

Figure 1.11: Penta-mix treated animals do not carry functional plasma virus. 25

Figure 1.12: Withdrawal of bNAb therapy results in viremic rebound. 26

Figure 1.13: Rebounding virus from bNAb-suppressed mice is not bNAb-resistant..... 27

Figure 2.1: 3BNC117 elicits viral resistance at CD4bs residues..... 30

Figure 2.2: An optimized bNAb tri-mix suppresses viral load and lowers intracellular HIV-1 DNA. 32

Figure 2.3: Daily oral cART rapidly lowers viral load in hu-mice..... 34

Figure 2.4: Individual bNAbs maintain virological suppression after ART withdrawal. .. 35

Figure 2.5: bNAb intensification of cART does not prevent viral rebound when stopped coincident with cART withdrawal. 37

Figure 2.6: Viral rebound following bNAb monotherapy is coincident with bNAb decay. 38

Figure 2.7: Viruses from mice suppressed by bNAb monotherapy remain neutralization-sensitive. 40

Figure 2.8: AAV-3BNC117 expresses 3BNC117 stably in hu-mice and selects for viral escape. 43

Figure 2.9: AAV-expressed 3BNC117 maintains stable titers and durably controls viremia. 45

Figure 2.10: A single dose of AAV-10-1074 durably maintains virological suppression. 47

Figure 3.1: Patient screening for virus sensitivity to 3BNC117 neutralization in a TZM-bl assay. 50

Figure 3.2: Study design and timeline. 51

Figure 3.3: Viral loads and serum 3BNC117 titers in HIV-1-infected subjects during ATI. 52

Figure 3.4: Moderate resistance to 3BNC117 is observed in subject viruses during rebound. 53

Figure 3.5: Viral gp160 sequences at rebound are different from those found before ATI. 55

Figure 3.6: Signature 3BNC117 resistance mutations are rarely observed in plasma rebound virus. 56

Figure 4.1: An HIV-1 reporter virus replicates in vitro, but does not establish viremia in vivo. 59

Figure 4.2: Infection spread of HIV-$1_{SV40HSA}$ variants in CEM.NKR.CCR5 cells. 61

Figure 4.3: Grafting a gp41 fragment from Q23.17 onto YU2 confers remarkable spread fitness. 62

Figure 4.4: Replacing SV40pro with a minimal human IL-16 promoter enhances marker expression. 63

Figure 4.5: HIV-1_{IL16HA} stably replicates at low levels in hu-mice. 64

Figure 4.6: Passaging HIV-1_{IL16HA} in vivo results in higher viral loads. 66

Figure 4.7: Further passage selects for a well-adapted, stably replicating reporter virus. 68

Figure 4.8: Viral sequencing reveals evolutionary selection for mutations in HIV-1_{IL16HA}. 70

Figure 4.9: An infectious molecular clone, HIVivoHA, recapitulates features of the primary isolate. 72

Figure 4.10: Rare HA+/Env- cells persist in reporter-infected hu-mice treated with cART. 73

Figure 4.11: In vivo-adapted reporter virus demonstrates stability and latency in vivo. 74

Figure 4.12: Single-cell analyses reveal that reporter virus-infected, Env- cells carry defective *env*. 77

Figure 4.13: A single-cell viral outgrowth assay to detect cells harboring intact viral genomes. 79

LIST OF TABLES

Table 4.1: List of reporter virus variants of HIV-$1_{SV40HSA}$ and their performance in vitro.60

Table 4.2: Modifications of YU2$(Q23)_{SV40HSA}$ to improve marker expression and staining. 63

Table 4.3: Summary of consensus mutations identified in ID#300 and HIV300-infected hu-mice 71

INTRODUCTION

HIV-1 virus and life cycle

HIV-1 is an enveloped, single-stranded, plus-strand RNA virus of the family *retroviridae*. HIV-1 infects human CD4+ T-lymphocytes through interaction of the viral envelope glycoprotein trimer, gp160, with CD4 molecules on the surface of the target cell(1-3). Following virus attachment, entry occurs by fusion of the viral envelope with the plasma membrane of the target cell. Virion-associated reverse transcriptases convert the RNA genome to a double-stranded DNA provirus. This process is highly error-prone, and is responsible for the high mutation rate of HIV-1 and the extensive genetic diversity of HIV-1 infection within even a single infected individual(4, 5). Following reverse-transcription, viral DNA pre-integration complexes are imported into the nucleus (6) and virion-associated integrases mediate proviral integration into the host cell genome. Once the provirus has become integrated, the cell is permanently infected. The integrated provirus is then transcribed by target cell transcription machinery into new sense-stranded viral RNAs, which are processed and translated into viral proteins, or assembled as full-length RNAs into new virions. Viral structural proteins accumulate at the target cell membrane, where they are proteolytically processed [either by the viral protease, in the case of Gag and Pol, or by cellular furin, in the case of Gp160(7)] and assemble into nascent viral buds. These buds then separate from the target cell membrane, at which point the virions mature and are free to initiate new rounds of infection.

Viral genetic material in tissues and cells

Virus released from productively infected cells can be detected in all lymphatic tissues in viremic and treated individuals(8), and is readily measured from human blood plasma by quantitative reverse-transcriptase polymerase chain reaction (qRT-PCR) assays(9) to measure HIV-1 RNA (referred to as viral load). HIV-1 DNA may also be detected in cellular genomic and extra-chromosomal DNA, in the forms of integrated or unintegrated provirus and reverse transcripts(6). Unintegrated HIV-1 DNA arises naturally from dysfunctional reverse transcription and failure to integrate. These HIV-1 DNA forms are generated during new infectious events, and are lost by dilution through cell division(10, 11), unlike integrated proviral DNA, which is copied along with chromosomal DNA during mitosis. Because HIV-1 replication is error-prone, assays that measure HIV-1 DNA may also detect integrated, but defective, proviruses that suffer deletions or mutations that render the provirus unable to initiate new rounds of infection(12). Depending on the nature of the aberration, these non-productively infected cells may also express certain viral antigens or exhibit normal levels of viral transcription, and may even support egress of defective virus particles harboring viral RNA (vRNA). Recent findings estimate that the vast majority of detectable integrated HIV-1 DNA is defective(13).

ART drugs and treatment

ART drugs are able to block the spread of HIV-1 infection by interfering with any of multiple steps in the viral life cycle. Nucleoside and nucleotide analogs, such as tenofovir disoproxil fumarate (Viread) and emtricitabine (Emtriva), inhibit reverse

transcription of viral RNA into DNA by incorporating false bases into reverse transcripts, resulting in premature termination. Non-nucleoside/ nucleotide reverse transcriptase inhibitors, such as efavirenz (Sustiva; Atripla), target the reverse transcriptase enzyme by blocking an allosteric site. Other classes of drugs target integration [such as raltegravir (Isentress)], proteolytic processing [indinavir (Crixivan)], or virus entry [enfuvirtide (Fuseon), maraviroc (Selzentry)]. Suppressive therapy in humans is achieved by combining at least three ART drugs, which guards against selection for drug-resistant viruses by requiring multiple resistance-conferring mutations to arise simultaneously. HIV-1 infection in the vast majority of treated individuals fails to escape this form of combination therapy, despite the high mutation rate of HIV-1. Treatment of infected individuals with ART leads to a rapid decline in viremia, which eventually falls below sensitive limits of detection (20 HIV-1 RNA copies per milliliter of blood plasma) within 3-12 weeks(14). This drop in viral load is caused by the death of virus-producing HIV-1-infected cells, which have an approximate half-life of 1.5 days(15). While several factors are believed to contribute to infected cell death, such as the apoptotic DNA damage response caused during virus integration(16), or the pyroptotic inflammatory response generated by interferon-stimulated genes during non-productive infection(17), ART drugs are not believed to contribute actively to the death of infected cells.

Human immune response to HIV-1 infection

In the absence of suppressive therapy, persistent HIV-1 viremia leads to gradual destruction of the host immune system, resulting in AIDS. ART drugs are necessary because the human immune response to HIV-1 infection is usually insufficient to

manage viremia. Certain HIV-1-infected persons, termed “elite controllers” or “long-term non-progressors”, can naturally suppress viremia without intervention, an effect which has been linked in some cases to human alleles known to improve effective T-cell responses(18). However, humoral immune responses have not been shown to impact viral loads or lead to elite control. Infected individuals always generate antibodies to gp160 during the course of infection, but such antibodies are largely ineffective at blocking virus infection (a property referred to as neutralization) or mediating clearance of infected cells (referred to as antibody-dependent cell-mediated cytotoxicity, or ADCC). However, a small percentage of HIV-1-infected individuals generate neutralizing antibodies that recognize epitopes on the gp160 trimer that are highly conserved among HIV-1 strains, despite the extensive intra- and inter-patient diversity of HIV-1(19). Termed “broadly neutralizing antibodies,” or bNAbs, these antibodies are unable to control viremia in the patients from which they are isolated due to the rapid selection of antibody-resistant virus that follows their generation in the host(20, 21). However, because of their ability to neutralize heterologous HIV-1 strains, bNAbs have long been proposed as both protective and therapeutic agents against HIV-1 infection in other individuals.

BNAbs in HIV-1 prevention and therapy

A number of early studies in animal models revealed that monoclonal bNAbs could be effective in protecting against HIV-1 infection(22, 23). These studies were initially conducted in macaques using a chimeric simian-tropic HIV-1 strain, termed SHIV, and were later corroborated with unmodified HIV-1 using humanized mouse models(24).

These results were highly encouraging, and suggested that vaccines capable of eliciting bNAb-like humoral responses could be similarly effective in protecting against new infections. However, studies that investigated the ability of bNAbs to treat established infection produced discouraging results, both in animal models and in humans(25-27). Administration of a cocktail of three bNAbs to humanized mice yielded only small transient reductions in viral load, and rapid selection for viral resistance(25). Likewise, in two clinical trials, a similar combination of three bNAbs failed to sustain virological suppression when ART-treated subjects were temporarily undergoing treatment interruption, yet selected for viral resistance to one of the bNAbs(26, 27). These results led to the conclusions that bNAbs could prevent new HIV-1 infections, and might serve as a model for protective vaccination, but were ineffective as therapeutic agents. However, these studies were done at a time when very few bNAbs had yet been discovered(28-31). The finding that certain bNAbs did select for viral resistance indicated that they were, in fact, triggering evolutionary bottlenecks in viral populations, and left open the possibility that more potent bNAbs could be therapeutically efficacious.

Significant advances in antibody cloning techniques eventually led to the discovery of many new bNAbs with diverse specificities, and these exhibited neutralizing potencies many orders of magnitude greater than first-generation bNAbs (summarized in Fig. 0.1). Several of these ‘second-generation’ bNAbs were identified in the Nussenzweig laboratory, including 3BNC117, an antibody that recognizes the CD4-binding pocket of

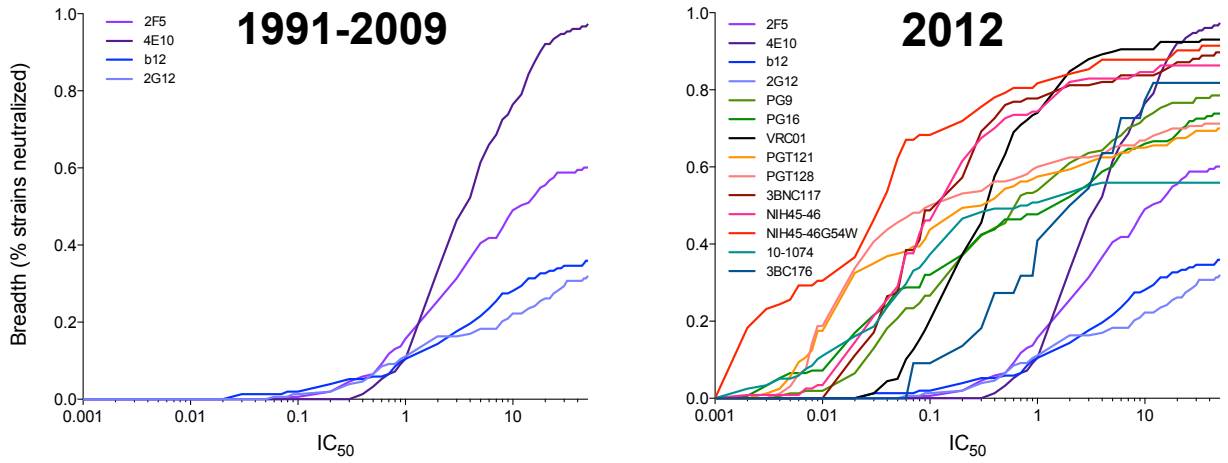

Figure 0.1: 1st and 2nd generation bNAbs.

Breadth and neutralizing potency of bNAbs before (left) and after advances in single-cell cloning techniques revolutionized bNAb discovery. Neutralizing potency refers to the IC_{50} (ug/ml) of a given bNAb against HIV-1 isolates in a luciferase-based single-round infectivity assay (TZM-bl assay, REF_Montefiori). Breadth refers to the percent of tested HIV-1 strains neutralized by a given bNAb among a panel of known HIV-1 isolates (Los Alamos National Laboratories).

gp120(32), 10-1074, an antibody that interacts with a mannose glycan-rich patch and the stem of the gp120 variable loop 3(33), and 3BC176, an antibody now known to recognize a quaternary epitope present on a transient intermediate conformation of the gp160 trimer(34). At the time I began my graduate studies, it remained unclear whether these and other new, highly potent “second-generation” bNAbs could be more effective than first-generation bNAbs when deployed against established HIV-1 infection in vivo.

Animal models of HIV-1 infection

Several animal models exist for studying various aspects of HIV-1 infection, and each has its advantages and disadvantages. Rhesus macaques and other non-human primate (NHP) models are readily infected with both simian immunodeficiency virus

(SIV) and SHIV, and are highly useful for studying immune responses to lentiviral infection because they are fully immunocompetent animals at the time of infection. As SHIV strains carry an SIV backbone, but are outfitted with HIV-1 *env* genes (and, therefore, express HIV-1 gp160 trimers on the surface of virus and infected cells), SHIV infection in macaques can be a useful model with which to evaluate the effectiveness of bNAbs in both protective and therapeutic contexts. However, NHPs are cost-prohibitive and difficult to obtain. Thus, while NHP models may be excellent for preclinical evaluation of potential anti-HIV-1 therapeutics due to their close genetic relation to humans, they are not ideal models for early-stage experimentation.

Humanized mouse models, in which immunocompromised mice are endowed with human immune cells, present an alternative and more accessible model with which to study HIV-1 infection. Unlike NHPs, which do not have human immune cells and cannot support HIV-1 infection, humanized mice (hu-mice) harbor human CD4+ T-lymphocytes that can readily propagate bona fide HIV-1 strains. Large colonies of hu-mice can be generated, permitting sufficient statistical powering of test groups for experimentation. However, hu-mouse models have several important shortcomings: human immune reconstitution levels and immune cell lineage composition are highly variable(35, 36), with several lymphatic tissues defective or absent (such as lymph nodes); murine and human immune functions are severely compromised, or are lacking altogether; and, because mice are three orders of magnitude smaller than humans, total body HIV-1 viral load in mice is necessarily far smaller than that of HIV-1-infected humans. Thus, while hu-mice are not ideal for studying immune responses to HIV-1 infection, they are

highly useful for evaluating anti-HIV-1 therapeutics such as bNAbs and ART drugs, which are best tested against bona fide HIV-1 infection in human CD4+ T-lymphocytes.

Latent HIV-1 infection

Latent HIV-1 infection, as described in this thesis, shall refer *only* to the behaviors of individual HIV-1-infected cells (a description of which follows), and *not* to a clinical stage of suppressed infection known as “clinical latency”(37). Because HIV-1 integration results in permanent infection of a cell, certain subsets of long-lived cells may become infected and persist for years, or even decades(38). These latently HIV-1-infected cells (LICs) can become spontaneously reactivated, resulting in the release of infectious virions. In the absence of suppressive therapy, virion release from LIC reactivation can initiate new infections, and rapidly re-establish active viremia in infected persons. Although the frequency of LICs among all CD4+ T-lymphocytes in ART-treated HIV-1-infected persons is thought to be low, on the order of 1 LIC per million resting CD4+ T-lymphocytes, the total body load of LICs is thought to number in the millions(38). The spontaneous reactivation of LICs is thought to be responsible for persistent, low-level viral loads (< 20 HIV-1 RNA copies per ml plasma, hereafter cpm) detectable by single-copy assays(39) in patients who are highly adherent to their suppressive ART regimens. In a majority of HIV-1-infected persons, withdrawal from suppressive ART results in virological rebound due to LIC reactivation within 2-3 weeks(40).

Current understanding of LICs holds that viral transcription (and, therefore, viral gene expression) is absent or highly suppressed during the latent state(41, 42). Due to this

apparent absence of identifiable antigenic signatures, combined with the extreme rarity of LICs in vivo, LICs at present are impossible to study *in situ*: they can neither be distinguished from uninfected cells, nor from infected cells harboring defective proviruses. Their existence *in vivo* has been demonstrated only by assays that were designed to reactivate and outgrow virus from the purified resting cells of ART-suppressed patients *ex vivo*(43). A number of studies have demonstrated that LICs are predominantly comprised of resting memory CD4+ T-lymphocytes(43, 44). LICs are thought to emerge by either of two possible routes: 1) rare, direct productive infection of resting memory cells; or 2) productive infection of activated CD4+ T-lymphocytes during a period of transition from an activated cell state to a resting state(42). Studies performed using models of LIC generation *in vitro* have suggested that either route is possible(45-48). However, the molecular determinants responsible for maintaining the latent state are largely unknown. Recent work has shown that only a fraction of LICs harboring fully intact proviruses are susceptible to reactivation *in vitro* using current methods(13). In that study, repeated reactivation of resting, non-induced cells led to further viral outgrowth, suggesting that viral reactivation in LICs is both rare and stochastic. These data indicate that latent reservoirs of HIV-1 infection are far larger than previously thought, although the nature and frequency of LIC reactivation in vivo remains very poorly understood.

It has been suggested that LICs may arise as a consequence of multiple factors, including (but not limited to): epigenetic silencing of the viral promoter; transcriptional interference from genetic promoters upstream of proviral integration; proviral integration

into sites that are, or that become, repressive for transcription; or the lack of critical transcription factors (such as NFAT) needed for efficient viral transcription, such as occurs during the transition from activated to resting cell states [reviewed in (42)]. However, the inability to purify individual bona fide LICs *ex vivo* has limited further interrogation of the molecular determinants of latency. A means with which to identify and dissect bona fide LICs, such as those that arise during the natural spread of HIV-1 infection *in vivo*, is required.

CHAPTER I: SUPPRESSION OF HIV-1 INFECTION IN VIVO BY COMBINATIONS OF BROADLY NEUTRALIZING ANTIBODIES

A humanized mouse model of HIV-1 infection

In order to investigate the dynamics of HIV-1 infection in response to therapeutic interventions *in vivo*, I opted to use NOD/Rag1$^{-/-}$/IL-2R$_{\gamma}^{null}$ (NRG) mice engrafted with human hematopoietic stem cells (hu-mice). To generate such hu-mice, human CD34+ cells were magnetically isolated from fetal liver tissue and injected intra-hepatically into neonate mice. Engraftment was confirmed by flow cytometric profiling of mouse PBMC at 8-12 weeks of age (Fig. 1.1).

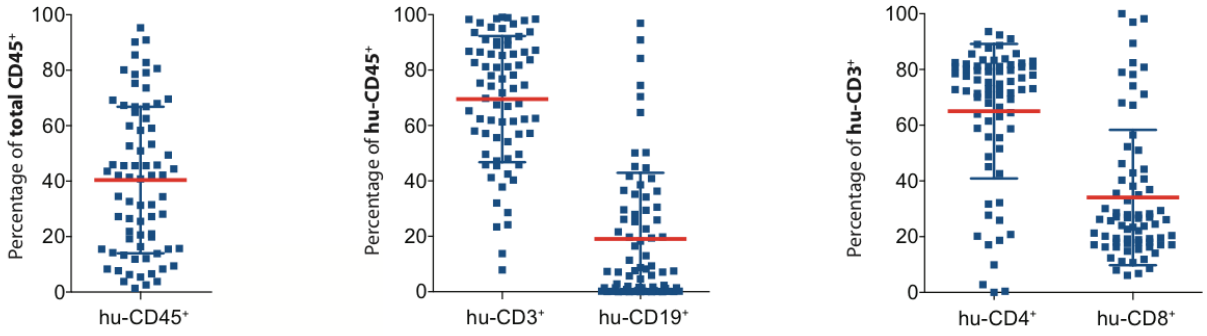

Figure 1.1: Hematopoietic reconstitution of hu-mice.

Each dot represents a single animal; red line indicates population geometric average. Left, percent human CD45+ cells among total CD45+ (mouse plus human). Middle, proportion of T- (CD3+) and B-lymphocytes (CD19) among total human CD45+. Right, proportion of CD4+ versus CD8+ T-lymphocytes among total CD3+. While the relative abundance of CD3+ versus CD19+ cells was highly variable, the presence of CD3+ cells generally resulted in consistent proportions of CD4+ and CD8+ cells.

Hu-mice harboring visible populations of human CD4+ T-lymphocytes were challenged with a laboratory-adapted HIV-1 strain, HIV-1$_{NL4/3}$ bearing the *env* gene of the clade B, Tier 2 strain YU-2, hereafter HIV-1$_{YU2}$. In order to measure viral load, I adapted a quantitative reverse-transcriptase PCR assay(9) to match the viral sequence of HIV-

1_{YU2}. Forward and reverse primers targeting the viral long terminal repeat (LTR) were 5'-GCCTCAATAAAGCTTGCCTTGA-3' and 5'-GGCGCCACTGCTAGAGATTTT-3', respectively; an internal probe (5'-AAGTAGTGTGTGCCCGTCTGTTRTKTGACT-3') contained a 5' 6-carboxyfluorescein reporter and an internal/3' ZEN-Iowa Black FQ double-quencher (Integrated DNA Technologies). Degenerate nucleotides reflect positions at which the published internal probe sequence differed from HIV-1_{YU2}. HIV-1 RNA was purified from mouse plasma using the QiaAmp MinElute Virus Spin Kit (Qiagen) and 20 ul purified RNA added to a one-step qRT-PCR reaction using the TaqMan RNA-to-Ct One Step Kit (Applied Biosystems) with 450nM forward and reverse primer and 125nM probe. Standard curves were generated using diluted virus stocks of known RNA copy number (as measured by a highly sensitive clinical assay). The resulting in-house HIV-1 qRT-PCR viral load assay was found to have a lower limit of quantitation of 800 copies per milliliter plasma (cpm) by probit analysis and was highly reproducible (Fig. 1.2).

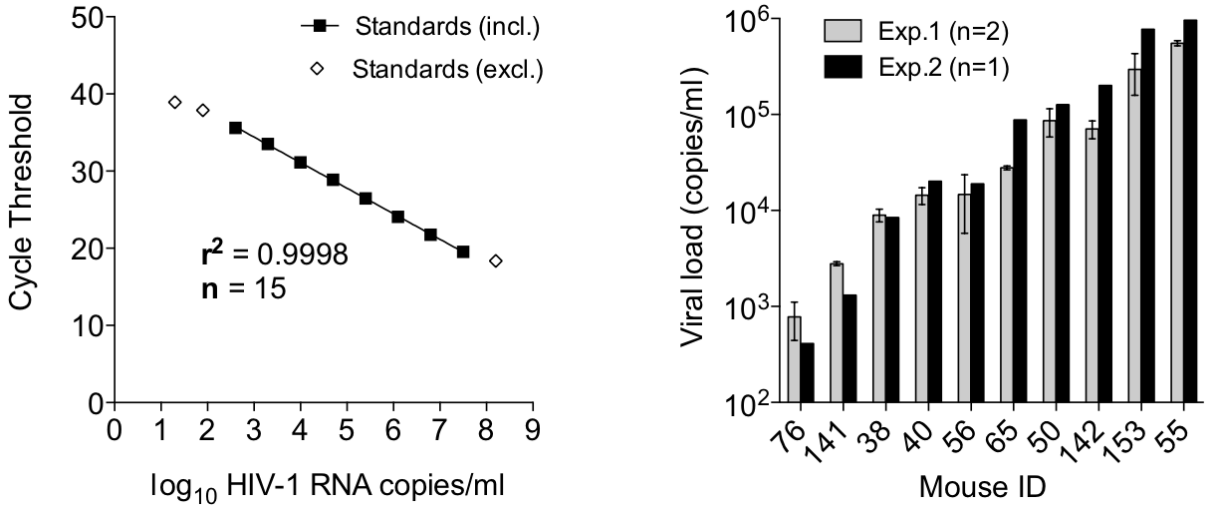

Figure 1.2: Validation of HIV-1 qRT-PCR plasma viral load assay.

Left, standard curve measurements averaged from fifteen consecutive qRT-PCR assays (error bars: standard deviation). Black, solid symbols reflect data points used for standard curve analysis. *Right*, test of inter-assay and intra-assay variation. Mice from which triplicate plasma samples could be obtained were analyzed in two independent experiments. In one experiment (gray bars), duplicate plasma samples were independently extracted and analyzed; in a second experiment (black bars), a third replicate plasma sample was independently extracted and analyzed. Intra-assay and inter-assay variation were always less than $\log_{10}(0.5)$ units. Peak viral loads were generally correlated with engraftment (data not shown).

Plasma viral loads in hu-mice reached concentrations equivalent to HIV-1-infected humans and SIV-infected macaques (Fig. 1.3). After many weeks of infection, human CD4 counts declined, as occurs in chronically HIV-1-infected humans (Fig. 1.3). To determine whether HIV-1 infection of hu-mice results in the high rates of viral diversification observed in humans, I utilized an assay to sequence the gp120 portion of *env* from individual plasma viruses. Briefly, purified RNA extracted as previously described was reverse-transcribed using the primer 5'-GGTGTGTAGTTCTGCCAATCA-GGGAAGWAGCCTTGTG-3' by SuperScript III first-strand synthesis (Invitrogen). The resulting cDNA was amplified by two rounds of nested PCR: primers

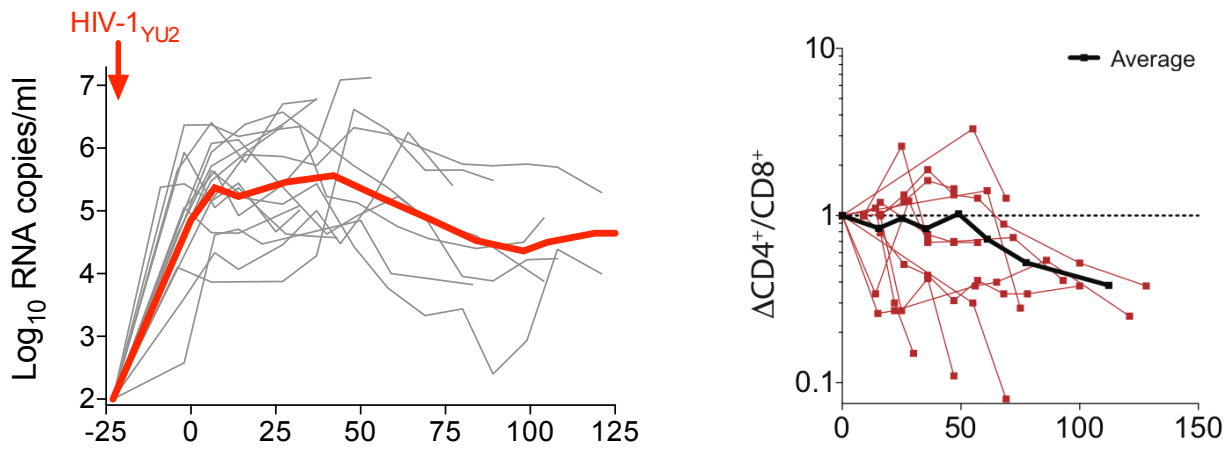

Figure 1.3: Viral load and CD4 T-cell depletion in HIV-1_{YU2}-infected hu-mice.

Left, plasma viral loads from untreated hu-mice. X-axis reflects days relative to subject enrollment. Red arrow indicates time of infection; each gray line reflects one animal; bold red line indicates population average over time. *Right*, change in CD4/CD8 ratios (normalized to baseline) in PBMC of infected mice over time. X-axis reflects days since infection. Each maroon line reflects a single animal; bold black line reflects the population average.

used for the first round of PCR were 5'-GGCTTAGGCATCTCCTATGGCAGGAAGAA-3' and 5'-GGTGTGTAGTTCTGCCAATCAGGGAAGWAGCCTTGTG-3', and primers for the second round of PCR were 5'-TAGAAAGAGCAGAAGACAGTGGCAATGA-3' and 5'-TCATCAATGGTGGTGATGATGATGTTTTTCTCTCTGCACCACTCTTCT-3'. PCR bands were cloned by topoisomerase-mediated ligation (pCR4 TOPO-TA kit, Invitrogen) and the resulting plasmids sequenced (Genewiz). Sequencing of plasma virus shortly after infection revealed rapid viral diversification (Fig. 1.4), but recurring mutations that would suggest a need for viral adaptation to hu-mice were not observed. Sequencing of clonal virus from purified viral stocks confirmed that the measured viral diversity in hu-mice was not merely an artifact of PCR errors (Fig. 1.4). These data indicated that HIV-1_{YU2} infection in hu-mice was robust and resembled many elements of acute HIV-1 infection in humans.

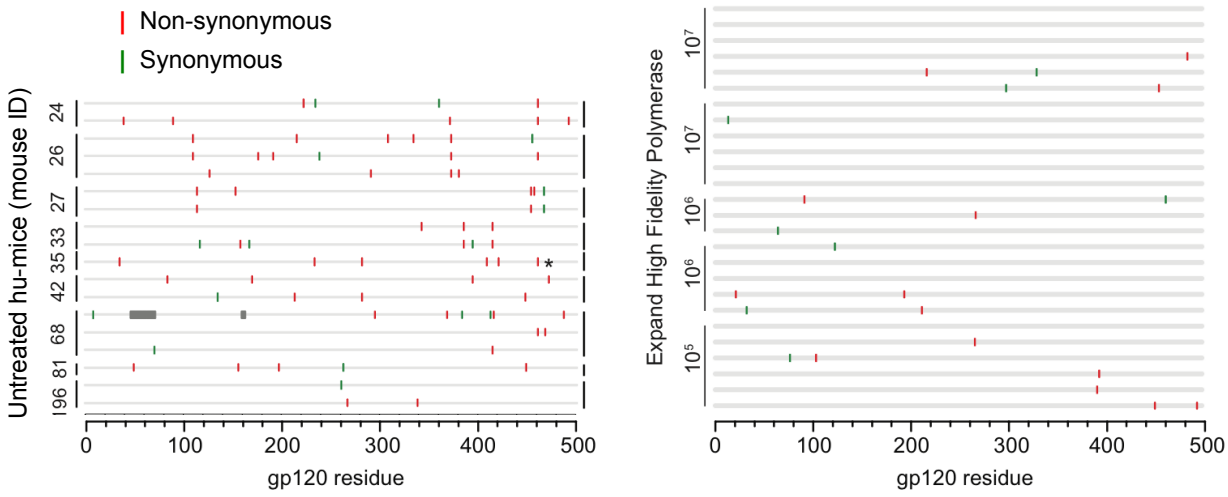

Figure 1.4: Rapid viral diversification after clonal infection.

Left, mutations in *env* gp120 in the plasma viruses of HIV-1_{YU2}-infected mice shortly after infection. Red and green bars reflect non-synonymous and synonymous mutations with respect to HIV-1_{YU2}, respectively. Horizontal lines reflect a single gp120 sequence from the animal indicated at left. *Right*, mutations due to PCR errors in single sequences obtained from gp120 cloning of the HIV-1_{YU2} viral stock. The indicated sample copy number (as measured by viral load) used for RT-PCR is given at left of each sequence. Mutation frequency due to PCR was significantly lower ($p < 0.01$) than that found in plasma viruses from untreated infected animals.

Individual bNAbs rapidly select for viral resistance

While early experiments in HIV-1-infected humans showed that first-generation bNAbs were therapeutically ineffective, none of the broader and substantially more potent second-generation bNAbs had yet been evaluated in any therapeutic context. To investigate whether second-generation bNAbs could suppress active HIV-1 infection in vivo, I treated viremic HIV-1_{YU2}-infected hu-mice with one of several different second-generation monoclonal bNAbs. Antibodies were chosen on the basis of their potency, breadth, and target site on the HIV-1 envelope trimer: PG16 is a glycan-binding antibody that targets a conformational epitope spanning gp120 variable loops 1 and 2(49); 10-1074 and PGT128 target the base of the gp120 variable loop 3 and interact

with a conserved glycan at position N332(33, 50); 3BC176 targets a quaternary epitope that exists as a conformational intermediate spanning the gp120-gp41 interface(34); and NIH45-46^{G54W} (45-46W) is a more potent, engineered variant of the bNAb NIH45-46, which targets the CD4-binding site on gp120(32, 51). All five antibodies exhibited strong neutralizing potency against HIV-1_{YU2} *in vitro*, with IC_{50}s ranging from 0.02-0.3(52) in a TZM-bl neutralization assay(53). Treatment of viremic animals with individual bNAbs led to transient reductions in plasma viral loads in a majority of animals for all but one of the bNAbs tested (Fig. 1.5).

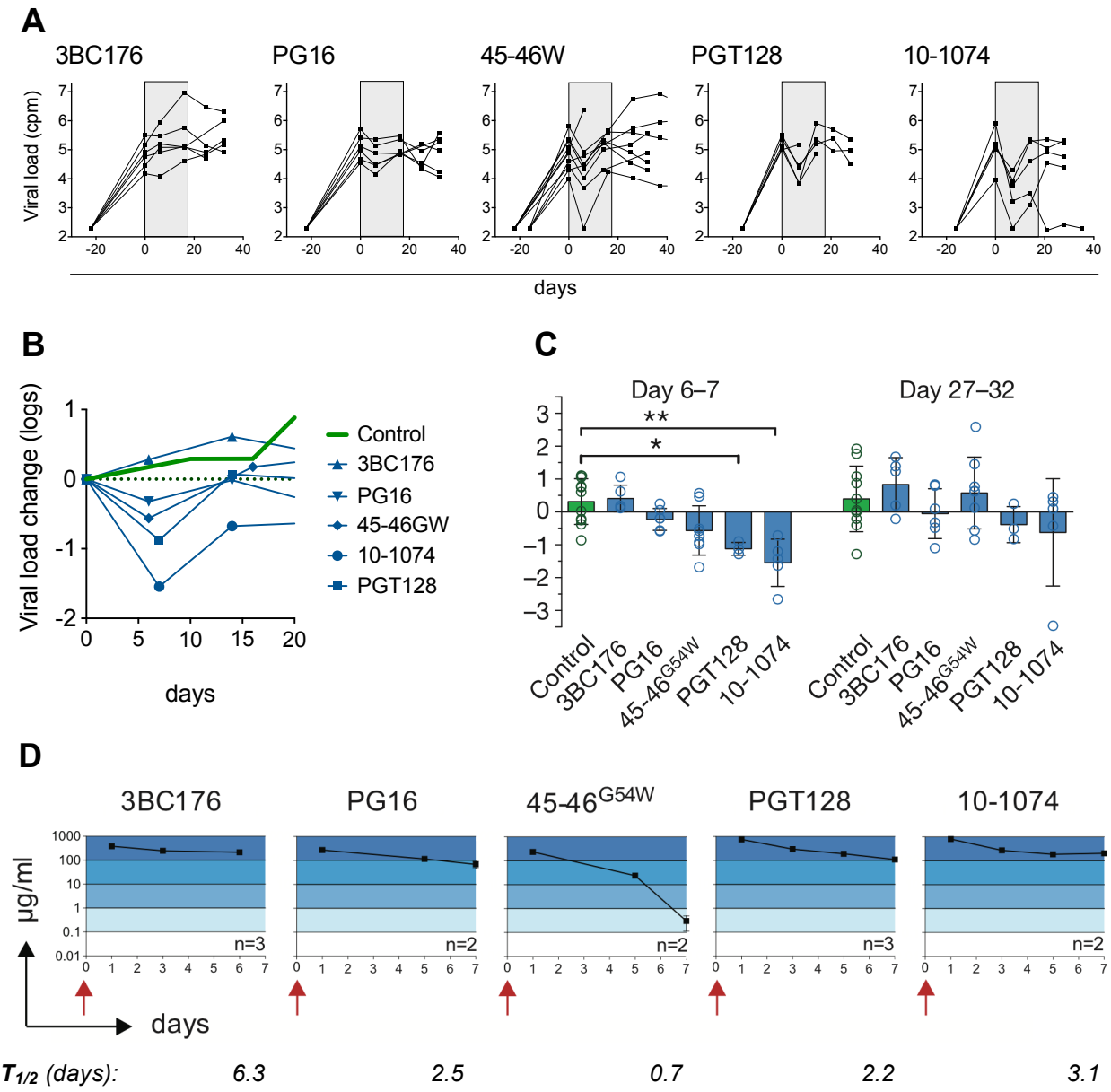

Figure 1.5: Individual bNAbs transiently lower viral load.

A, viral loads (log_{10} cpm) in hu-mice treated with the indicated bNAb. Antibodies were administered during the period shaded in gray. Each line reflects a single animal. *B*, population average viral loads (normalized to baseline) for each group of animals in *A* (and control animals from Fig. 1.3). Averages were computed by moving average (geometric mean). *C*, quantitation of viral load changes (normalized to baseline) at the indicated number of days after initiation of bNAb treatment. Viral load changes one week after treatment initiation were significantly different from control animals for two bNAbs (* = p <0.05, ** = p <0.01, Kruskal-Wallis test). Viral loads for all groups returned to baseline levels four weeks after treatment initiation. Scale, as in *B*. *D*, bNAb IgG concentrations in plasma of NRG mice and corresponding half-lives are shown. Mice were injected intravenously with 0.5mg of each antibody (red arrows) and the plasma concentration over time was measured by anti-human IgG1 ELISA.

Strong reductions in viral load were observed after one week of bNAb treatment for all bNAbs except 3BC176 (Fig. 1.5A,B). Viral loads returned to baseline levels in bNAb-treated animals two weeks after treatment initiation (Fig. 1.5C), when antibody was still being administered. It was therefore anticipated that the viruses had acquired mutations conferring resistance to bNAb neutralization. The *env* gp120 sequences from plasma virus of treated animals were sequenced to identify mutations that might have arisen in response to bNAb treatment. As expected, nearly all viral sequences obtained from animals treated with PG16, 45-46W, PGT128, or 10-1074 carried amino acid changes at sites known to be critical for their interaction with gp120 (Fig. 1.6). PG16-associated mutations universally removed the putative N-linked glycosylation site (PNGS) at residue 160 by mutation of either N160 or T162. 45-46W-associated mutations occurred at CD4bs residues spanning either 279-281 or 458/459, with a highly prevalent mutation to A281T. PGT128-associated mutations universally removed the PNGS at residue 332 by mutation of either N332 or S334. 10-1074-associated mutations were extremely restricted, with 51 of 53 sequences mutated to N332K. Viruses obtained from animals treated with bNAb 3BC176, for which viral loads increased acutely following therapy initiation, did not contain recurring mutations in gp120, despite that antibody having the longest half-life in mouse plasma (Fig. 1.5D). These data suggested that 3BC176 was sub-therapeutic against HIV-1_{YU2} infection in hu-mice.

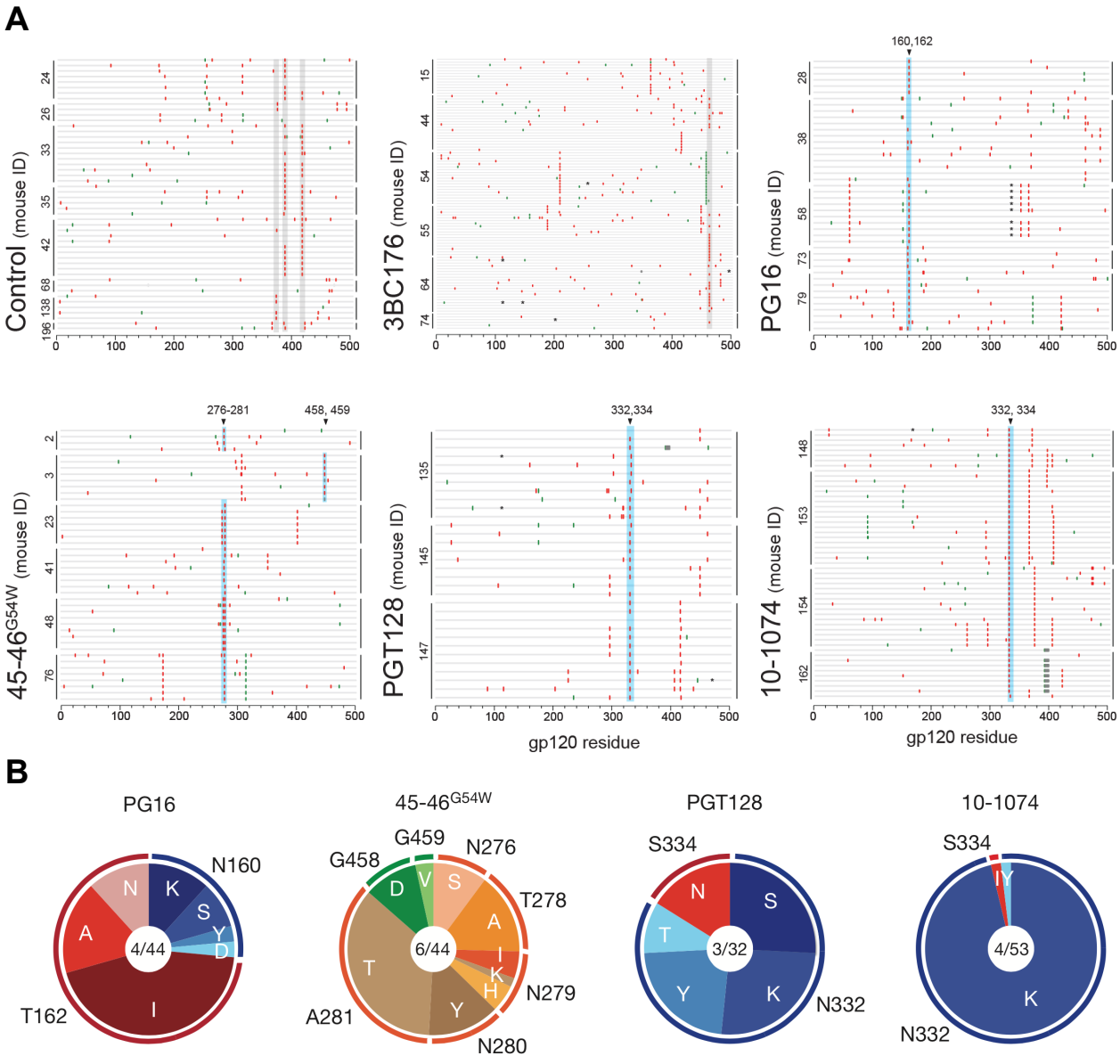

Figure 1.6: *env* gp120 sequences reveal amino acid substitutions at antibody contact sites.

A, individual viral sequences from animals treated with the indicated bNAb (or controls), annotated as in Fig. 1.4. Gray shaded vertical lines reflect recurring mutations not found in bNAb contact sites; blue shaded vertical lines reflect recurring mutations in bNAb contact sites. The Hxb2-aligned gp120 residues are shown above each blue shaded line. *B*, summary of amino acid changes (from *A*) in bNAb contact sites for animals treated with the indicated bNAb. Original residues in HIV-1_{YU2} are given at the perimeter, while colored slices and corresponding letters reflect the mutation observed. Numbers in the center of each pie chart give the number of mice, followed by the number of discrete gp120 sequences obtained.

To determine whether the amino acid changes in gp120 found in antibody contact sites conferred resistance to neutralization, I introduced selected point mutations into HIV-

1_{YU2} pseudoviruses and assayed for bNAb neutralization *in vitro* by TZM-bl assay. This work was performed in collaboration with the laboratory of Dr. Michael S. Seaman (Beth Israel Deaconess Medical Center, Boston, MA). Expectedly, amino acid changes arising in bNAb contact sites fully abrogated neutralizing activity of the respective bNAbs in a majority of cases (Fig. 1.7). Strikingly, the number of amino acid positions on gp120 that were mutated in response to bNAb pressure was very low, suggesting that the strong *in vivo* neutralizing potency of each effective bNAb overwhelmingly restricted the possible routes of viral escape.

		IC_{50} (µg/ml) in TZM.bl neutralization assay				
YU2	Identified in (mouse ID)	**3BC176**	**PG16**	**45-46^{G54W}**	**PGT128**	**10-1074**
wt	-	**0.319**	**0.612**	**0.024**	**0.169**	**0.312**
Frequent mutation in 3BC176-treated mice						
G471R*	44, 55, 64, 74	**0.159**	**0.154**	**0.008**	**0.020**	**0.091**
Frequent mutations in PG16-treated mice						
N160K	22, 25, 38, 43, 49, 56, 73	**0.145**	>50	**0.007**	**0.086**	**0.155**
T162N	22, 25, 56, 79	**0.154**	>50	**0.013**	**0.166**	**0.175**
Frequent mutations in 45-46^{G54W}-treated mice						
N279H	2	**0.209**	**0.294**	>50	**0.064**	**0.177**
N280Y	25, 49, 76	**0.276**	**0.145**	>50	**0.031**	**0.126**
Frequent mutations in PGT128 or 10-1074-treated mice						
N332K	135, 147, 148, 153, 154, 162	**0.232**	**0.988**	**0.017**	>50	>50
N332Y	135, 145, 162	**0.269**	**0.632**	**0.010**	>50	**13.596**
S334N	135, 145	**0.218**	**0.615**	**0.020**	>50	**7.308**

Figure 1.7: Amino acid changes found in bNAb contact sites confer bNAb resistance.

HIV-1_{YU2} point mutants were generated based upon the gp120 sequences of animals treated with the indicated bNAb at left. Pseudoviruses carrying the indicated point mutants (in bold at left, Hxb2-aligned gp120 residue) were tested for neutralization *in vitro* by the indicated bNAbs at right. IC_{50} (ug/ml) is shown for each condition. Red shading, < 0.1 ug/ml; orange shading, < 1.0 ug/ml; yellow-orange shading, < 10 ug/ml; yellow shading, < 50 ug/ml.

Of note, two of the bNAbs tested, PGT128 and 10-1074, share a common epitope comprised of a glycan moiety at position N332. While both bNAbs exhibited similar neutralizing potencies against unmutated HIV-1_{YU2} (Fig. 1.7), the viral sequences that emerged after bNAb treatment of infected hu-mice reflected key differences in bNAb resistance profiles (Fig. 1.6B). Whereas PGT128 treatment elicited any of several different mutations at either N332 or S334, all of which merely removed the N-linked glycan at position 332, 10-1074 treatment elicited a highly restricted escape profile limited almost exclusively to N332K. When pseudoviruses harboring various mutations at the 332 position were tested for neutralization by PGT128 or 10-1074, it was evident that mere removal of the 332 glycan was sufficient for PGT128 resistance, but only the N332K mutation resulted in complete resistance to 10-1074 (Fig. 1.7). This restrictive escape requirement may explain why viremia in one of the six mice treated with 10-1074 alone became suppressed and failed to escape antibody pressure (Fig. 1.5A), despite a very high pre-treatment viral load.

In conclusion, individual highly potent bNAbs can transiently depress viral loads in hu-mice, and rapidly select for bNAb-resistant viruses through restricted patterns of escape conferred by amino acid changes in the antibody binding sites on gp120.

Combinations of bNAbs can suppress viral loads in hu-mice

As treatment of hu-mice with individual bNAbs imposed strong selective pressure on viral populations, I sought to test whether combinations of multiple highly potent bNAbs could further restrict virus escape pathways and possibly prevent viral escape. As was

done for individual bNAbs, HIV-1_{YU2}-infected, viremic hu-mice were treated with a combination of three bNAbs: 3BC176, PG16, and 45-46W (tri-mix, Fig. 1.8). While a plurality of tri-mix-treated animals exhibited transient viral load depression followed by rebound to pre-treatment levels, three animals fell below the assay LOQ (800 cpm) 2-3 weeks after initiation of bNAb therapy. Viral blips were occasionally observed thereafter, but these three animals exhibited sustained viremic suppression during the antibody treatment period. These data stand in contrast to animals treated with individual bNAbs, in which virus nearly always rebounded to pretreatment levels after two weeks of bNAb therapy.

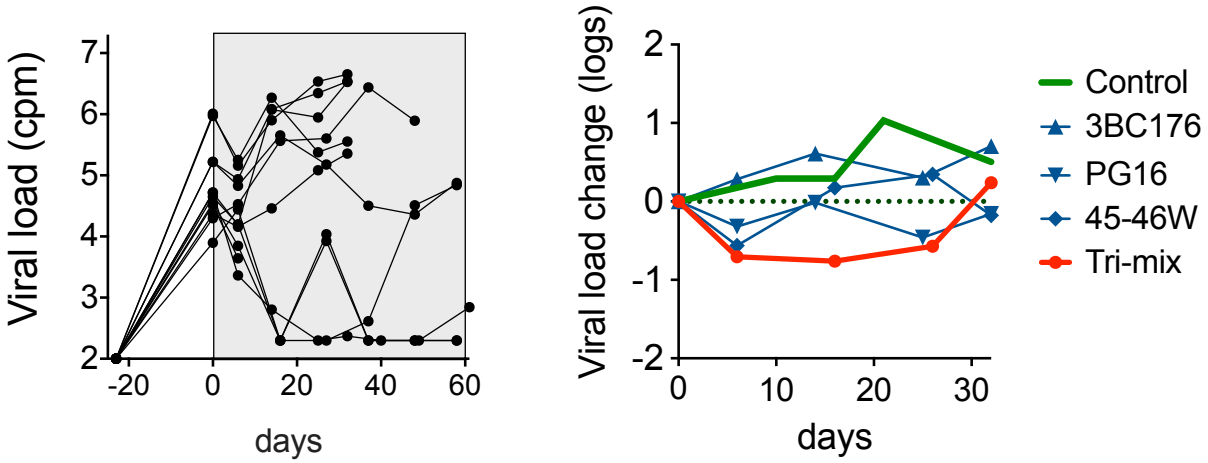

Figure 1.8: A bNAb tri-mix can durably suppress viremia in some hu-mice.

Left, viral loads (log_{10} cpm) of twelve hu-mice treated with a bNAb tri-mix of 3BC176, PG16 and 45-46W (lines and shading as in Fig. 1.5A). *Right*, population average changes in viral loads for the indicated treatment groups (as in Fig. 1.5B).

To determine whether the viruses that rebounded to pre-treatment levels carried escape mutations to the antibodies comprising the tri-mix, I again obtained individual gp120 sequences from plasma virus (Fig. 1.9). Almost without exception, discrete gp120 sequences carried mutations in both PG16 and 45-46W contact sites, many of which

were previously shown to confer complete resistance to the respective bNAbs (Fig. 1.7). No recurring mutations were observed that could confer resistance to 3BC176, as expected from individual bNAb therapy with that antibody. This result yields two observations: first, extensive viral diversification occurs within 2-3 weeks of infection that is sufficient to form clones harboring simultaneous resistance mutations to PG16 and 45-46W; and second, the co-existence of resistance mutations to both PG16 and 45-46W is not deleterious to viral fitness.

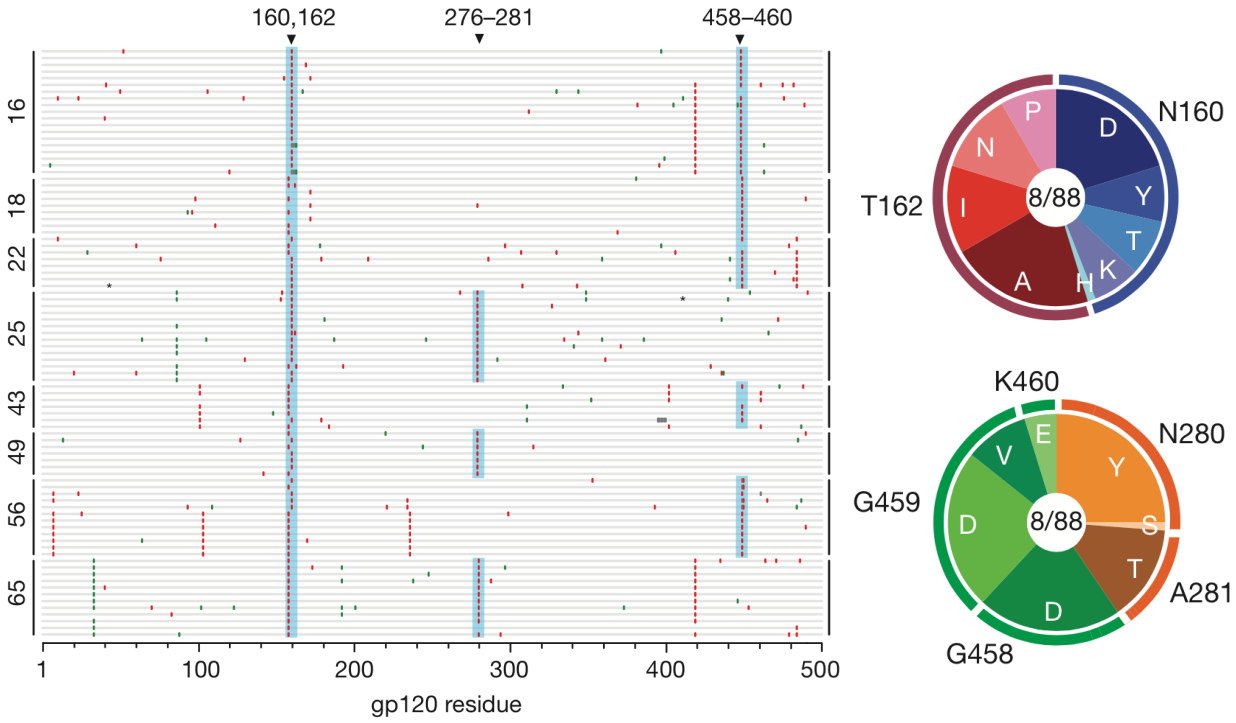

Figure 1.9: Simultaneous bNAb escape mutations arise in tri-mix treated animals.

Left, plasma virus gp120 sequences (as in Fig. 1.6A) of tri-mix treated animals after viral rebound (2-6 weeks after treatment initiation). *Right*, pie charts (as in Fig. 1.6B) showing the prevalence of amino acid changes at PG16 (top) or 45-46W contact sites.

While tri-mix therapy resulted in most animals developing viral resistance to both PG16 and 45-46W, the finding that viral suppression did occur in some animals suggested

that the requirement for two simultaneous bNAb resistance mutations severely restricted the likelihood of viral escape. To test whether requiring additional resistance mutations would increase the likelihood of viremic control, I added two additional bNAbs, PGT128 and 10-1074, to the tri-mix (penta-mix). These two antibodies target the same viral epitope, which does not overlap with PG16 or 45-46W, and they were found to share consistent resistance mutations when used individually to treat hu-mice (Fig. 1.6). Strikingly, penta-mix treatment (Fig. 1.10) resulted in viremic control in all fourteen animals. Viral loads in all animals remained below baseline during the entire treatment period, and most also remained below the assay LOQ during that time.

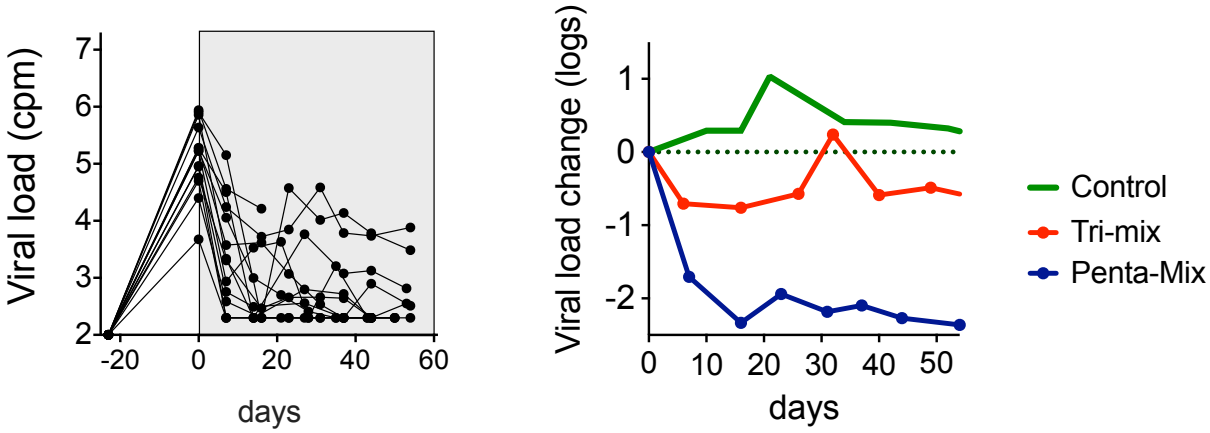

Figure 1.10: A bNAb penta-mix suppresses viremia in hu-mice.

Left, viral loads (log_{10} cpm) of penta-mix treated hu-mice (as in Fig. 1.5A). *Right*, population average viral load changes for the indicated treatment groups (as in Fig. 1.5B).

A minority of animals had detectable viral loads, despite continued penta-mix therapy. To determine whether these animals harbored resistance mutations to the entire penta-mix, I again obtained individual plasma virus gp120 sequences. Surprisingly, all viral sequences in all animals from which sequences could be obtained were defective, replete with STOP codons reflecting APOBEC3G/3F signature mutations (Fig. 1.11). It

remains unclear whether these defective RNA sequences reflect egress of Env-free particles, or whether they are instead the products of infected cell apoptosis.

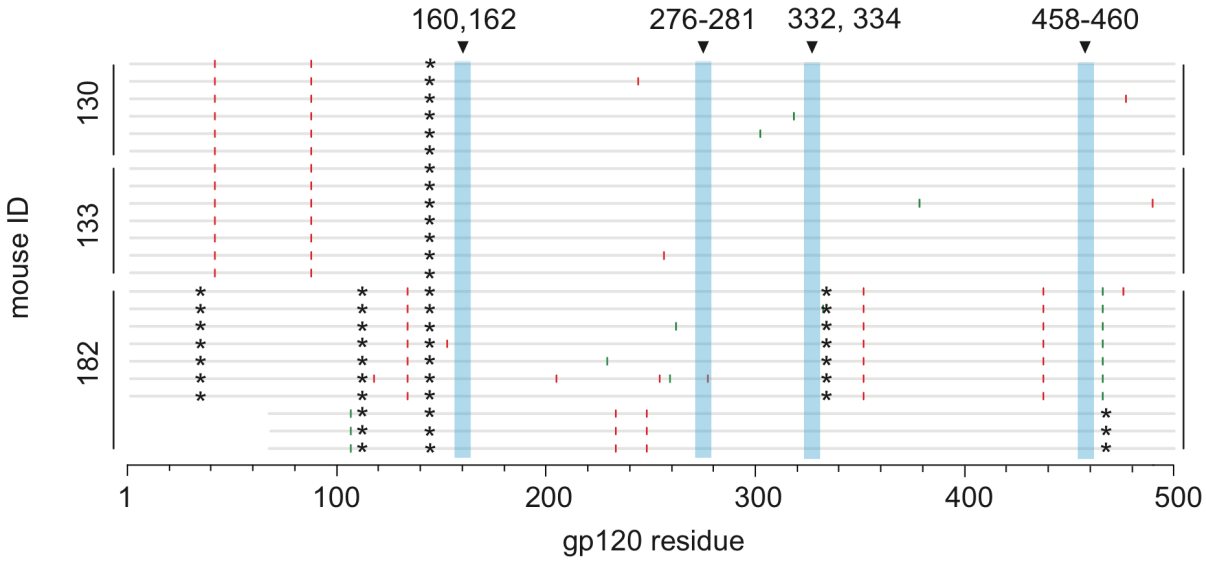

Figure 1.11: Penta-mix treated animals do not carry functional plasma virus.

Gp120 sequences (as in Fig. 1.6) from penta-mix treated animals that were persistently viremic at low levels are shown. Asterisks indicate mutations resulting in STOP codons.

To validate that viral suppression by bNAbs was the result of an inability to generate simultaneous resistance mutations, as opposed to low-level persistence and ongoing replication of resistant virus, I withdrew suppressed tri-mix and penta-mix treated animals from antibody therapy (Fig. 1.12). In a majority of cases, viremia returned coincident with the disappearance of bNAbs from mouse plasma (as measured by anti-gp120 ELISA). The rapid re-emergence of viremia upon antibody decay suggested that the presence of the bNAbs was, indeed, responsible for sustained virological suppression. Furthermore, when penta-mix treated animals were re-treated with the same penta-mix after viremia had returned, their viral loads again became rapidly

suppressed, indicating that the rebounding virus remained sensitive to neutralization by the penta-mix.

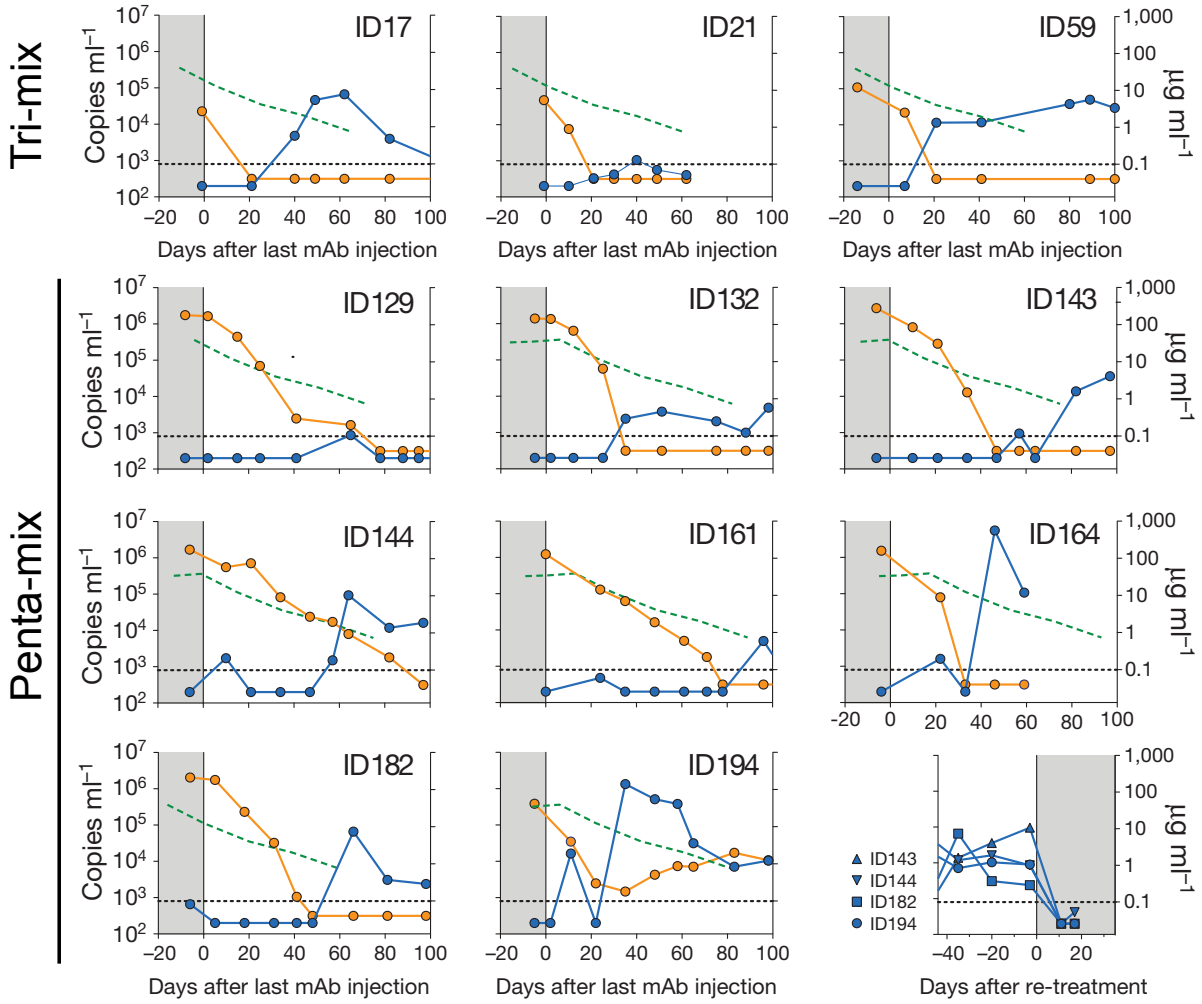

Figure 1.12: Withdrawal of bNAb therapy results in viremic rebound.

Viral loads (blue lines/symbols, left y-axis) and HIV-1-specific human IgG1 (yellow lines/symbols, right y-axis) for each animal suppressed by either tri-mix (top) or penta-mix bNAb therapy are shown. Green dashed line gives the average viral load of control mice at equivalent times post-infection. *Bottom-right*, retreatment of penta-mix treated animals (viral loads shown in blue lines/symbols) post-rebound re-suppresses viral loads.

To confirm that the rebounding virus in bNAb-suppressed animals did not carry simultaneous bNAb resistance mutations, I obtained plasma gp120 sequences from rebound plasma virus (Fig. 1.13). As expected, no viral sequences were found that

carried mutations expected to confer resistance to either the tri-mix or the penta-mix, although occasional mutations could be identified to one of the bNAbs in some mice.

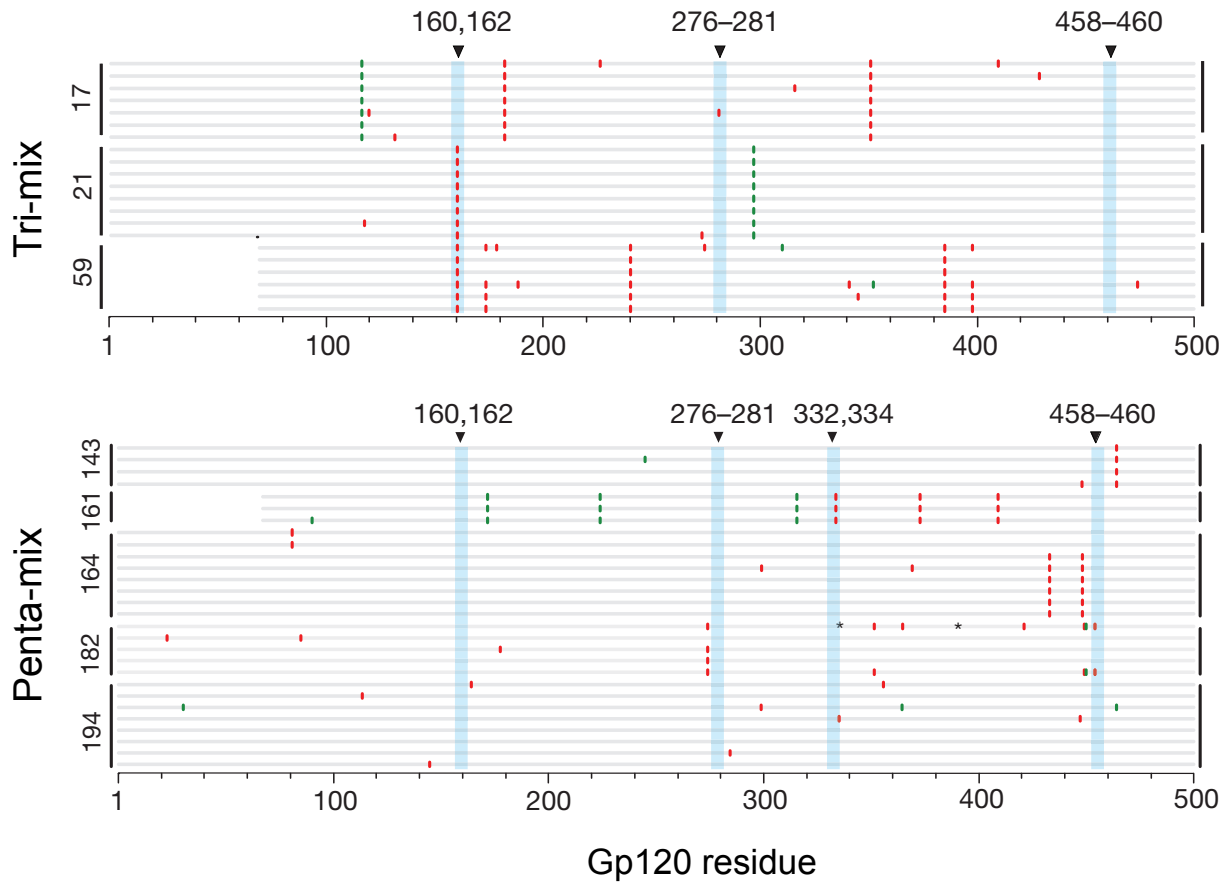

Figure 1.13: Rebounding virus from bNAb-suppressed mice is not bNAb-resistant.

Plasma gp120 sequences (as in Fig. 1.6) from tri-mix (top) or penta-mix treated animals maintaining viremic suppression during treatment.

In summary, these experiments demonstrated that bNAbs can apply strong selective pressure on viral populations in the context of active HIV-1 viremia in infected hu-mice. Due to the high mutation rate of HIV-1, bNAb-resistant viruses were rapidly selected in response to treatment of infected animals with individual monoclonal bNAbs. However, combinations of bNAbs resulted in durable viremic suppression, and increasing the

number of bNAbs targeting different epitopes dramatically improved rates of control. Antibody decay in bNAb-suppressed animals revealed that viremia returned after prolonged periods of control, and that re-emergent viruses remained bNAb-sensitive. These data stand in stark contrast to earlier studies in hu-mice and in humans, which found that the weaker, first-generation bNAbs were largely ineffective in suppressing established HIV-1 infection. I conclude that second-generation bNAbs are potent antiviral agents against active HIV-1 infection in hu-mice.

CHAPTER II: DURABLE CONTROL OF HIV-1 INFECTION BY SINGLE BNABS FOLLOWING SUPPRESSIVE ANTI-RETROVIRAL THERAPY

3BNC117 and 45-46W elicit similar profiles of HIV-1$_{YU2}$ resistance

I previously found that the CD4bs bNAb 45-46W was strongly selective for viral resistance in hu-mice [Figs. 1.5-1.7 and (52)]. However, this antibody is an engineered variant of a naturally occurring CD4bs bNAb, and may not arise or be tolerated in humans. Additionally, 45-46W had the shortest half-life in mice of any bNAb tested (0.7 days). To test whether a naturally arising CD4bs bNAb would be effective against HIV-1 *in vivo*, I tested the effectiveness of a similar bNAb, 3BNC117(32), as a mono-therapeutic against established HIV-1$_{YU2}$ infection in hu-mice. 3BNC117, like 45-46W, dramatically and transiently reduced viral loads (Fig. 2.1A). 3BNC117 also exhibited an improved half-life over 45-46W, at 2.0 days (Fig. 2.1B). Viral sequencing identified resistance mutations that highly resembled those found in 45-46W-treated hu-mice (Fig. 2.1C).

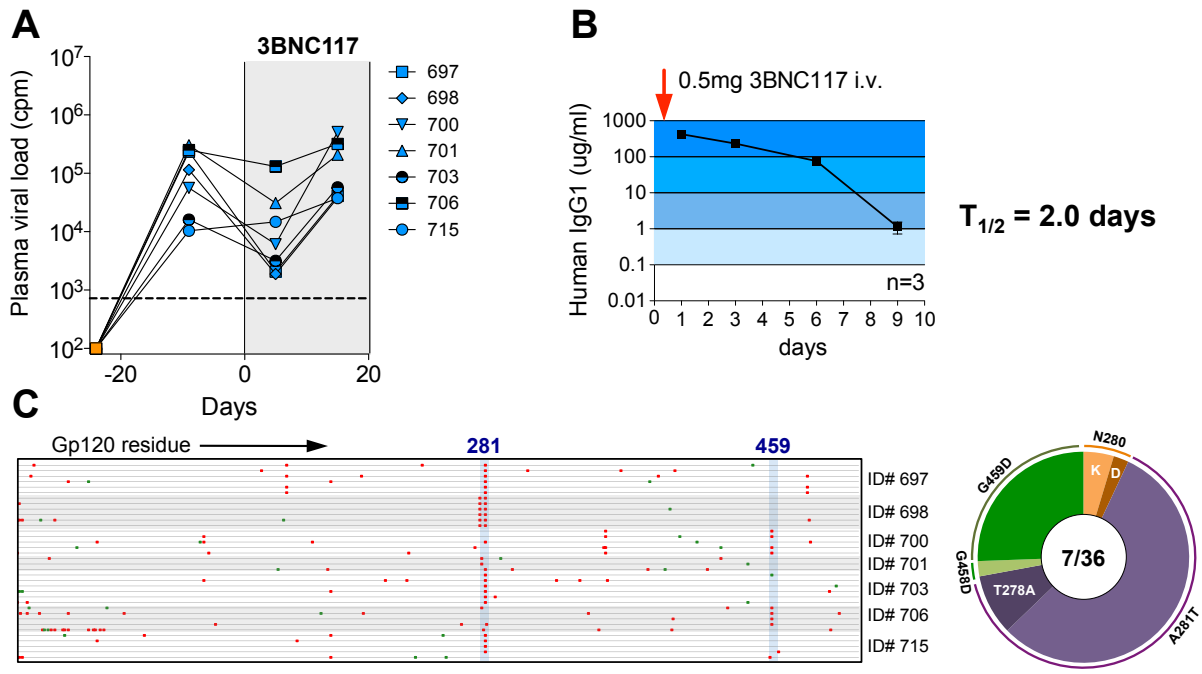

Figure 2.1: 3BNC117 elicits viral resistance at CD4bs residues.

A, Viral loads are transiently depressed by treatment of HIV-1_{YU2}-infected hu-mice with 3BNC117. *B*, Serum half-life of 3BNC117 in NRG mice, as in Fig. 1.5D. *C*, mutations identified in gp120 from 3BNC117-treated mice (in *A*). The profile of CD4bs mutations among all clones is shown at right, as in Fig. 1.6B.

An optimized bNAb tri-mix controls viremia and lowers cell-associated HIV-1 DNA

I previously found that treating HIV-1-infected hu-mice with a combination of five bNAbs suppressed viral loads in all treated animals. However, one antibody (3BC176) was found to be therapeutically ineffective, while another (PGT128) resulted in a less-restricted escape profile than a highly similar antibody (10-1074). Additionally, I opted to replace 45-46W with 3BNC117 because of its more favorable serum accumulation and similar viral resistance profile (Fig. 2.1). Thus, three antibodies were chosen that target three distinct viral epitopes and elicit three distinct restrictive viral escape pathways: PG16, 10-1074, and 3BNC117. Treatment of hu-mice with this new combination

resulted in strong viral load suppression in all animals (Fig. 2.2), as was previously found with the original penta-mix.

In addition to suppressing plasma viral loads, the optimized tri-mix also reduced levels of cell-associated HIV-1 DNA in peripheral blood (Fig. 2.2). DNA levels dropped by an average of 0.8 $\log_{10}$ HIV-1 DNA copies per million human PBMC over the six-week treatment period. This result stands in contrast to the limited effects of HAART on cell-associated DNA in humans, which may become reduced by 0.5-1 $\log_{10}$ HIV-1 DNA copies per million PBMC after more than a year on HAART(54). However, it should be noted that these experiments did not include untreated or ART-treated control animals, and a strong conclusion that the decline in cell-associated HIV-1 DNA is due to active clearance of infected cells by bNAbs cannot be made.

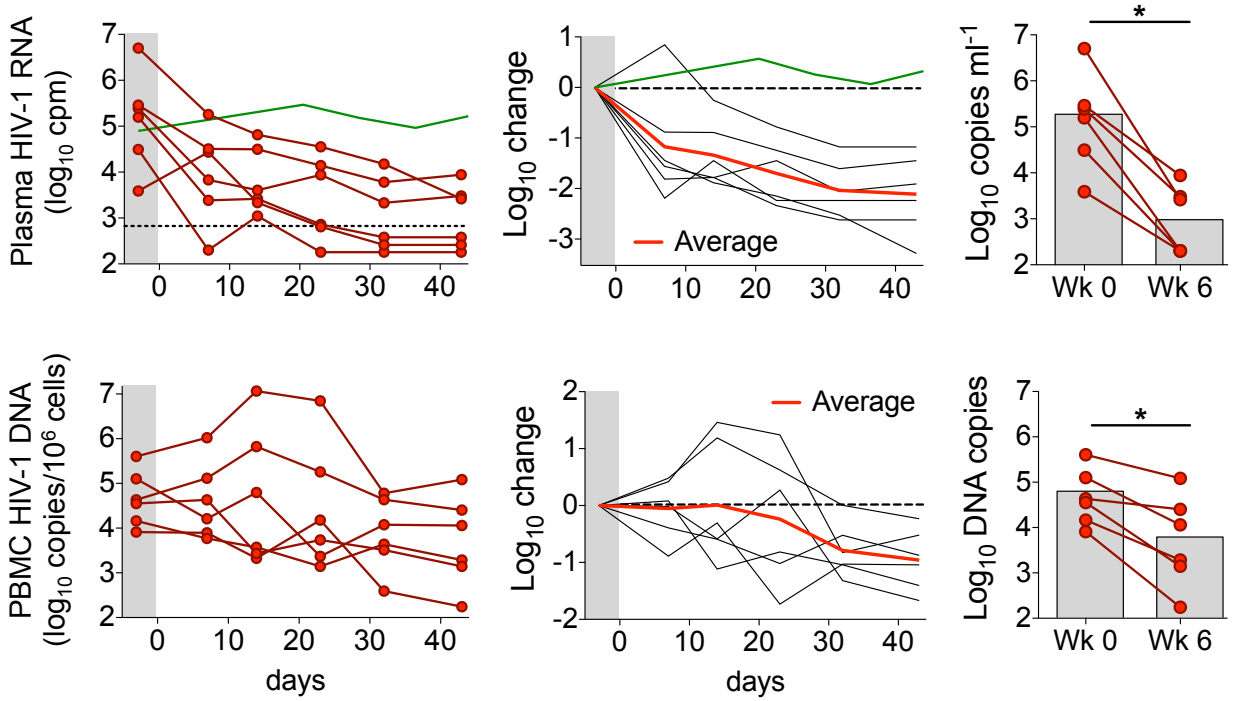

Figure 2.2: An optimized bNAb tri-mix suppresses viral load and lowers intracellular HIV-1 DNA.

Top, plasma viral loads of hu-mice treated with 3BNC117, PG16, and 10-1074. At left and right, absolute plasma viral loads at the indicated time points are shown; in the middle, the viral load change in logs over time (red line and green line reflect population averages of treated and untreated mice respectively, geometric mean). *Bottom,* intracellular HIV-1 DNA from PBMC of hu-mice at top. At left and right, absolute DNA copies per million PBMC at the indicated time points; in the middle, HIV-1 DNA load change in logs over time (red line, as in top-middle).

An oral ART regimen suppresses viral loads in hu-mice

As I sought to explore whether bNAbs could prevent viremic rebound in hu-mice already suppressed by ART, it was critical to develop a means of delivering ART drugs to hu-mice that would effectively suppress viral loads. Based on the work of previous groups(55, 56), I developed an oral ART regimen (cART) comprised of three drugs commonly used to treat HIV-1-infected humans: tenofovir disoproxil fumarate (TDF, 1.23 mg/animal p.o., Gilead); emtricitabine (FTC, 1.48 mg/animal p.o., Gilead); and raltegravir (RTV, 2.46 mg/animal p.o., Merck). Drugs were crushed into fine powder, suspended in sterile PBS, and administered daily by gavage to hu-mice (Fig. 2.3). In

contrast to untreated animals, viral loads in hu-mice treated for three weeks with cART dropped by an average of 2.0 $\log_{10}$ cpm (Fig. 2.3A). Withdrawal of cART resulted in immediate viral rebound to pre-treatment levels, which were sustained thereafter. To ensure that ART did not select for specific mutations in gp120 that might later confound bNAb treatment experiments, viral gp120 sequences were obtained from untreated and cART-treated mice (Fig. 2.3B). Fortunately, and expectedly, no cART-associated recurring mutations could be identified in gp120, validating that *env* is not under selection by cART. While viral clones revealed, on average, one consensus mutation per animal, none of the identified mutations would be expected to confer resistance to any of the bNAbs under study. Therefore, cART is a suitable means by which to suppress viral loads in hu-mice for the purposes of investigating the ability of bNAbs to prevent post-suppression viral rebound.

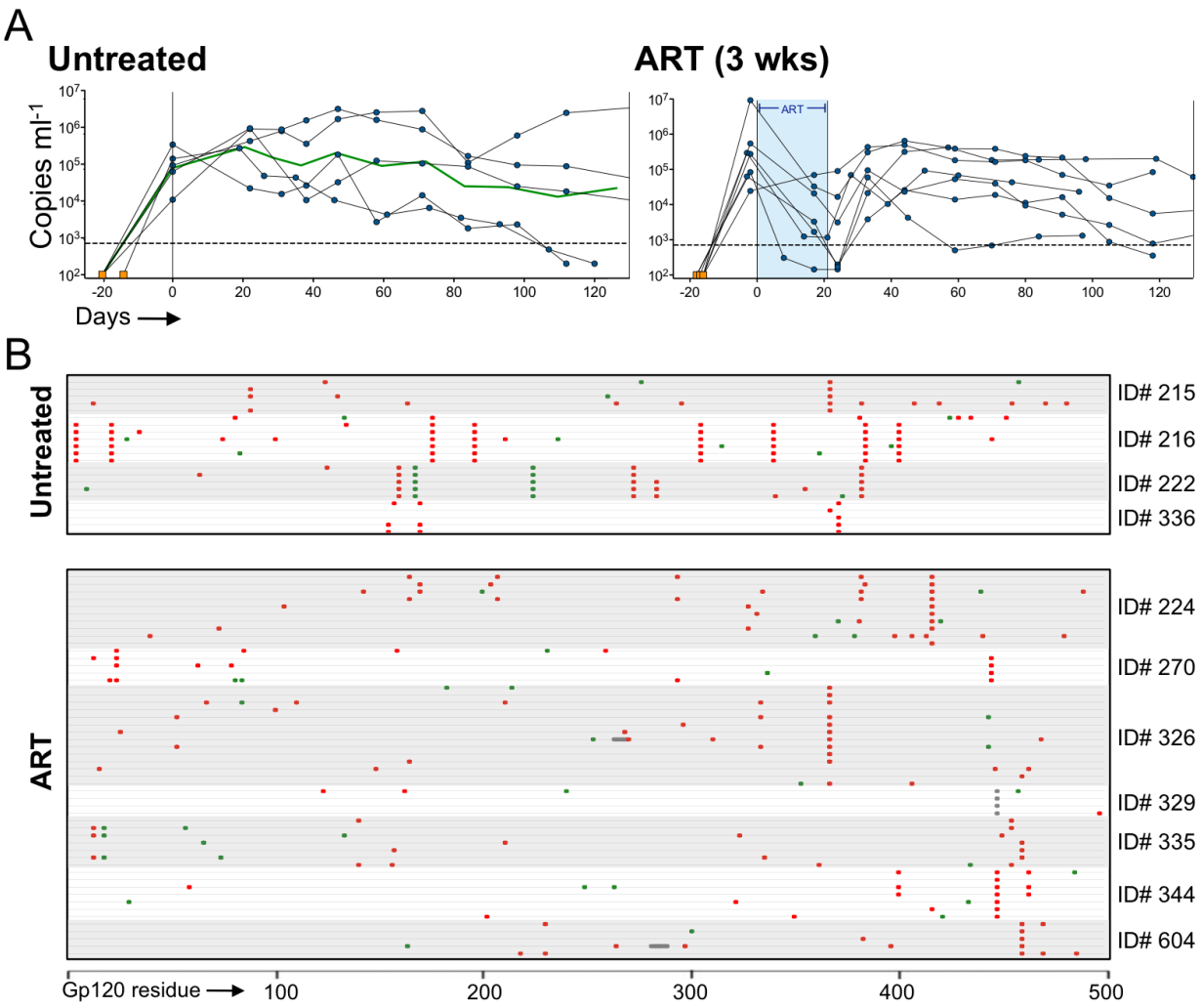

Figure 2.3: Daily oral cART rapidly lowers viral load in hu-mice.

A, plasma RNA viral loads in untreated (left) and cART-treated hu-mice over time. cART was administered by daily gavage during the time points shaded in blue. *B*, gp120 sequences from untreated (top) and cART-treated hu-mice following viral rebound.

Suppressing viral load reduces the likelihood of viral escape from bNAbs

It is understood that combinations of ART drugs with distinct antiviral mechanisms rapidly suppress viral loads in HIV-1-infected humans by requiring the simultaneous occurrence of viral strains resistant to all drugs used. Similarly, my work has shown that combinations of potent bNAbs targeting different viral epitopes suppress viral loads in hu-mice, while bNAb monotherapy rapidly selects for viral resistance. The

aforementioned experiments involving cART treatment of hu-mice showed that viral rebound occurs rapidly following withdrawal of cART, just as occurs in humans undergoing ART treatment interruption(57), suggesting that the viral reservoirs which persist despite suppressive ART are substantial. I therefore sought to determine whether suppression of active viremia, thereby reducing the total body load of HIV-1, has a measurable impact on the likelihood of viral escape from bNAbs. To answer this question, I suppressed HIV-1_{YU2}-infected hu-mice with cART, later adding a monoclonal bNAb and withdrawing cART (Fig. 2.4) to observe viral escape.

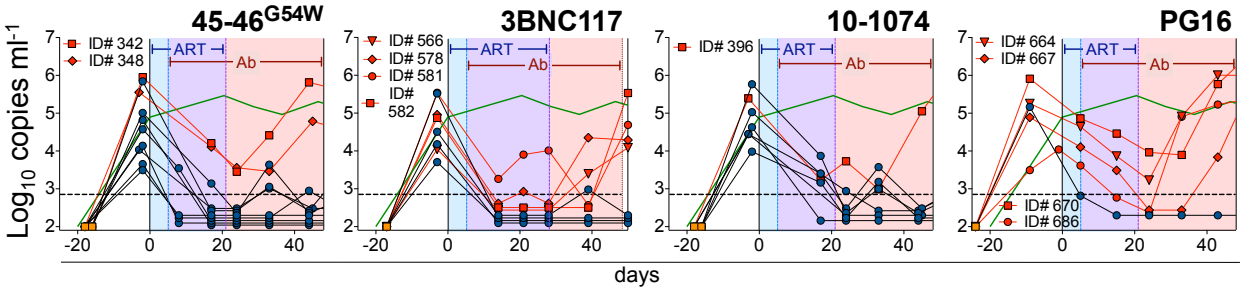

Figure 2.4: Individual bNAbs maintain virological suppression after ART withdrawal.

Viral loads are shown of hu-mice suppressed with cART, followed by withdrawal of cART in the presence of the indicated bNAb. cART treatment is shown in blue shading, cART plus the indicated bNAb in purple shading, and treatment with the indicated bNAb alone in red shading. Dark blue lines/symbols, mice that remain suppressed following cART withdrawal; red lines/symbols, mice that escape bNAb pressure following cART withdrawal; green line, population average of untreated animals at similar times post-infection.

Contrary to what had previously been observed in humans(26, 27), hu-mice treated with single bNAbs when withdrawn from cART largely remained suppressed under bNAb pressure. Of 10 mice treated with 45-46W, eight mice remained suppressed, as did four of eight mice treated with 3BNC117, seven of eight mice treated with 10-1074, and one of five mice treated with PG16. Of note, hu-mice with detectable viral loads above 10^3

cpm at time of cART withdrawal uniformly escaped bNAb pressure, as might have been expected from the aforementioned bNAb monotherapy experiments (Fig. 1.5). However, the vast majority of hu-mice that had viral loads below 10^3 cpm following cART withdrawal were successfully maintained on bNAb monotherapy (eight of eight 45-46W-treated animals, four of seven for 3BNC117, seven of seven for 10-1074, and one of three for PG16). These data suggest that bNAb monotherapy can successfully contain HIV-1 viremia once already suppressed (by ART, e.g.).

To verify that sustained virological suppression under bNAb monotherapy was not the result of intensification of the ART regimen prior to cART withdrawal, I conducted an experiment identical to that shown in Fig. 2.4 with 45-46W, with the following modification: 45-46W was used to intensify cART for two weeks, but was withdrawn coincident with cART withdrawal, and raltegravir monotherapy was maintained instead (Fig. 2.5). 45-46W was chosen for this experiment because all eight mice with undetectable viral loads after cART withdrawal remained suppressed on 45-46W monotherapy, and because its short half-life (Fig. 1.5D) would render continuation with raltegravir to be properly monotherapeutic. In contrast to hu-mice continuing with 45-46W monotherapy, which all remained suppressed, viremia in all hu-mice continuing on raltegravir monotherapy rapidly returned to baseline levels (Fig. 2.5).

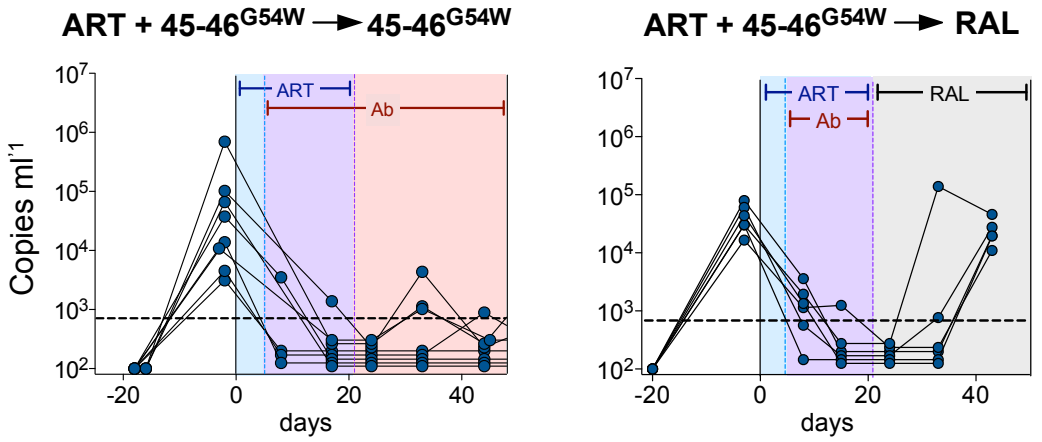

Figure 2.5: bNAb intensification of cART does not prevent viral rebound when stopped coincident with cART withdrawal.

Left, viral loads of cART-treated mice intensified with 45-46W and continued on 45-46W monotherapy following cART withdrawal (copied from Fig. 2.4). *Right,* cART-treated mice intensified with 45-46W and continued on raltegravir monotherapy following cART and 45-46W withdrawal.

To confirm that sustained virological suppression under bNAb monotherapy was, indeed, the result of bNAb pressure, I withdrew hu-mice (from Fig. 2.4) from bNAb therapy and followed them to observe viral rebound. As expected from earlier experiments (Fig. 1.12), in the vast majority of suppressed animals, viremia rebounded coincident with the disappearance of antibody from blood plasma (Fig. 2.6) at time points that were expected based upon antibody half-lives. The vast majority of viral rebound events occurred when antibody concentrations were low (<1 ug/ml) or undetectable, indicating that bNAb monotherapy was, indeed, responsible for the sustained virological suppression observed in these animals.

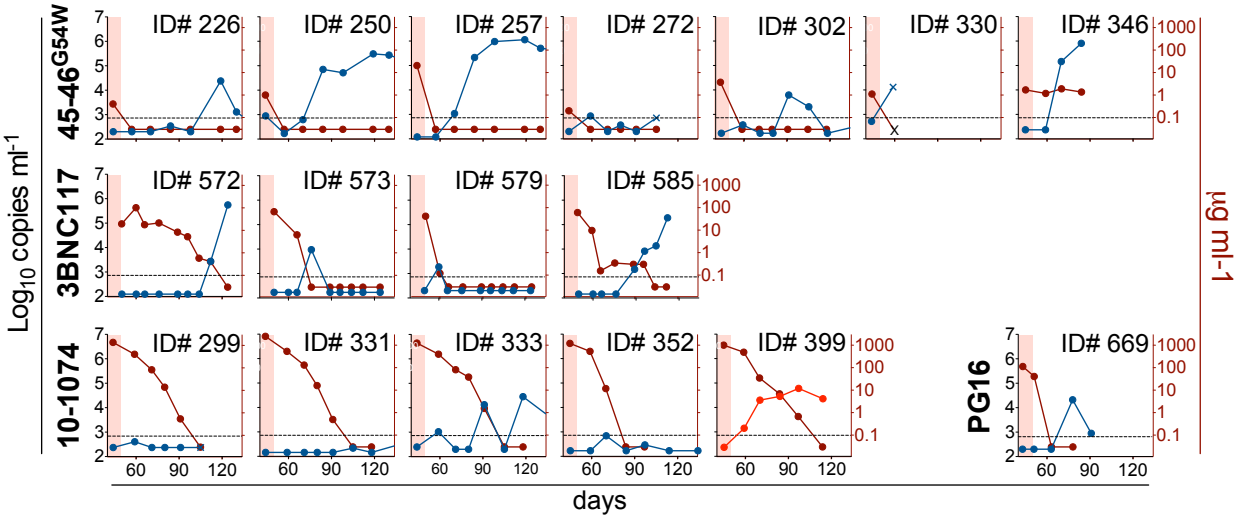

Figure 2.6: Viral rebound following bNAb monotherapy is coincident with bNAb decay.

Plasma viral loads (blue lines/symbols) and human IgG1 (maroon lines/symbols) are shown for hu-mice suppressed during bNAb monotherapy (from Fig. 2.4). Each plot reflects a single animal. X-axis reflects days since cART initiation. End of bNAb treatment is shown in red shading. Only in ID#399 did viremia rebound prior to antibody decay (viral load line/symbols shown in red).

To determine whether rebounding viruses remained sensitive to bNAb neutralization, I obtained gp120 sequences from animals that rebounded to detectable levels before and after antibody decay (Fig. 2.7). Expectedly, animals that rebounded during bNAb monotherapy carried signature resistance mutations to the respective bnAbs (Fig. 2.7A), as had been previously identified (Figs. 1.6, 2.1). In contrast, animals that rebounded after suppressive bNAb monotherapy did not harbor resistant viruses (Fig. 2.7B), with one exception (ID#399). These data are in line with previous observations from mice that were successfully suppressed by combinations of bNAbs (Figs. 1.12-13), whose rebounding viruses also did not carry signature resistance mutations. To verify that the sequences arising from animals rebounding after suppressive bNAb monotherapy indeed remained sensitive to the bNAbs, near-complete gp120 sequences were grafted into an HIV-1_{YU2} *env* pseudovirus vector (by direct cloning of the KpnI-MfeI region of

each viral gp120 clone into the respective restriction sites of pSVIII-HIV-1_{YU2}) and tested for neutralization by the respective bNAb used in treatment experiments for each animal (Fig. 2.7C). As a control, viruses from animals rebounding during bNAb monotherapy were also cloned and tested for neutralizing sensitivity. Expectedly, viruses that carried signature resistance mutations (arising during bNAb monotherapy) were highly resistant to bNAb neutralization, whereas those without signature mutations (arising after suppressive bNAb monotherapy) remained sensitive to neutralization.

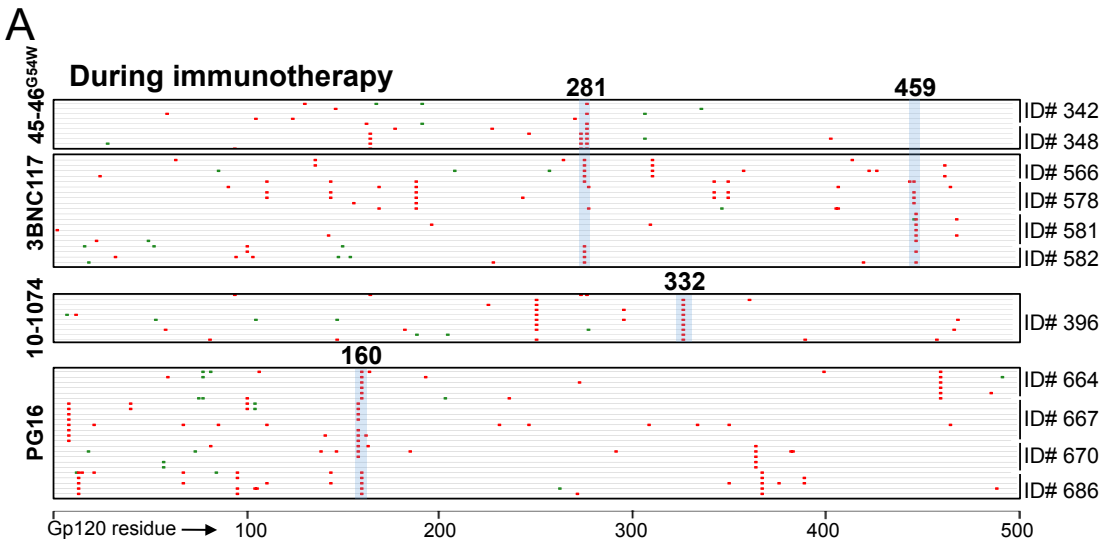

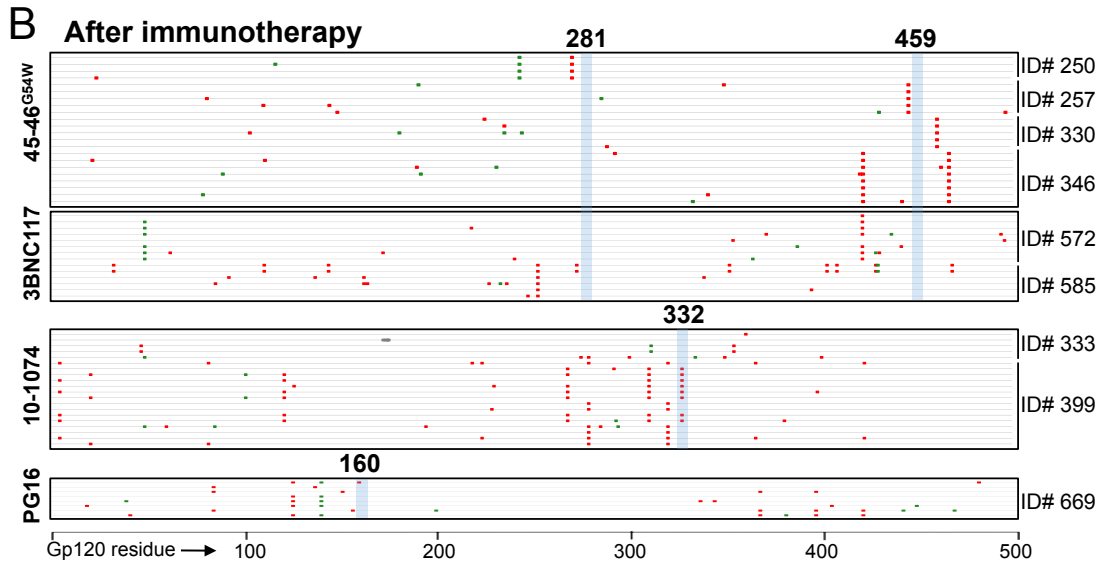

C

Rebound during bNAb therapy

Animal	IC_{50}	bNAb
ID# 342	5.067	*4546W*
ID# 348	>50	*4546W*
ID# 396	>50	*10-1074*
ID# 664	>50	*PG16*
ID# 566	>50	*3BNC117*
ID# 582	>50	*3BNC117*

Rebound after bNAb therapy

Animal	IC_{50}	bNAb
ID# 250	0.066	*4546W*
ID# 257	0.005	*4546W*
ID# 330	0.018	*4546W*
ID# 346	0.036	*4546W*
ID# 333	0.173	*10-1074*

Figure 2.7: Viruses from mice suppressed by bNAb monotherapy remain neutralization-sensitive.

Gp120 sequences from mice rebounding during bNAb monotherapy (*A,* Fig. 2.4, red lines/symbols) or after suppressive bNAb monotherapy (*B,* Fig. 2.4, 2.6) are shown. *C,* Neutralizing sensitivities of pseudoviruses derived from mice rebounding before or after bNAb monotherapy are shown. Box shading, as in Fig. 1.7.

Whereas individual bNAbs were fully unable to suppress established viremia and rapidly selected for resistant viruses (Figs. 1.5-7), these experiments showed that suppressing viral loads with cART prior to bNAb monotherapy enabled high rates of sustained virological control (Figs. 2.4-7). Taken together, these data show that suppressing viral loads (e.g. with cART) significantly improves the ability of bNAbs to control HIV-1 viremia *in vivo*, and suggest that bNAbs could effectively replace ART in HIV-1-infected humans who suffer from the burdens of daily ART.

Gene therapy enables durable virological control by individual bNAbs alone

My experiments thus far had demonstrated that administration of a single monoclonal bNAb to cART-suppressed hu-mice could maintain virological suppression when cART was withdrawn. However, this approach required constant administration of purified bNAb protein twice per week at high doses (0.5mg per injection). I hypothesized that repeated administration of antibody could be unnecessary if a gene therapy-based approach were possible that permitted stable antibody expression from a one-time intervention. Adeno-associated virus (AAV) vectors offered a promising solution to this problem: their genome size permits the insertion of a complete immunoglobulin gene that could be optimized for high stable expression in mice, and they exhibit a low immunogenicity profile both in mice and in humans(24, 58, 59). To determine whether an AAV-based gene therapy platform would support stable expression of bNAbs in hu-mice, bNAb-encoding AAVs were developed in collaboration with Dr. James Wilson at the University of Pennsylvania. I injected 10^{11} genomes of an AAV vector encoding

recombinant 3BNC117 (AAV-3BNC117) per animal intramuscularly into HIV-1_{YU2}-infected hu-mice (Fig. 2.8). 3BNC117 titers increased steadily until 21 days post-injection (Fig. 2.8A), as expected from previous studies(24) given the time required for AAV infection to establish a double-stranded episome capable of being transcribed. While titers were lower than those obtained by passive administration of 3BNC117 protein, which usually accumulated around 100 ug/ml (Figs. 2.1, 2.6), I found that the viruses in all mice harbored signature resistance mutations to 3BNC117 (Fig. 2.8B) bearing a high degree of similarity to those identified following passive bNAb monotherapy (Fig. 2.1). Interestingly, the overall profile of mutations observed in AAV-3BNC117 treated animals was noticeably more diverse than that of mice treated with passive 3BNC117 protein, which had higher serum accumulation. This likely reflects that a wider resistance profile is tolerated when serum 3BNC117 concentrations are low. In sum, a single injection of AAV-3BNC117 treatment led to durable 3BNC117 titers and imposed selective pressure on viral populations in hu-mice.

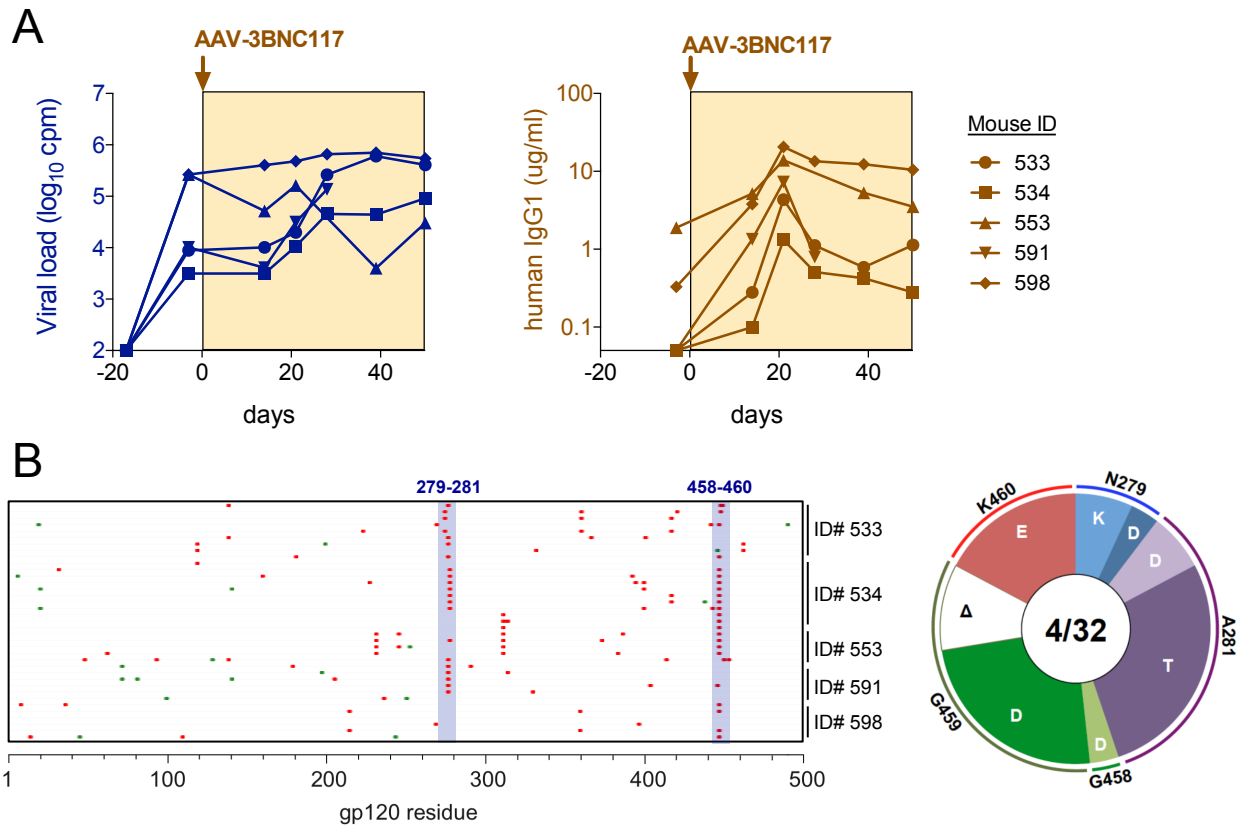

Figure 2.8: AAV-3BNC117 expresses 3BNC117 stably in hu-mice and selects for viral escape.

A, Viral loads of HIV-1_{YU2}-infected hu-mice treated at day 0 with AAV-3BNC117 (left) and gp120-binding human IgG1. *B*, gp120 sequences of mice after injection of AAV-3BNC117. Individual sequences from each animal (left) and the summary of amino acid changes in CD4bs residues are shown.

To determine whether AAV-expressed bNAbs could durably maintain virological suppression, as I had shown for passively administered bNAb protein, I conducted experiments in HIV-1_{YU2}-infected hu-mice combining cART viral load suppression with bNAb-encoding AAVs. Because of the need to wait three weeks before peak bNAb titers (Fig. 2.8), I administered AAV-3BNC117 two days after initiation of cART (Fig. 2.9). Unfortunately, expression levels of 3BNC117 21 days after AAV injection were significantly lower than titers obtained from injection of cART-naïve animals, with no detectable antibody in a majority of animals (Fig. 2.9A). (It is possible that this effect

may have been the direct result of some cART drugs interfering with AAV infectivity: the nucleotide analogue reverse-transcriptase inhibitor, TDF, has some reactivity with mammalian DNA polymerase, and may have impaired completion of the double-stranded AAV genome following AAV transduction.) For this reason, only animals with detectable plasma gp120-binding human IgG1 at 21d post-AAV injection were followed (Fig. 2.9B). cART was withdrawn in the presence of AAV-expressed 3BNC117, and viral loads and antibody titers were monitored over time. Three of five mice remained durably suppressed for more than 75 days after cART withdrawal, while two mice rebounded shortly following cART withdrawal (one of which had detectable viral loads at the time cART was withdrawn).

To validate that the durably suppressed animals were, indeed, controlled by bNAb expression (as opposed to being unable to support viremia due to loss of the human graft, e.g.), I challenged the two surviving mice with serum from mice carrying 3BNC117-resistant virus. Both mice rapidly became viremic upon re-challenge, demonstrating that control was conferred directly by AAV-3BNC117. Serum 3BNC117 titers in all five mice remained stable over the ~100-day observation period (Fig. 2.9C). Virus gp120 sequences from both mice that rebounded shortly following cART withdrawal confirmed the presence of 3BNC117 signature resistance mutations (Fig. 2.9D), and pseudoviruses derived from each animal confirmed their resistance to 3BNC117. Following reinfection of AAV-3BNC117-suppressed animals, re-emergent virus was sequenced and the presence of 3BNC117 resistance mutations from the re-infecting inoculum was confirmed (Fig 2.9E), validating that viral rebound post-

reinfection was, indeed, due to re-infection. Together, these data show that a single dose of AAV-3BNC117 can achieve stable titers in hu-mice and durably maintain virological suppression.

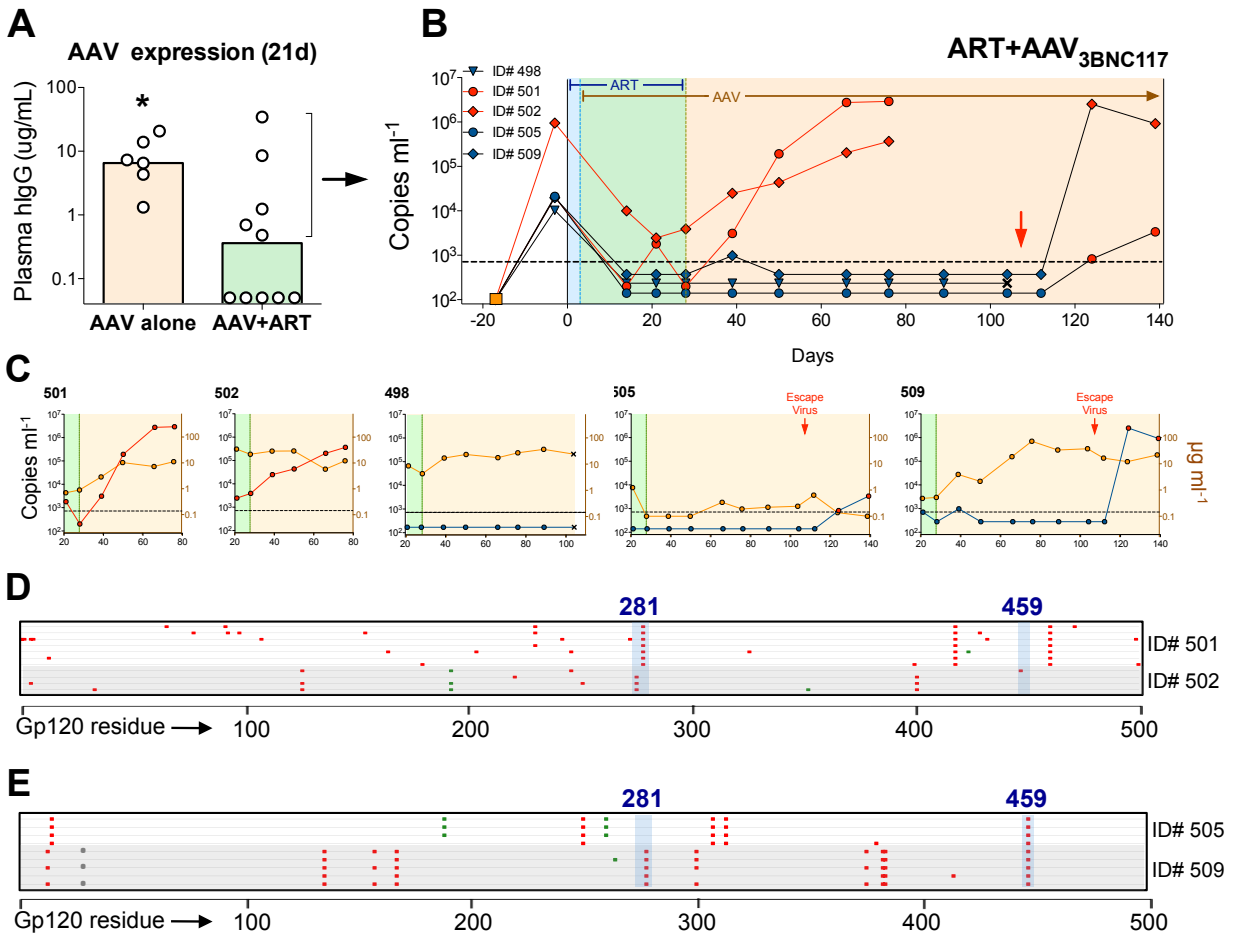

Figure 2.9: AAV-expressed 3BNC117 maintains stable titers and durably controls viremia.

A, Plasma gp120-binding human antibody titers in mice injected with a single dose of AAV-3BNC117 in the presence or absence of daily cART. *B*, Single-shot AAV-3BNC117 monotherapy following viremic suppression with cART. Blue shading, cART only; green shading, cART plus AAV-3BNC117; pink shading, AAV-3BNC117 only. Red arrow, point where mice were injected with 3BNC117-resistant virus. *C*, Viral loads (red or blue lines/symbols, left y-axis) and antibody titers (yellow lines/symbols, right y-axis) for each animal in *B* at the indicated number of days after starting cART (x-axis). *D*, gp120 sequences from the two animals that rebounded shortly after cART withdrawal. *E*, gp120 sequences from the two animals that were re-infected after prolonged viral suppression on AAV-3BNC117 monotherapy.

As cART unexpectedly impaired AAV transduction in hu-mice, I attempted an alternative approach to circumvent the need for AAV delivery during cART. To test whether an AAV vector encoding the bNAb 10-1074 could replicate the encouraging results I obtained for AAV-3BNC117, I first treated cART-suppressed mice passively with 10-1074 IgG (biotinylated for detection purposes) to bridge cART withdrawal before injecting AAV-10-1074 (Fig. 2.10). In this experiment, mice that remained viremic after cART withdrawal in the presence of passive 10-1074 were un-enrolled because of incomplete viremic suppression, and were not administered AAV-10-1074 (Fig. 2.10A). Passive 10-1074 administration was terminated following AAV-10-1074 injection, and the decay of passive 10-1074 IgG from plasma was measured (Fig. 2.10B). While precise quantitative results could not be obtained for biotinylated 10-1074 protein, the disappearance of a measurable signal by ELISA indicated the complete decay of passively administered protein by experiment day 80 in all animals, as would have been predicted based on the half-life of 10-1074 in hu-mice (Fig. 1.5D). Because total gp120-binding human IgG concentrations remained largely unchanged during this period, the antibody titers after experiment day 60 were assumed to reflect those of the AAV-derived 10-1074 antibody. A single injection of AAV-10-1074 produced high titers that were extremely stable, with many animals retaining titers in excess of 100 ug/ml 70 days after AAV injection.

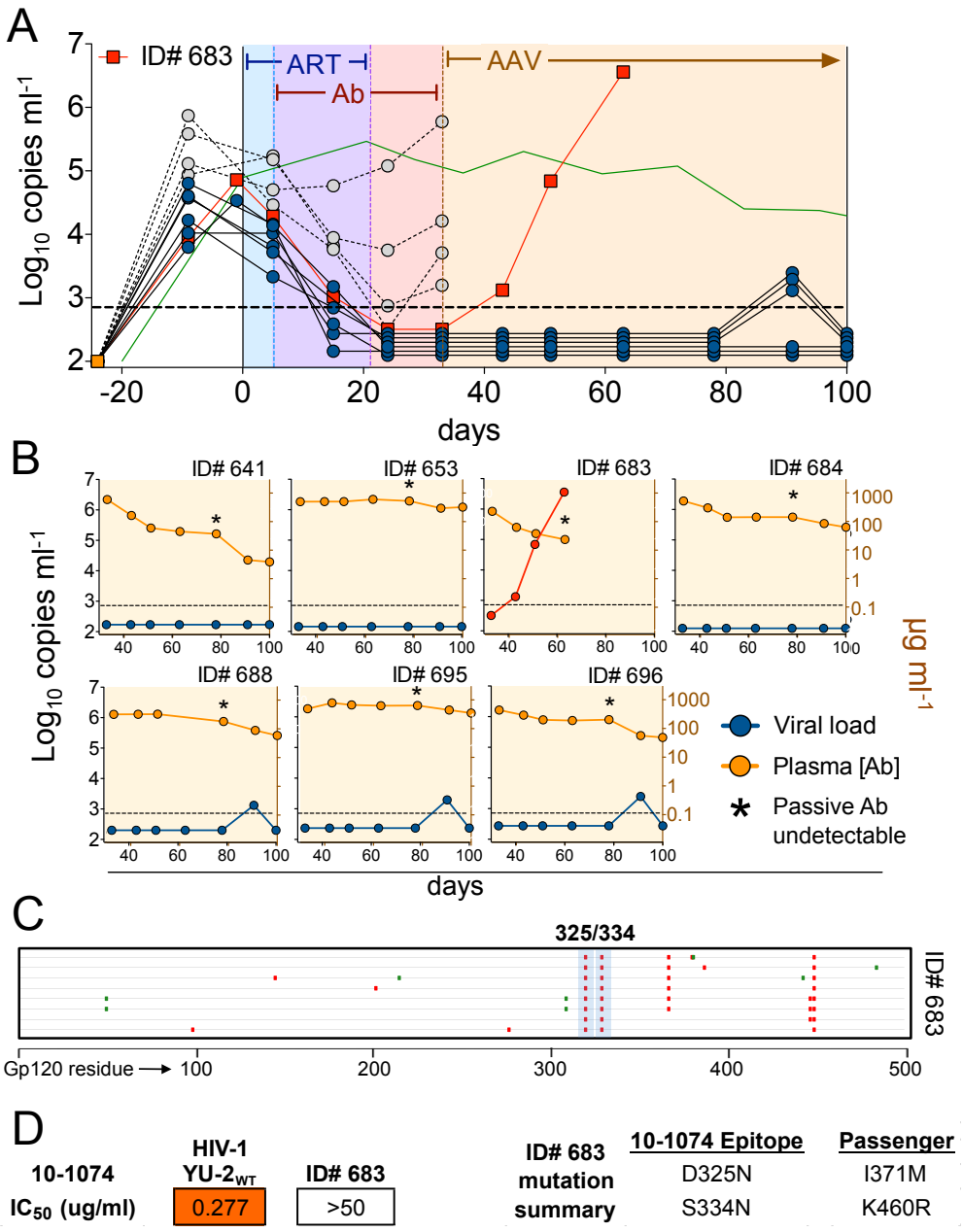

Figure 2.10: A single dose of AAV-10-1074 durably maintains virological suppression.

A, Viral loads in cART-suppressed hu-mice bridged with passive, biotinylated 10-1074 IgG prior to AAV-10-1074 injection (annotated as in Fig. 2.2). Dashed lines/gray symbols reflect mice that were un-enrolled due to measurable viral loads after passive 10-1074 administration; yellow shading, AAV-10-1074 monotherapy. *B*, viral loads and gp120-binding human IgG1 from individual mice (in A), annotated as indicated (ID#683, red line indicates viral load). *C*, gp120 sequences from ID#683 after viral rebound. *D*, Neutralization sensitivity and mutation summary of pseudovirus from ID#683 (in C) against 10-1074.

Of the seven animals that were injected with AAV-10-1074, only one animal rebounded during AAV-10-1074 monotherapy (ID#683), and gp120 sequences from that animal were found to harbor mutations that rendered the virus completely resistant to neutralization by 10-1074 (Fig. 2.10C, D). The remaining six mice receiving AAV-10-1074 remained suppressed for the duration of the experiment, despite receiving no further interventions after the single dose of AAV-10-1074. As these six animals failed to rebound after decay of the passively administered antibody, I concluded that a single injection of AAV-10-1074 durably sustained viremic control in six of seven animals. Together with the aforementioned results from AAV-3BNC117, these experiments demonstrate that AAV-driven expression of individual bNAbs can durably sustain virological control in cART-suppressed hu-mice.

In summary, the experiments conducted herein demonstrate that suppressing viral load can dramatically improve the ability of individual bNAbs to control HIV-1_{YU2} viremia as monotherapeutics in hu-mice. AAV-driven bNAb expression was as effective as passive bNAb monotherapy in achieving this virological control, and these experiments provide proof-of-concept support for the idea that bNAbs delivered by a gene therapy approach could comprise a single-shot, functional cure for HIV-1 infection.

CHAPTER III: 3BNC117 DELAYS VIRAL REBOUND IN HIV-1-INFECTED HUMANS DURING TREATMENT INTERRUPTION

I previously found that individual bNAbs could maintain virological suppression in hu-mice that were withdrawn from cART. To test whether similar effects could be observed in humans, we conducted a clinical trial to determine whether the bNAb 3BNC117 could maintain virological suppression in HIV-1 infected humans undergoing analytical treatment interruption (ATI) of their HAART regimen. 3BNC117 had previously been tested for safety in humans in a phase I clinical trial(60) and a single infusion of 3BNC117 antibody was well tolerated up to 30 mg/kg. In that study, viremic individuals were administered 3BNC117 at various doses. Pharmacokinetics, safety profile, and effects on viral load and neutralizing sensitivity to 3BNC117 were monitored. It was found that intravenous infusion of 3 - 30 mg/kg 3BNC117 transiently reduced viral loads, resulting in viral load rebound to pre-treatment levels within 3-5 weeks and selection for 3BNC117-resistant mutations. These results were in line with previous observations in both 3BNC117-treated, HIV-1-infected hu-mice (Chapter 1) and SHIV-infected macaques(61, 62). To determine whether multiple infusions of 3BNC117 would be safe in humans and could maintain virological suppression during ATI, we performed a phase IIa open-label trial.

HIV-1-infected patients were screened for neutralizing sensitivity to 3BNC117 by a bulk viral outgrowth assay (Fig. 3.1). Patients whose culture viruses had a 3BNC117 IC_{50} below 2.0 ug/ml in the TZM-bl assay were subsequently enrolled. Of 90 viral outgrowth

cultures from 85 patients screened, 11 (12%) were resistant to 3BNC117 (IC_{50} >20ug/ml) while 57 (63%) were highly sensitive (IC_{50} > 2ug/ml). By comparison, the same cultures assayed for sensitivity to the bNAbs 10-1074 and PG16 yielded 14% and 21% resistance, and 80% and 59% high sensitivity, to those respective antibodies.

			3BNC117		10-1074		PG16	
Culture	Virus ID	$TCID_{50}$/ml	IC50	IC80	IC50	IC80	IC50	IC80
1	B69D2	267,184	1.281	4.647	0.974	5.741	>50	>50
2	B73-13	2,795	0.102	0.288	0.024	0.084	0.023	0.077
3	B73-13/2	31,250	0.094	0.267	0.028	0.086	0.023	0.067
4	B74-13	69,877	0.542	1.622	0.062	0.198	0.023	<0.023
5	B76-14	3,655	2.331	8.516	>50	>50	>50	>50
6	B77	456,878	0.077	0.221	0.128	0.292	0.014	0.068
7	B80	6,679,594	0.248	0.908	0.126	0.366	>50	>50
8	B82	91,376	2.347	6.781	0.674	2.435	0.04	0.344
9	B88	6,679,594	0.904	3.111	3.551	23.522	4.533	>50
10	B89	39,493,845	3.189	11.365	0.825	2.223	9.81	>50
11	B92	13,471,913	6.625	27.427	0.658	1.768	0.012	0.106
12	B93	1,335,919	>50	>50	15.464	>50	1.318	>50
13	B96	3,906,250	0.415	1.116	0.096	0.268	0.721	45.948
14	B98	2,284,389	5.787	17.308	0.758	2.031	0.006	0.034
15	B99	781,250	0.387	1.430	0.330	0.919	>50	>50
16	B100	69,877	4.384	16.923	0.051	0.124	0.124	>50
17	B103	69,877	0.138	0.645	>50	>50	0.001	0.005
18	B104	31,250	0.237	0.843	>50	>50	0.053	36.619
19	B105	349,386	13.994	>50	0.537	1.816	0.022	0.324
20	B106	349,386	0.346	1.605	0.246	0.843	0.002	0.008
21	B107	2,284,389	>50	>50	0.732	2.024	>50	>50
22	B109	349,386	0.486	2.133	0.040	0.109	>50	>50
23	B112	349,386	0.355	1.206	0.299	0.982	>50	>50
24	B114	349,386	0.134	0.362	>50	>50	0.176	1.014
25	B114BV2	156,250	0.514	1.873	ND		ND	
26	B115	91,376	1.462	2.634	0.197	0.690	0.015	0.033
27	B116	1,746,928	3.652	12.244	26.072	>50	0.094	0.764
28	B119	1,746,928	0.525	2.418	0.089	0.410	6.672	>50
29	B123	18,275	0.269	0.768	0.152	0.346	0.291	7.603
30	B124	349,386	0.772	2.572	0.198	0.675	<0.001	0.003
31	B125	85,449	0.348	1.123	0.088	0.187	0.016	0.039
32	B127	349,386	0.857	7.362	0.043	0.101	>50	>50
33	B129	1,746,928	0.572	2.833	1.395	14.138	0.016	0.051
34	B130	1,746,928	1.989	5.285	>50	>50	0.027	0.303
35	B133	1,579,754	0.875	2.369	15.587	>50	0.269	6.092
36	B136	53,437	0.181	0.502	0.010	0.039	>50	>50
37	B139	1,746,928	0.499	3.380	0.044	0.493	9.192	>50
38	B140	597,441	0.239	1.032	0.175	0.739	0.004	0.014
39	B143	349,386	0.488	1.595	>50	>50	>50	>50
40	B144	156,250	0.139	0.456	0.132	0.426	0.005	0.017
41	B144AB	11,421,944	>50	>50	0.417	1.450	0.008	0.020
42	B148	456,878	1.142	3.043	0.521	1.373	0.014	0.087
43	B149	1,132,637	0.632	2.088	0.043	0.114	>50	>50
44	B121	69,877	>50	>50	ND		ND	
45	B123	18,275	0.269	0.768	0.152	0.346	0.291	7.603

			3BNC117		10-1074		PG16	
Culture	Virus ID	$TCID_{50}$/ml	IC50	IC80	IC50	IC80	IC50	IC80
46	B125	85,449	0.348	1.123	0.088	0.187	0.016	0.039
47	B148	456,878	1.142	3.043	0.521	1.373	0.014	0.087
48	B151	18,275	0.075	0.368	0.025	0.086	0.004	0.010
49	B152	69,877	0.154	0.417	0.012	0.034	0.008	0.342
50	B153	267,184	1.170	4.099	>50	>50	1.572	>50
51	B155	5,663,186	2.725	7.564	>50	>50	14.735	>50
52	B155-2	781,250	2.251	7.874	>50	>50	3.421	>50
53	B155BV2	1,132,637	3.843	8.731	ND		ND	
54	B156	31,250	>50	>50	ND		ND	
55	B161	69,877	0.158	0.538	0.500	3.408	0.103	4.989
56	B164	69,877	0.486	1.620	0.459	1.461	0.240	11.974
57	B165	156,250	0.385	0.750	ND		ND	
58	B166	69,877	0.185	0.404	ND		ND	
59	B167	91,376	>50	>50	0.489	2.574	3.220	>50
60	B168	53,437	35.349	>50	0.280	0.745	0.007	0.019
61	B169	91,376	4.989	15.443	>50	>50	0.008	0.069
62	B175	349,386	0.291	0.810	ND		ND	
63	B177	456,878	12.387	>50	ND		ND	
64	B183	13,975	15.489	>50	0.021	0.056	>50	>50
65	B184V2	6,250	0.187	0.667	0.043	0.118	0.202	>20
66	B185	156,250	1.839	5.152	ND		ND	
67	B191	349,386	2.508	7.031	ND		ND	
68	B193	10,687	12.007	>50	ND		ND	
69	B194	91,376	0.370	0.998	ND		ND	
70	B195	69,877	11.939	28.190	ND		ND	
71	B196A	349,386	>50	>50	ND		ND	
72	B196B	69,877	>50	>50	ND		ND	
73	B197	5,108,049	3.031	9.205	ND		ND	
74	B199	2,284,389	3.206	8.671	ND		ND	
75	B200	781,250	0.411	0.790	ND		ND	
76	B211	781,250	>20	>20	0.402	2.413	>20	>20
77	B212	69,877	0.655	2.207	0.390	1.304	1.504	>20
78	B214		0.941		0.130		0.071	
79	B219		0.417		1.257		7.569	
80	B220	31,250	3.423	10.461	0.083	0.222	>20	>20
81	B221	18,275	0.641	2.913	0.072	0.241	0.003	0.008
82	B224		0.385		0.022		0.007	
83	B226		6.001		0.198		0.011	
84	B228	91,376	>20	>20	0.084	0.293	0.003	0.029
85	B236	10,687	0.735	2.532	0.320	1.105	0.010	0.038
86	B244	53,437	0.315	1.063	1.174	4.106	13.120	>20
87	B248	781,250	>20	>20	0.355	0.981	>20	>20
88	B254	53,437	0.324	1.091	0.028	0.122	2.800	>20
89	B258	556,278	1.385	5.319	0.816	3.346	0.005	0.018
90	B266	33,397,968	0.927	3.324	0.399	1.395	0.366	>20

Figure 3.1: Patient screening for virus sensitivity to 3BNC117 neutralization in a TZM-bl assay.

Culture virus sensitivity (IC_{50} and IC_{80}) to the indicated bNAbs are shown. Cultures with 3BNC117 IC_{50}s < 2 ug/ml are shaded in dark orange, while cultures with IC_{50}s < 2 ug/ml to 10-1074 or PG16 are shaded in light orange. Samples that were not analyzed are marked “ND.”

Study design included two infusions, three weeks apart, with the first infusion given two days prior to starting ATI (Fig. 3.2). ATI was maintained until subjects received two consecutive viral load measurements > 200 cpm. In addition to having sensitive virus at the time of screening, subjects were enrolled on the basis of good heath, high CD4+ T-cell counts, and repeated viral load measurements < 20 cpm. Subjects whose ART

regimens included an NNRTI were switched to Dolutegravir four weeks prior to ATI because of the comparatively longer half-lives of NNRTIs. In total, eight subjects were enrolled, though two subjects were later excluded because their viral loads were not fully suppressed at the time the first infusion was given.

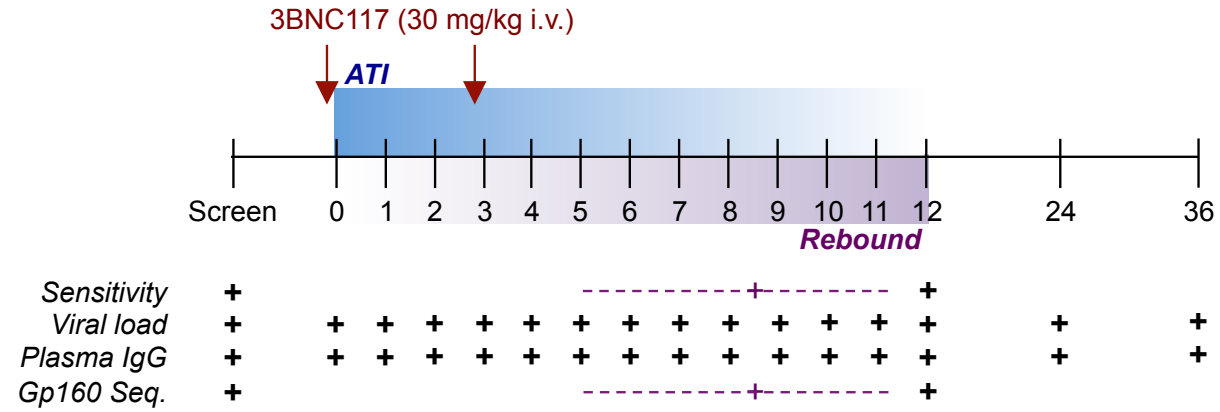

Figure 3.2: Study design and timeline.

Axis numbers indicate study week. ATI was initiated at week zero. Two infusions of 3BNC117 were administered three weeks apart, where indicated. Assays performed at each study time point are indicated with a "+" (dashed lines, purple crosshairs reflect assays conducted at time of viral rebound). Sensitivity was performed by bulk viral outgrowth culture of patient PBMC (as in Fig. 3.1). Viral load was measured from 1 ml EDTA-blood plasma by clinical assay. Plasma IgG concentrations of 3BNC117 were measured by an anti-idiotype ELISA to detect 3BNC117 (CellDex Pharmaceuticals). Gp160 sequencing was performed by single-genome amplification(63) of either culture supernatant or plasma virus, when possible.

Viral loads of all six subjects remained suppressed below 200 cpm during the first three weeks after the first infusion (Fig. 3.3). Viral loads remained suppressed until two to six weeks after the second infusion (study weeks 5-9), when plasma concentrations of 3BNC117 had declined well below peak levels (Fig. 3.3). Rebound occurred at plasma 3BNC117 concentrations ranging from 18.2 – 123.3 ug/ml, indicating that this may reflect the therapeutic threshold for 3BNC117-mediated viral suppression. These data

stand in stark contrast to results obtained in earlier clinical trials(26, 27), in which a combination of three first-generation bNAbs were unable to delay viral rebound during ATI in a majority of subjects.

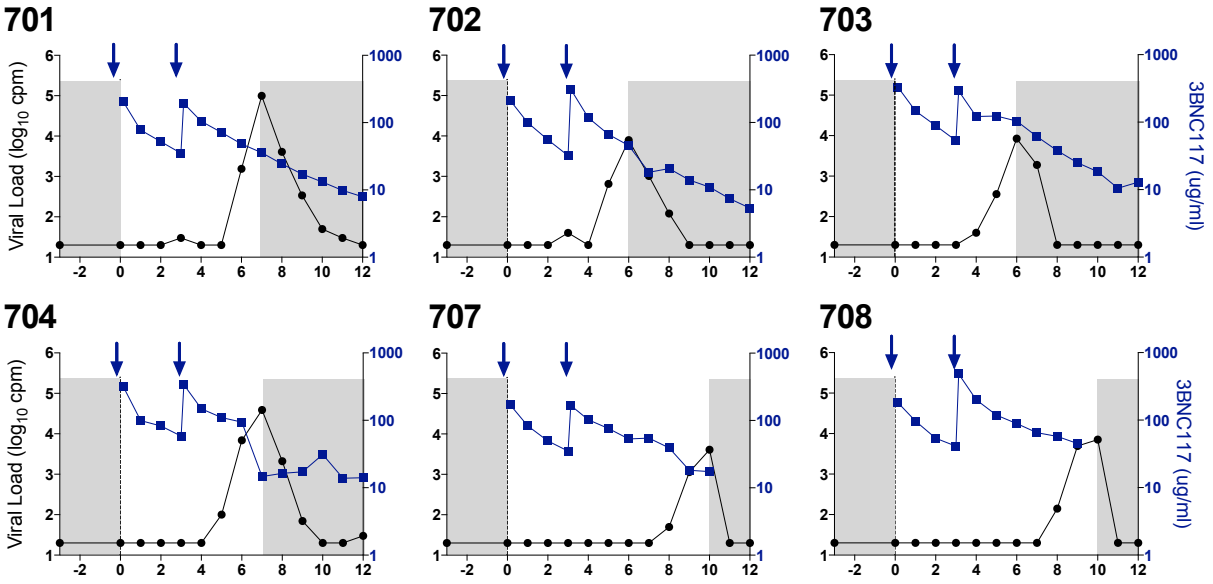

Figure 3.3: Viral loads and serum 3BNC117 titers in HIV-1-infected subjects during ATI.

Viral loads (black lines/symbols) and serum 3BNC117 titers (blue lines/symbols) for each of the six ATI subjects are shown (x-axis: weeks post-ATI). Gray shading indicates ART treatment before and after ATI; blue arrows indicate 3BNC117 infusions.

To determine whether viral rebound after 3BNC117 infusion was associated with viral resistance to 3BNC117, we cultured subject viruses before, during and after viral rebound, and assayed for 3BNC117 neutralization (Fig. 3.4). While moderate decreases in 3BNC117 neutralizing sensitivity were observed for most patients at the time of rebound (noted by an increase in 3BNC117 IC_{50}), sensitivities returned to baseline levels in nearly all cases after re-treatment with ART. On average, 3BNC117 neutralizing sensitivities were 6.2-fold higher at rebound than at baseline (geometric mean), but retained sensitivity < 5 ug/ml in all but one case (#708). These data

indicated that the rebounding viruses in 3BNC117-infused subjects were those against which low serum 3BNC117 titers were sub-therapeutic due to their reduced sensitivity.

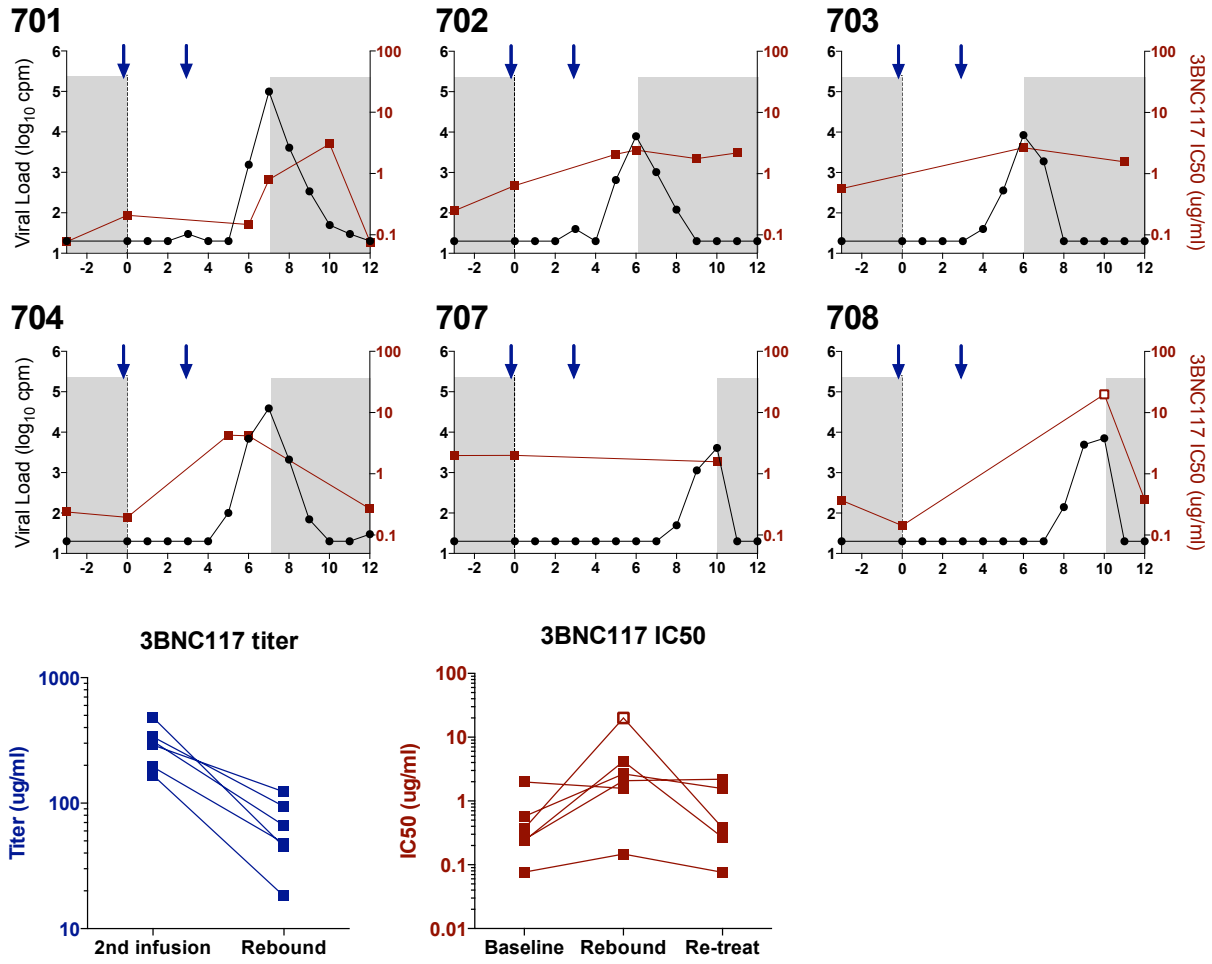

Figure 3.4: Moderate resistance to 3BNC117 is observed in subject viruses during rebound.

Top, viral loads (copied from Fig. 3.3) and cultured virus sensitivity to 3BNC117 (IC_{50}, red lines/symbols) are shown; open red symbol, IC_{50} >20 ug/ml. All other features as in Fig. 3.3. *Bottom,* summaries of subject 3BNC117 titers and cultured virus IC_{50}s at the indicated time points. Baseline was defined as either the screen or Week 0 time point; rebound was defined as any time point at which viral load exceeded 200 cpm; re-treat was defined as any time point after resuming ART when viral load was < 20 cpm.

To further evaluate whether rebounding viruses harbored resistance to 3BNC117, I sequenced plasma viruses at rebound and analyzed them for signature resistance mutations in gp160 (Figs. 3.5, 3.6). For comparison, sequences were also obtained

from viral cultures at screen or prior to 3BNC117 infusion for each subject. Whereas viral sequences from pre-treatment cultures uniformly clustered separately from viruses obtained in plasma sequences at rebound, plasma sequences from both rebound time points always clustered closely together and were highly clonal (Fig. 3.5). These data indicate that viral rebound was characterized by rapid expansion of a viral clone. Individual sequences were also analyzed for the presence of signature mutations known to confer resistance to 3BNC117 (Fig. 3.6). Clear mutations likely to confer resistance to 3BNC117 neutralization could be identified in three of six subjects: one mutation, A281D, arose in both #702 and #703, while R456S arose in #704. Other changes between pre-ATI and rebound viruses could be identified, but none that could be expected to confer resistance to 3BNC117.

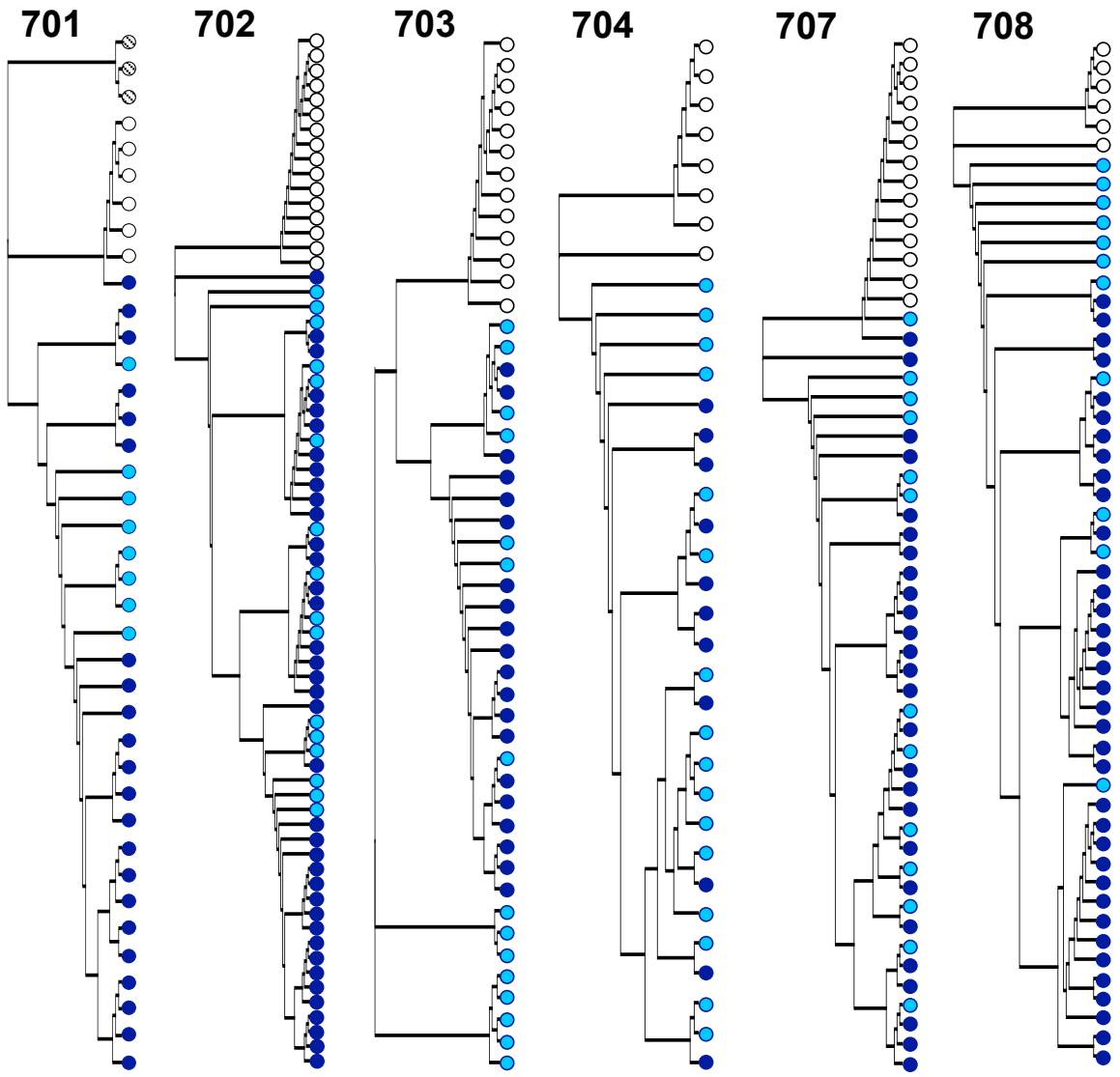

Figure 3.5: Viral gp160 sequences at rebound are different from those found before ATI.

Proportional alignment trees of gp160 sequences obtained by SGA for each subject before ATI and during viral rebound are shown. White circles, pre-ATI culture-derived sequences; light blue circles, early rebound plasma sequences; dark blue circles, late rebound plasma sequences.

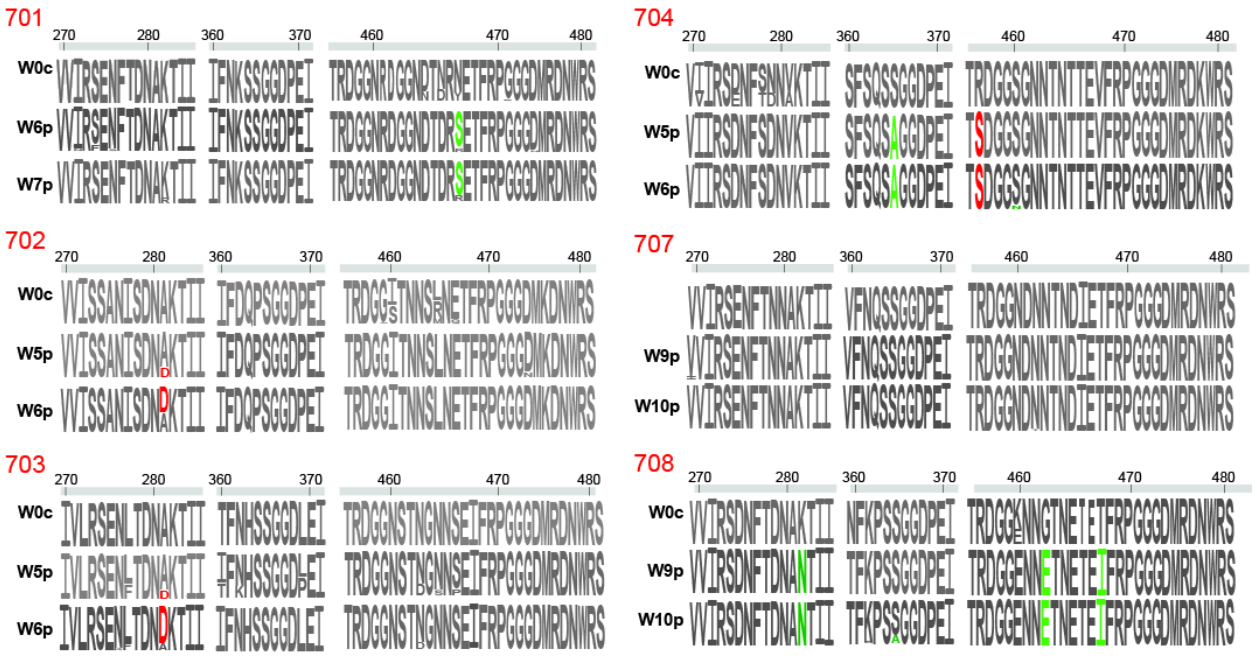

Figure 3.6: Signature 3BNC117 resistance mutations are rarely observed in plasma rebound virus.

Amino acid profiles of SGA sequences obtained for each subject's virus at the indicated time points are shown over regions known to be important for 3BNC117 neutralization. Where indicated at left, "c" reflects culture virus, while "p" reflects plasma virus. Signature resistance mutations arising during rebound are highlighted in red, while mutations arising that are not known to affect neutralizing sensitivity are in green.

Taken together, these data demonstrate that two infusions of 3BNC117 delayed virological rebound in all six patients. Rebound occurred when serum titers of 3BNC117 were low, and viruses at rebound exhibited only moderate viral resistance to 3BNC117 neutralization.

CHAPTER IV: A REPLICATION-COMPETENT, IN VIVO-ADAPTED HIV-1 REPORTER VIRUS

Design of a replication-competent HIV-1 reporter virus

My aforementioned experiments in hu-mice and humans uniformly encountered a common scenario in which HIV-1 viremia returns following withdrawal of suppressive therapy (or during suppressive therapy, if the outgrowing virus is resistant to that therapy). These events are understood to reflect the outgrowth of virus from spontaneously reactivated, latently HIV-1-infected cells (LICs, described in the introduction to this thesis). Because these cells are poorly understood, and as they comprise the major barrier to eradicating HIV-1 infection in humans, I sought to develop a means by which to identify and characterize LICs.

HIV-1$_{SV40HSA}$

To construct a replication-competent HIV-1 strain capable of reporting latent infection, I first modified the HIV-1$_{YU2}$ molecular clone (used in my hu-mice experiments) to carry a small transcription cassette decoupled from the viral promoter that would express a cell surface marker on any infected cell (latent or otherwise). This virus contained an SV40 virus immediate early promoter (SV40pro) upstream of a murine cell surface marker, CD24/heat-stable antigen (HSA), in between the *env* and *nef* open reading frames (Fig. 4.1A). Such a design was intended to constitutively label infected cells, such that LICs could be identified by HSA despite the absence of viral gene expression. The resulting recombinant strain, HIV-1$_{SV40HSA}$, produced well at high infectious titers and replicated in

human PBMC (Fig. 4.1B, C), albeit with reduced kinetics relative to the parental HIV-1_{YU2}. Expression of the heterologous marker, HSA, was robust and clearly labeled p24+ cells (Fig. 4.1D) by flow cytometry. Infection of seven hu-mice with HIV-$1_{SV40HSA}$ initially resulted in two animals becoming infected, but neither animal carried the intact reporter virus: the plasma virus from one animal (ID#802) had excised much of the SV40HSA cassette (as evidenced by RT-PCR spanning the *env-nef* region), while the second animal (ID#691) had no detectable HSA+ cells among p24+ cells in the spleen when sacrificed. The failure of five of seven animals to become infected at all, despite good humanization, was a clear and further indication that HIV-$1_{SV40HSA}$ was not able to replicate stably in vivo.

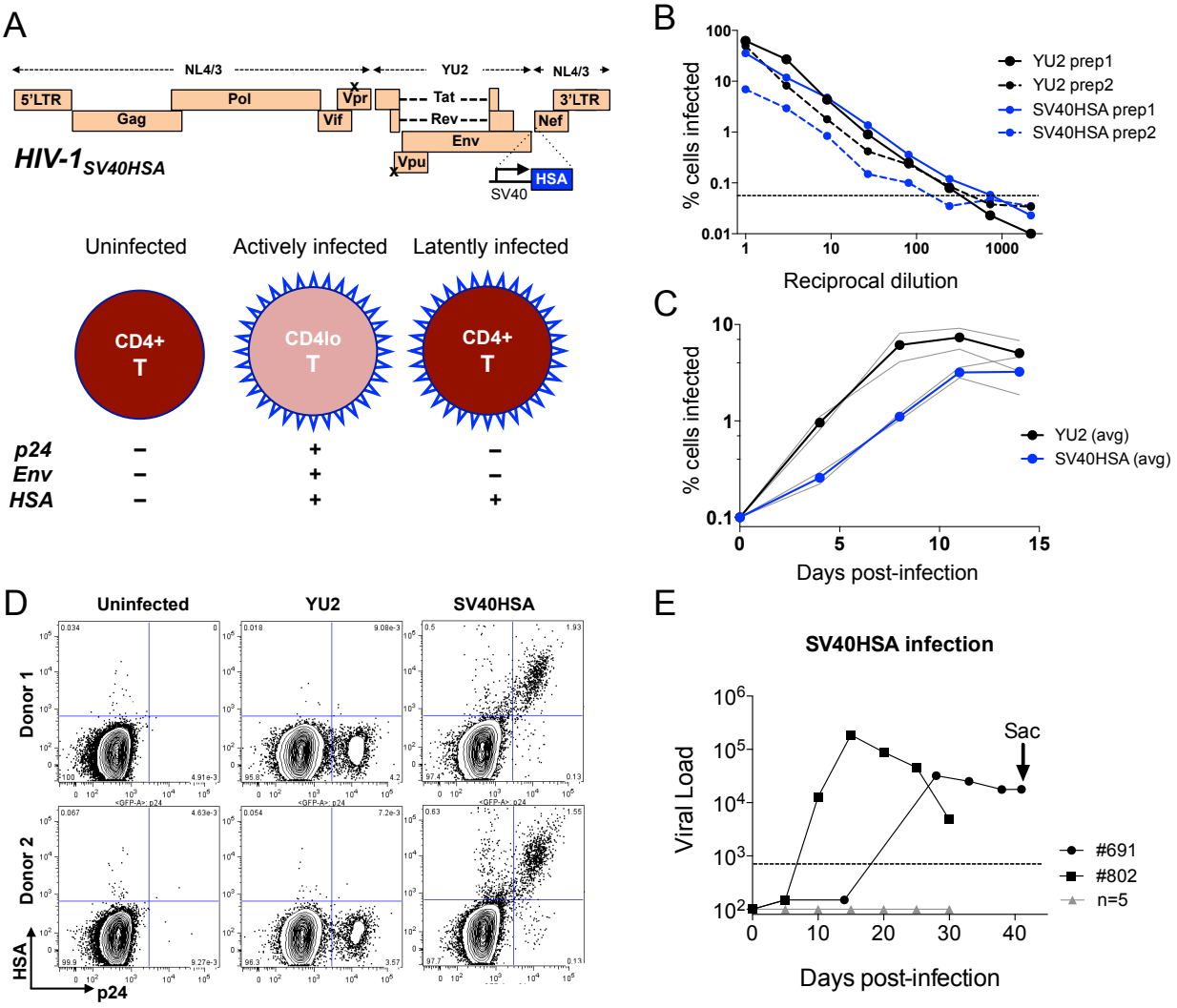

Figure 4.1: An HIV-1 reporter virus replicates in vitro, but does not establish viremia in vivo.

A, Schematic and design of an HIV-1 reporter virus, HIV-$1_{SV40HSA}$. At top, the recombinant HIV-1 viral genome with the SV40pro and HSA marker gene inserted as shown; at bottom, a summary of the viral and cellular markers anticipated upon HIV-$1_{SV40HSA}$ infection for identification of infected cells. *B*, Infectivity of two independent viral preparations of HIV-1_{YU2} (YU2) and HIV-$1_{SV40HSA}$ (SV40HSA) in a HeLa-based cell line capable of being infected by HIV-1. *C*, Infection spread in human PBMC challenged at day 0 with equivalent infectious titers of YU2 and SV40HSA. Average of two human PBMC donors infected in parallel are shown. *D*, Viral and recombinant marker expression in human PBMC (from *C*) eight days after infection with the indicated virus. *E*, Infection of hu-mice with HIV-$1_{SV40HSA}$. ID#691 was sacrificed at the indicated timepoint and splenocytes assayed for p24+ and HSA+ cells.

Improving the fitness of HIV-1$_{SV40HSA}$

To improve the replicative fitness of HIV-1$_{SV40HSA}$, I constructed a number of variants rationally designed to attempt enhancement of viral fitness (Table 4.1). For brevity, a simple description of the outcomes of each virus is provided. Viruses that could be produced at useful infectious titers were assayed for spread in a human acute lymphoblast CD4+ T-cell line (CEM.NKR.CCR5, NIH AIDS reagent program, hereafter CEMs) by tracking the percent of infected cells (by p24+ staining on flow cytometry) over time in the presence or absence of an HIV-1 protease inhibitor, indinavir sulfate (IS), to inhibit viral spread (Fig. 4.2). In this assay, CEMs were infected with equivalent titers of each virus (41 – 355 $TCID_{50}$/well) and assayed every three days for p24+ cells by flow cytometry. Spread was determined as the ratio of the frequency of p24+ cells in non-IS-treated and IS-treated conditions. Because CEMs rapidly spread infection, high-titer conditions did not always yield striking differences between viral variants, while low-titer conditions permitted strong separation of variants on the basis of spread fitness.

Table 4.1: List of reporter virus variants of HIV-1$_{SV40HSA}$ and their performance in vitro.

Variant name	Modification relative to HIV-1$_{SV40HSA}$	Infectivity	Marker expression	Virus spread
SV40HSA	(none)	+++	+++	+
vavHSA	human *vav* promoter replacing SV40pro	+++	-	n/d
SV40HSA_SA	splice acceptor added after HSA	+++	+++	+
SV40HSArev	SV40HSA in antisense	-	n/d	n/d
SV40HSApArev	SV40HSA with poly-A signal, in antisense	-	n/d	n/d
SV40HSA(dVprHA)	Additional marker for LTR expression in *vpr*	++	+++/+++	-
dVpr(SV40HSA)	SV40HSA cassette relocated to *vpr*	+++	+	n/d
SV40HSA(TM2)	YU2 *env* triple-bNAb escape mutant	(+)	n/d	n/d
SV40HSA_UbiNef	Nef ORF fused to HSA with Ubi cleavage site	+++	++	+
SV40HSA_Vpu+	Vpu ORF restored by replacement of ATG	+++	+++	-
89.6_SV40HSA	YU2 *env* swapped for dual-tropic 89.6 *env*	-	n/d	n/d
Q23_SV40HSA*	YU2 *env* swapped for Q23.17 *env*	+++	++++	+++

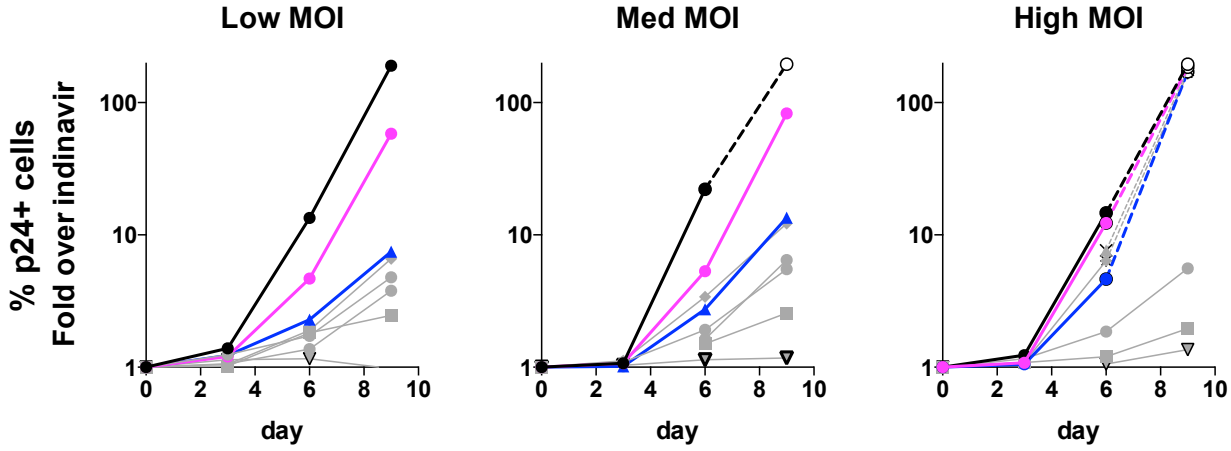

Figure 4.2: Infection spread of HIV-$1_{SV40HSA}$ variants in CEM.NKR.CCR5 cells.

Results from one of two identical experiments is shown (data points are the average of duplicate experimental replicates). Y-axis reflects the ratio of p24+ cells in non-indinavir sulfate-treated and indinavir sulfate-treated cultures. Black lines/symbols, wild-type HIV-1_{YU2}; blue lines/symbols, HIV-$1_{SV40HSA}$; pink lines/symbols, Q23_SV40HSA; gray lines/symbols, other variants (from Table 4.1) performing worse than or equivalent to HIV-$1_{SV40HSA}$. Dashed lines/open circles reflect points at which data could not be reliably obtained due to depletion of culture cells by viral cytopathic effects. Results from this assay are summarized in Table 4.1 under "Virus spread."

Of all variants tested, none replicated with enhanced fitness relative to the original HIV-$1_{SV40HSA}$ except for one virus bearing a different *env* gene, from the strain Q23.17 (Q23_SV40HSA). As this virus was found to spread significantly better than HIV-$1_{SV40HSA,}$ and with near-wild type kinetics, I sought to determine the mechanisms responsible for this enhancement. It was particularly curious that swapping the viral *env* gene would have such dramatic effects on spread, as the original HIV-$1_{SV40HSA}$ bearing the YU2 *env* gene did not appear to exhibit defects in infectivity. However, the HIV-1 *env* gene contains numerous features beyond the Gp160 open reading frame that may impact replicative fitness: in particular, the second exons for genes *tat* and *rev,* a splice site critical for their expression, and a *rev*-responsive DNA element, are all encoded within a small region of gp41. Therefore, a variant of HIV-$1_{SV40HSA}$ was constructed

bearing the original YU2 *env* gene, but in which a 432bp segment of gp41 spanning the AleI/BamHI sites was replaced with the Q23.17 sequence [YU2(Q23)_SV40HSA]. This minimal segment was sufficient to confer all of the enhanced replicative capacity of the full Q23.17 *env* gene, but in the context of a predominantly YU2-based *env* (Fig. 4.3).

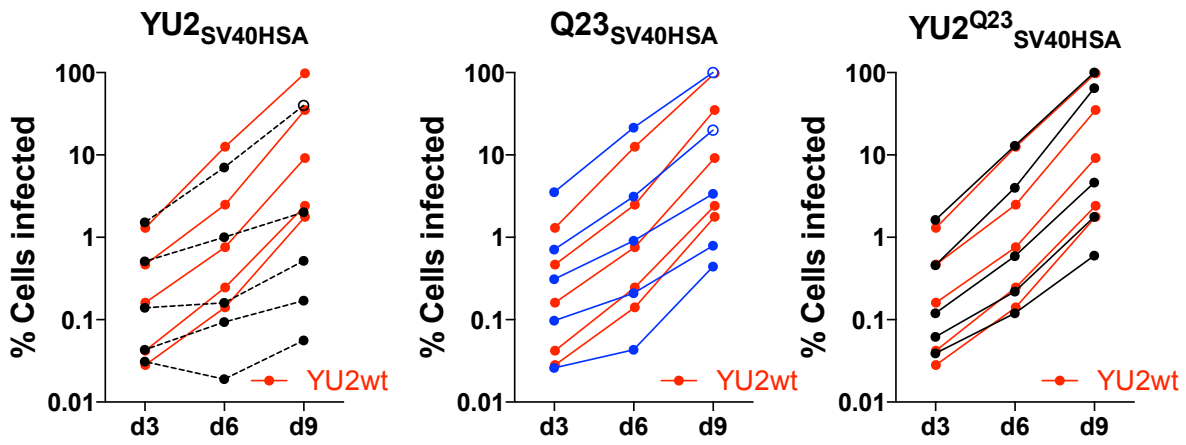

Figure 4.3: Grafting a gp41 fragment from Q23.17 onto YU2 confers remarkable spread fitness.

Virus spread in CEMs infected at a range of titers is shown as the % p24+ cells at each time point. Open circles indicate points at which extensive viral cytopathic effects prevented reliable data collection. Dashed black lines/symbols: HIV-$1_{SV40HSA}$; blue lines/symbols, Q23_SV40HSA; solid black lines/symbols, YU2(Q23)_SV40HSA. The wild-type HIV-1_{YU2} is underlaid on each graph as a reference.

HIV-1_{IL16HA}

Further modifications included evaluation of different minimal promoter sequences to optimize heterologous marker expression, as well as replacement of the HSA ectodomain with an influenza haemagglutinin tag (HA)(64), to reduce background staining. For brevity, a summary of the respective variants tested is provided (Table 4.2). An optimized virus was identified, HIV-1_{IL16HA}, that exhibited both strong replicative fitness and high marker expression in vitro (Fig. 4.4).

Table 4.2: Modifications of YU2(Q23)$_{SV40HSA}$ to improve marker expression and staining.

Variant name	Modification relative to YU2(Q23)$_{SV40HSA}$	Infectivity	Marker expression	Virus spread
YU2/Q23_SV40HSA	(none)	+++	++++	+++
YU2/Q23_SV40HA	HSA ectodomain replaced with HA-tag	+++	+++	+++
YU2/Q23_CD4HA	SV40pro replaced with minimal CD4 promoter	+++	++	+++
YU2/Q23_IL16f.HA	SV40pro replaced with full IL16 promoter	+++	++++	n/d
YU2/Q23_IL16s.HA*	SV40pro replaced with minimal IL16 promoter	+++	++++	+++

*This virus later re-named "HIV-1$_{IL16HA}$"

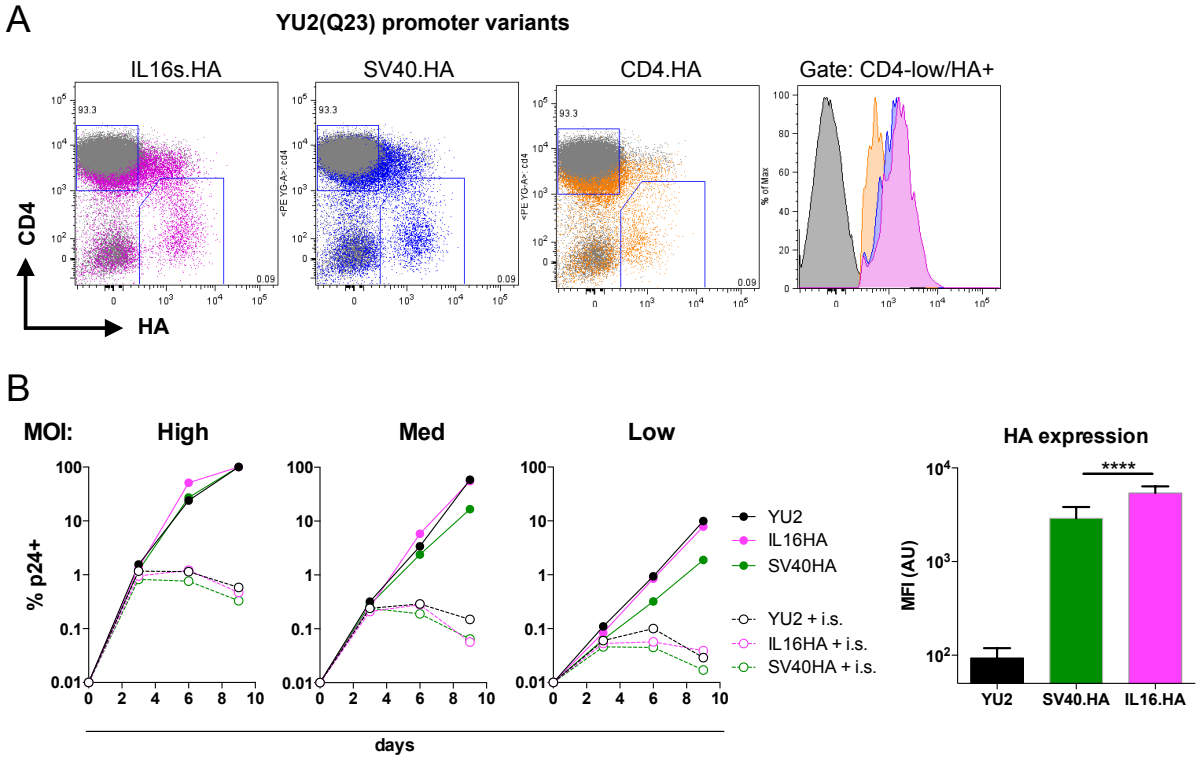

Figure 4.4: Replacing SV40pro with a minimal human IL-16 promoter enhances marker expression.

A, In vitro infection of human PBMC with the indicated YU2(Q23) promoter variant. Uninfected cells are shown in gray. Histogram populations are gated on CD4-low/HA+ (except for uninfected controls, gated on CD4+/HA-). *B*, At left, viral spread in CEMs (% p24+ cells at each time point are shown, for both non-IS-treated and IS-treated conditions). At right, HA expression (MFI) of p24+ CEMs infected with the indicated YU2(Q23) promoter variant (or wild-type HIV-1$_{YU2}$). Bars reflect averages of five cultures each.

An in vivo-adapted HIV-1$_{IL16HA}$

To determine whether HIV-1$_{IL16HA}$ was capable of launching stable viremia in hu-mice, I infected mice with either a high-titer virus prep of HIV-1$_{IL16HA}$ or cells from a culture of human PBMC highly infected with the same virus (Fig 4.5). All animals became viremic five days after infection, but at low viral loads (Fig. 4.5A). Viral loads failed to increase after two to three weeks of infection. To validate that the originating virus, indeed, replicated stably in the animals, infected animals were sacrificed and splenocytes assayed for infection. 10% of cells were assayed by flow cytometry for the presence of HA+ cells, while the remaining 90% were added to viral outgrowth cultures. While extremely few HA+ cells could be observed in the spleens directly (data not shown), viral outgrowth cultures revealed that the viruses in some animals largely retained expression of the HA marker (Fig. 4.5B), signifying that the low-level viral replication in these animals faithfully maintained the recombinant reporter cassette.

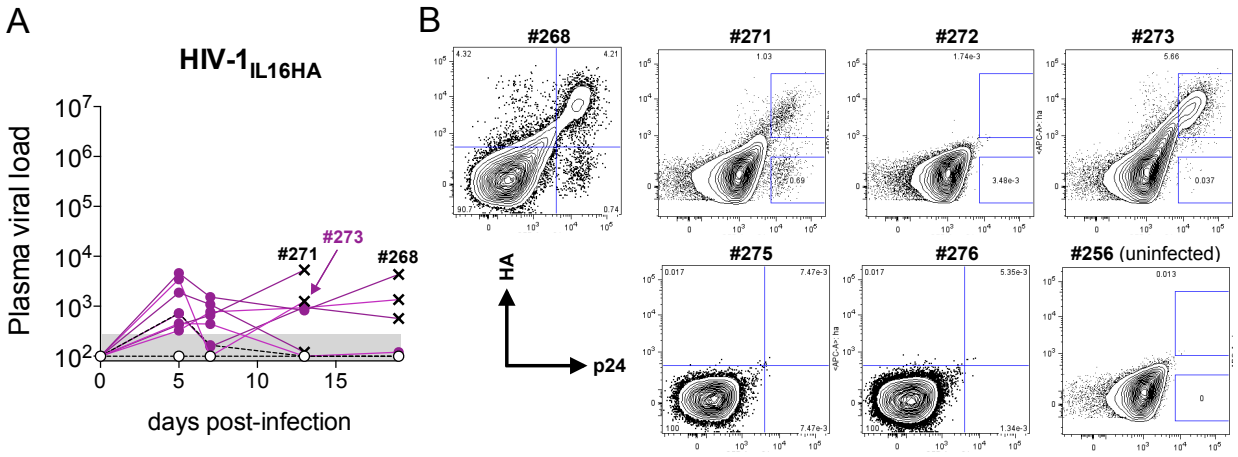

Figure 4.5: HIV-1$_{IL16HA}$ stably replicates at low levels in hu-mice.

A, viral loads in HIV-1$_{IL16HA}$-infected animals. Mice were sacrificed where "X"-marks are indicated; mice with positive outgrowth cultures (*B*) are identified. *B*, spleen viral outgrowth cultures from the indicated animals after 1-2 weeks of co-culture.

As the intact outgrown virus from HIV-1_{IL16HA} infected animals may have acquired adaptive mutations that could enhance replicative fitness in vivo, I attempted serial passaging of the virus in hu-mice (Fig. 4.6). Cultured cells from the splenic outgrowth culture of ID#273 were injected intravenously into four animals (P1 mice), and viral loads were monitored. All animals became viremic, with viral loads steadily climbing to peak levels by three weeks post-infection. Mice were sacrificed and spleens analyzed for the presence of HA+ cells, this time revealing clear populations of infected cells (Fig. 4.6B). Animals had varying degrees of retention of the HA reporter, with ID#283 being the most intact. Interestingly, the HA+ cells in splenic outgrowth cultures from these animals were CD4-high (unlike the majority of cells infected with either HIV-1_{IL16HA} or the parental ID#273 virus), providing further evidence of viral evolution (Fig. 4.6C).

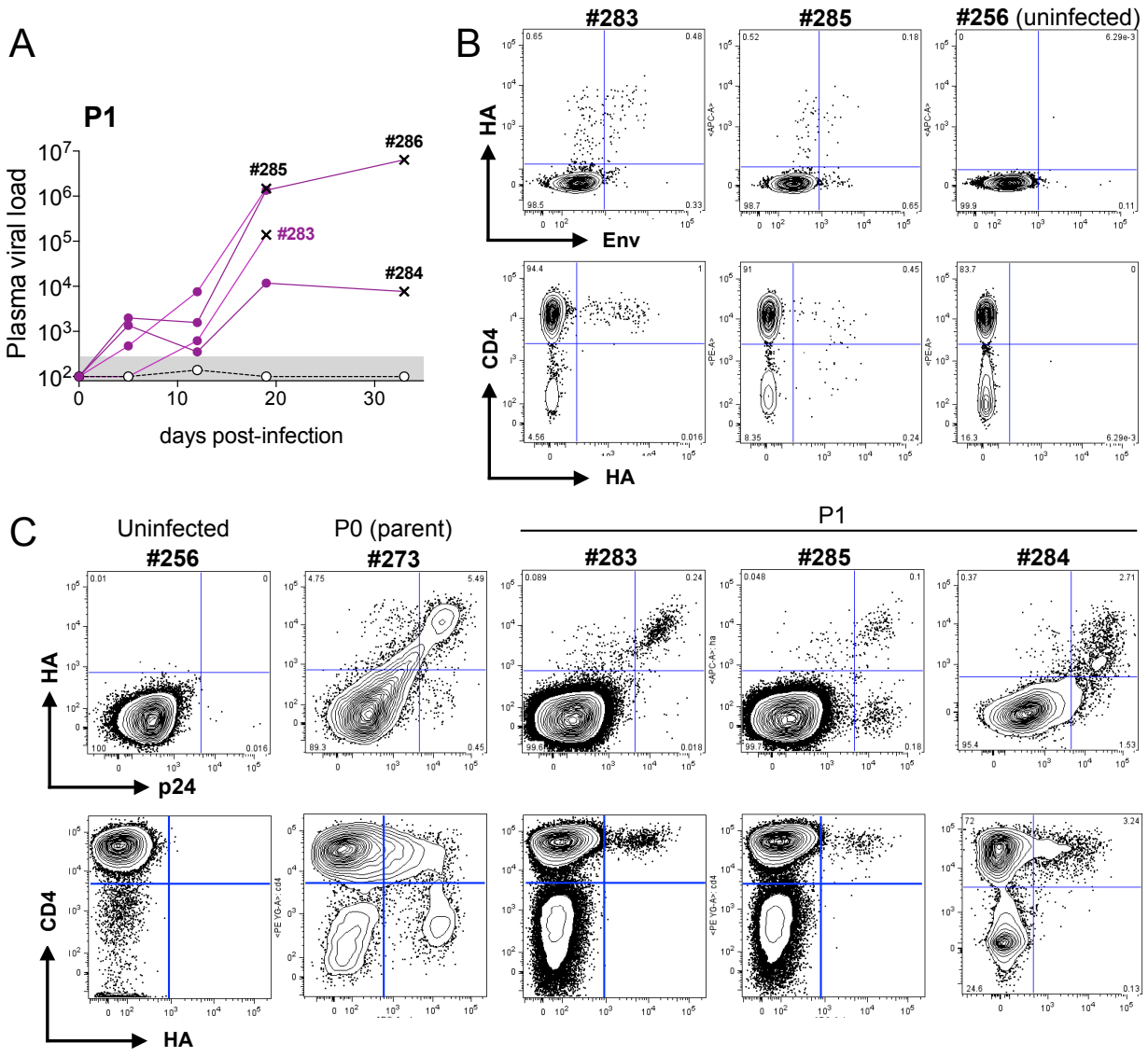

Figure 4.6: Passaging HIV-1_{IL16HA} in vivo results in higher viral loads.

A, Viral loads of hu-mice infected with virus outgrown from ID#273 (P1 mice). Animal IDs are indicated. *B*, Spleen cells stained for HA, Env, and CD4 by flow cytometry (gated on CD3+/CD8-/mCD45-/live). *C*, Viral outgrowth cultures from bulk splenocytes (in *B*) of P1 mice after 1-2 weeks of co-culture. As a reference, the outgrowth culture from the parental virus, ID#273, is shown along with an uninfected mouse outgrowth culture.

The ID#283 virus grown in splenic outgrowth culture was again passaged in new animals (by intra-peritoneal injection), resulting in high level viremia in ID#300 three weeks after infection (Fig. 4.7A). Sacrifice revealed that the HA reporter remained intact

among infected ID#300 splenocytes (Fig. 4.7B), indicating that the viral species circulating in that animal carried adaptive mutations that permitted both high viral loads and stable retention of the HA reporter in hu-mice. To determine whether the ID#300 virus had improved over the ID#283 virus, I infected new animals intravenously with cultured cells highly infected with supernatant harvested from splenic outgrowth cultures of each virus (Fig. 4.7C, D). Eight days after infection, nearly all animals infected with either virus had high viral loads $>10^4$ cpm, and HA+ cells could be clearly seen in the PBMC of some animals. Animals infected with the ID#300 virus had significantly higher viral loads than those infected with the ID#283 virus, indicating that further adaptation rendered the ID#300 virus more infectious in hu-mice. Of note, HA+ cells in the ID#300 culture appeared to regain some ability to down-regulate CD4, indicating continuing evolution over the ID#283 virus. To preserve the adapted virus from ID#300 for experimentation, the ID#300 splenic outgrowth culture was expanded and a high-titer prep was obtained by collection of the culture supernatant. The resulting prep is referred to as HIV300.

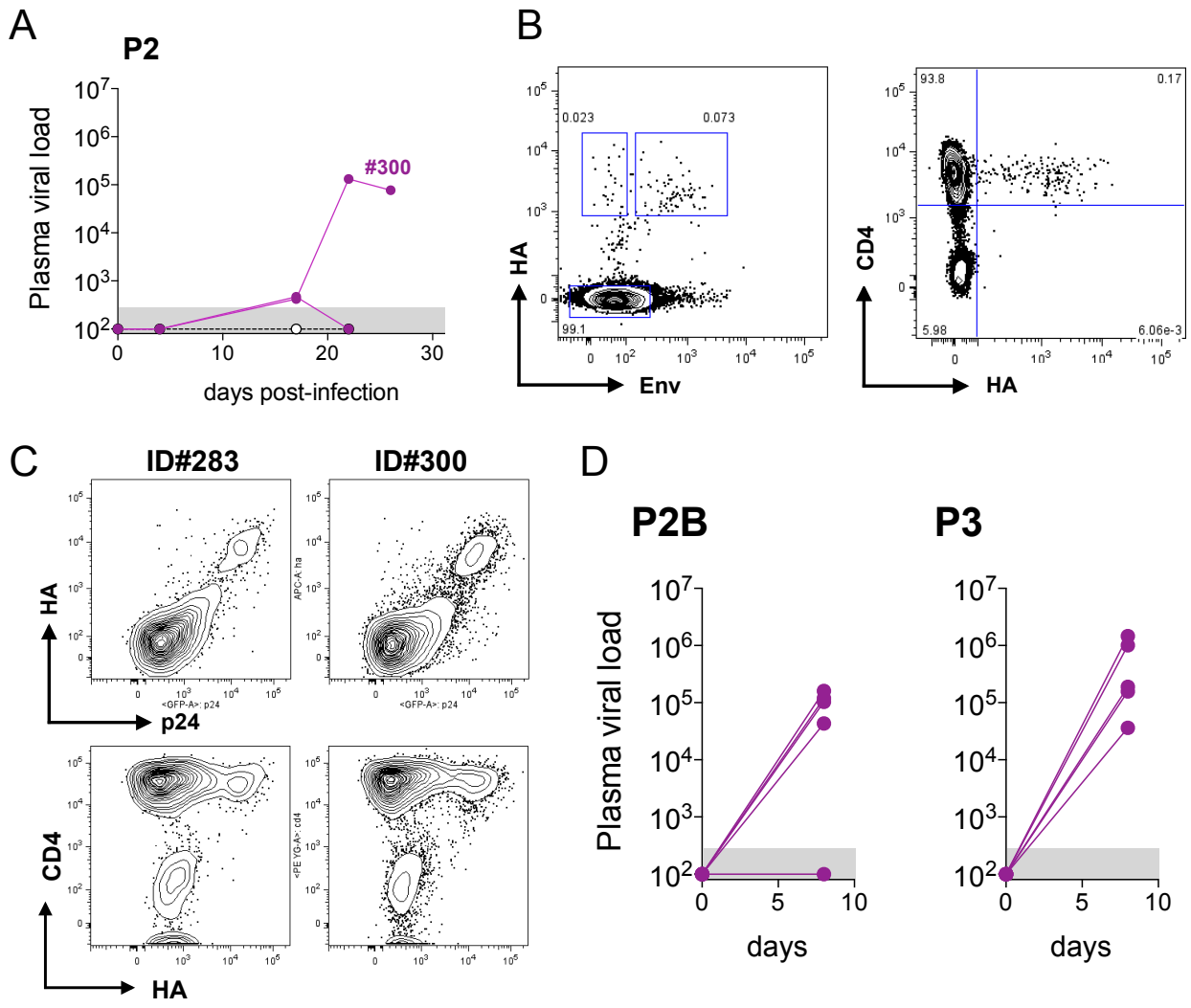

Figure 4.7: Further passage selects for a well-adapted, stably replicating reporter virus.

A, Viral loads of hu-mice infected with virus from ID#283 by intra-peritoneal injection of cultured cells (P2 mice). *B*, Spleen cells from ID#300 sacrificed 27 days after infection (gated on CD3+/CD8-/mCD45-/live). *C*, Human PBMC cultures infected with virus harvested from ID#283 and ID#300 splenic outgrowth cultures (infection day 6). *D*, Viral loads of hu-mice injected intravenously with cultured cells (from *C*) infected with either ID#283 (P2B mice) or ID#300 (P3 mice).

To determine whether serial passage of HIV-1_{IL16HA} resulted in selection of adaptive mutations, I attempted to sequence the viruses at each passage by RT-PCR (Fig. 4.8). Near-full length genomes could be constructed for some viruses, while partial genomes could be obtained for most. Sequences revealed clear viral evolution through serial

passage, with several coding mutations becoming fixed. A consensus adapted genome could be obtained from the sequences of animals infected with the ID#300 virus, with numerous mutations relative to the originating HIV-1_{IL16HA} (Table 4.3). These mutations included four coding changes in *env*, two coding changes in *nef* (one reflecting a 16bp frame-shifting deletion in the 3' end of *nef*, resulting in a 44aa elongation of the Nef C-terminus), and restoration of the *vpu* ATG start codon (naturally mutated in the originating YU2-derived sequence). These mutations may explain the loss of CD4 down-regulation classically seen for actively infected cells, as Nef is known to down-regulate CD4 via interaction of its C-terminus with the AP-2/Clathrin adaptor(65). This effect is specifically known to be abolished by any of several mutations, including mutation of V180 (as found in the adapted viruses). It is noteworthy that Nef expression may have been achieved through translation of a continuous open reading frame initiated within the *HSA-HA* gene, rather than from its own ATG, which could result in a failure to myristoylate the N-terminus of Nef that would impact its ability to localize to the plasma membrane. Additionally, restoration of the *vpu* ATG in the final passages may explain the partially regained ability to down-regulate CD4, as Vpu is known to bind CD4 directly to mediate its degradation(66, 67).

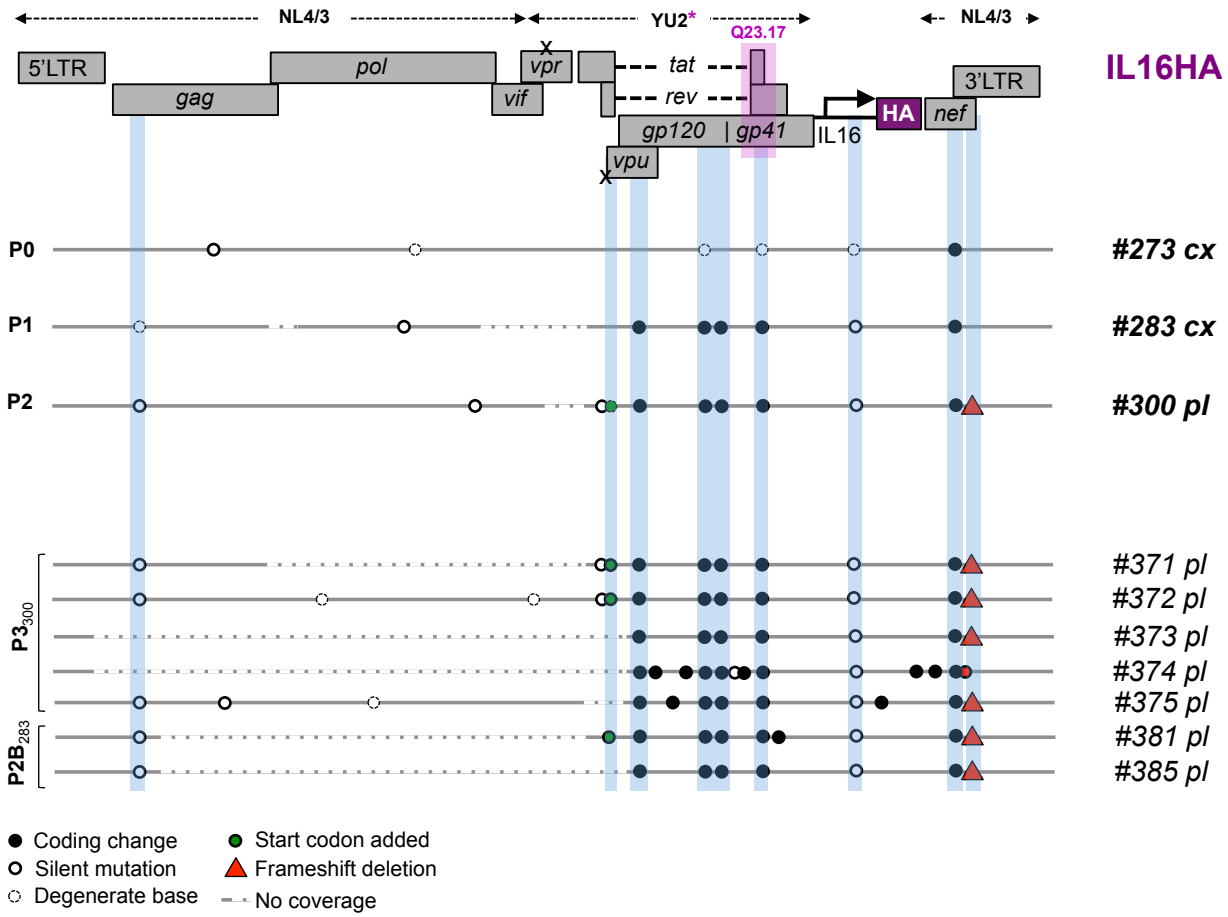

Figure 4.8: Viral sequencing reveals evolutionary selection for mutations in HIV-1_{IL16HA}.

A schematic of the originating virus, HIV-1_{IL16HA}, is shown at top. Each horizontal line below reflects a spatially aligned viral genome sequence, with identified mutations annotated as described. At right, the animal ID is shown; "cx" refers to viral sequencing performed on culture supernatant from splenic outgrowth culture of the indicated animal; "pl" refers to viral sequencing from plasma virus.

Table 4.3: Summary of consensus mutations identified in ID#300 and HIV300-infected hu-mice

Nt pos. (Hxb2)	*Nt pos. (HIV-1_{IL16HA})*	*Nt mutation*	*Gene*	*AA mutation (Hxb2)*	*AA mutation (HIV-1_{IL16HA})*	*Notes*
826	826	T/C	*gag*	-	-	
6043	6043	G/A	*tat*	-	-	*Falls within splice donor*
			rev	S25N	S25N	
6063	6063	C/T	*vpu*	+fMet	+fMet	*Restores Vpu ATG start codon*
6310	6307	G/A	*env*	S29N	S29N	
7516	7477	G/A	*env*	G431E	G431E	*Adjacent to CD4 contacts*
7647	7608	A/G	*env*	M475V	M475V	*Adjacent to CD4 contacts*
8244	8205	G/A	*env*	D664N	D674N	*Falls within MPER*
-	8923	G/A	*IL16pro*	-	-	*Downstream of TSS*
9335	9709	T/A	*nef*	V180E	V180E	
9349	9722	16bp del.	*nef*	Δ185-207	Δ185-207	*Results in frameshift at R184 causing elongated Nef C-terminus (extra 44 aa)*

To determine whether the consensus mutations identified from ID#300 virus-infected animals were sufficient to launch high-level viremia in hu-mice, I constructed a molecular clone bearing the mutations listed in Table 4.3. The resulting virus, hereafter referred to as $HIVivo_{HA}$, was produced and tested for infectivity in vitro and in vivo (Fig. 4.9). In vitro infection of human PBMC resulted in very high infectivity (>10% of cells infected 2d after infection) and recapitulated the cellular and viral gene expression profile of HIV300-infected cells by flow cytometry (Fig. 4.9B). Following intra-peritoneal challenge of hu-mice, $HIVivo_{HA}$ infection yielded high viral loads comparable to those obtained by HIV300 infection 8 days after infection (Fig. 4.9C). These data validate that $HIVivo_{HA}$ is an in vivo-adapted, highly infectious molecular clone of a recombinant HIV-1 reporter virus. To my knowledge, this is the first demonstration of a recombinant HIV-1 reporter virus that can stably replicate with high viral loads in vivo.

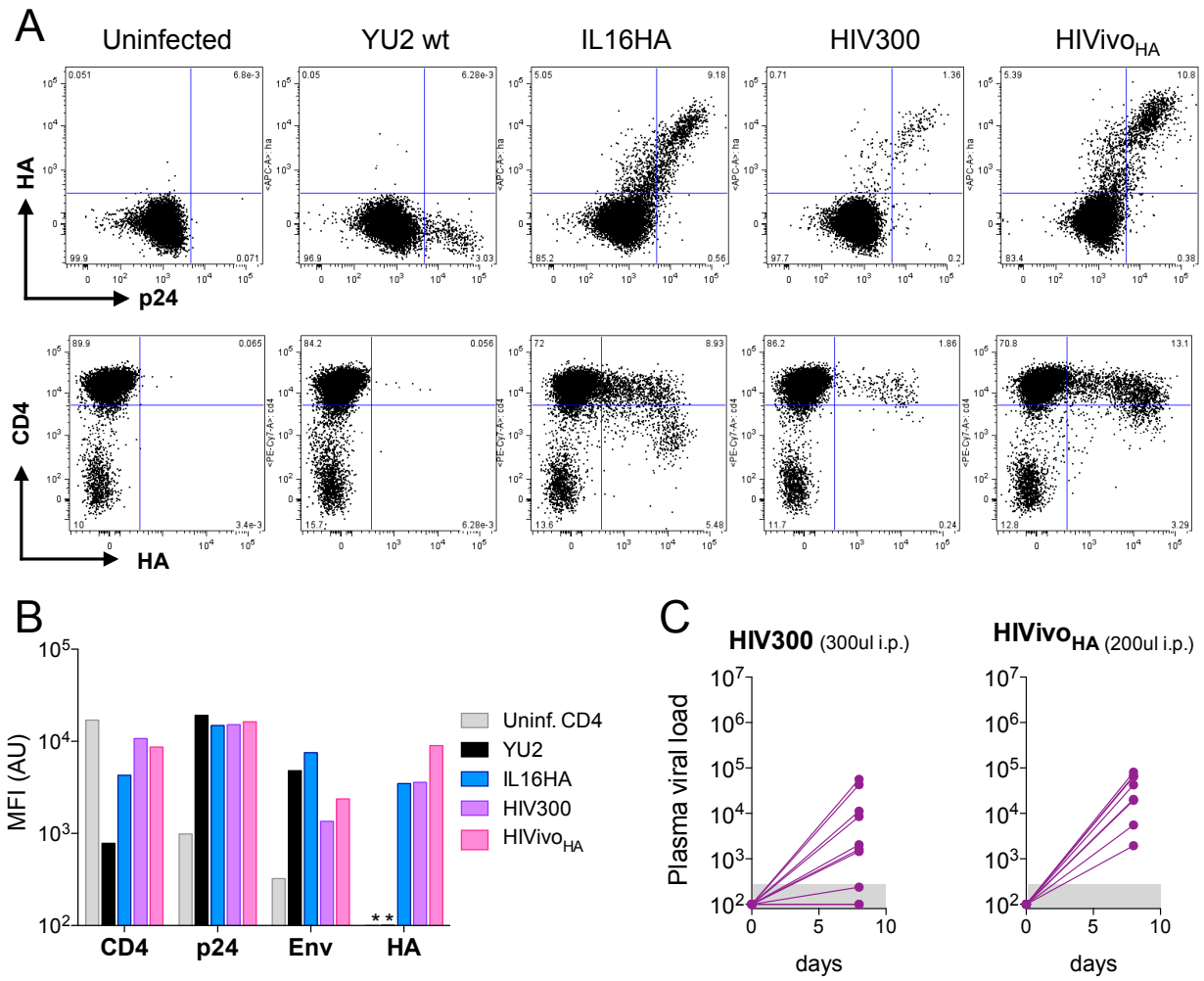

Figure 4.9: An infectious molecular clone, HIVivoHA, recapitulates features of the primary isolate.

A, Flow cytometry analysis of viral and cellular gene expression in healthy donor human PBMC infected with the indicated viruses (2d after infection). *B*, Expression levels of p24+ cells (from samples in *A*) by flow cytometry; geometric mean fluorescence intensity is shown for the indicated viruses. *C*, Viral loads 8d after infection by intra-peritoneal injection of the indicated viral prep.

To determine whether the in vivo-adapted viruses identified from ID#283 or ID#300 were capable of establishing latent infection in hu-mice, I treated animals infected with each virus with cART to suppress viral loads (Fig. 4.10). For these experiments and those that follow, an optimized cART regimen was used in which higher doses than those I had used previously were administered by incorporation of drugs into animal

food(68). Viral loads became suppressed over three to four weeks of continuous cART. Animals infected with ID#283 virus were sacrificed after all three cART-treated animals had dropped to undetectable viral loads. Spleen cells were assayed for the presence of HA+ cells. As expected, the two mice that did not receive cART had detectable populations of Env+/HA+ cells indicative of active infection (as well as Env-/HA+ cells, which may or may not reflect latent infection). The three cART-treated animals, in contrast, only had Env-/HA+ cells, and at extremely low frequencies (Fig. 4.10B). This rare population of Env-/HA+ cells may reflect (or may include) bona fide LICs, but significant further experimentation is required.

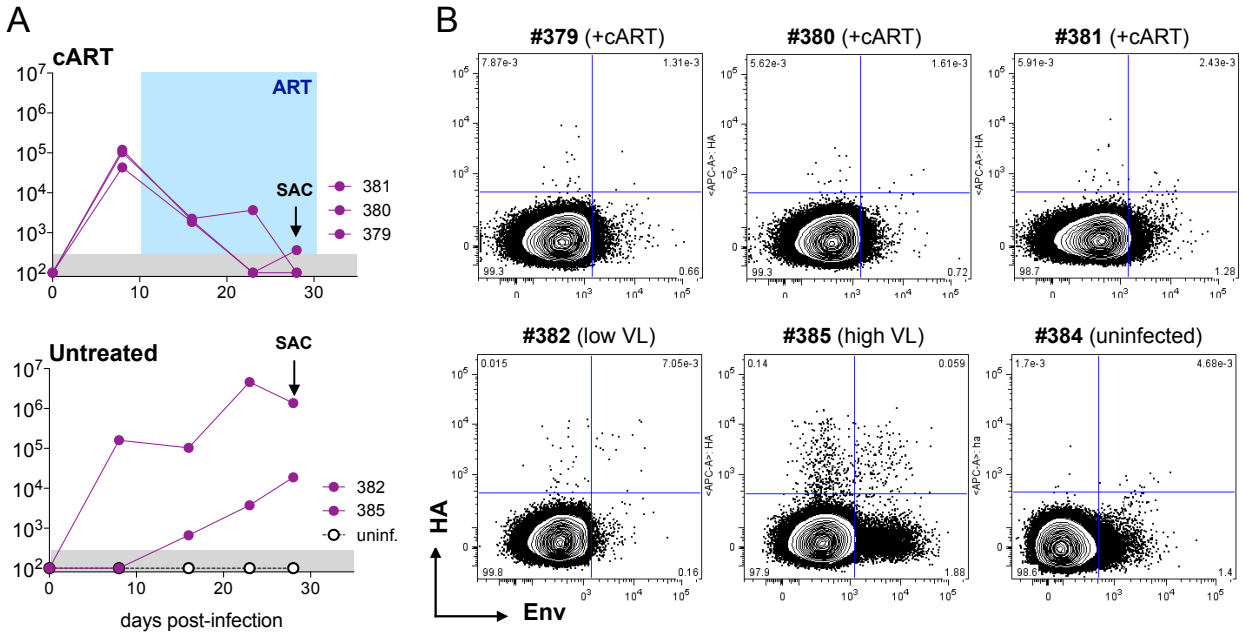

Figure 4.10: Rare HA+/Env- cells persist in reporter-infected hu-mice treated with cART.

A, Viral loads of P2B mice (Fig. 4.7D) over time with (top) or without cART treatment, sacrificed where indicated. *B*, Spleen cells of sacrificed P2B mice (from *A*) and an uninfected control, analyzed by flow cytometry for the presence of HA+ cells. Events shown were gated on CD3+/CD8-/mCD45-/live (from a total of 10^6 un-gated events). Spleen samples yielded approximately 2 – 15 x 10^6 events each, depending on the animal.

To test whether latent infection was possible with the adapted reporter viruses, I treated P3 mice (Fig. 4.7D) with cART until their viral loads dropped below detection, then withdrew them from cART. Viral loads and PBMC were assayed (Fig. 4.11). As expected, cART treatment led to a disappearance of HA+/p24+ cells from PBMC coincident with viral load suppression (Fig. 4.11). Withdrawal of cART after viral loads dropped below detection resulted in rapid viral rebound to pre-treatment levels, coincident with the re-appearance of HA+/p24+ cells in all animals. These data suggested that the in vivo-adapted reporter virus (from ID#300) was capable of establishing latent infection in hu-mice, and provided further confirmation that the reporter virus could stably and faithfully replicate in hu-mice.

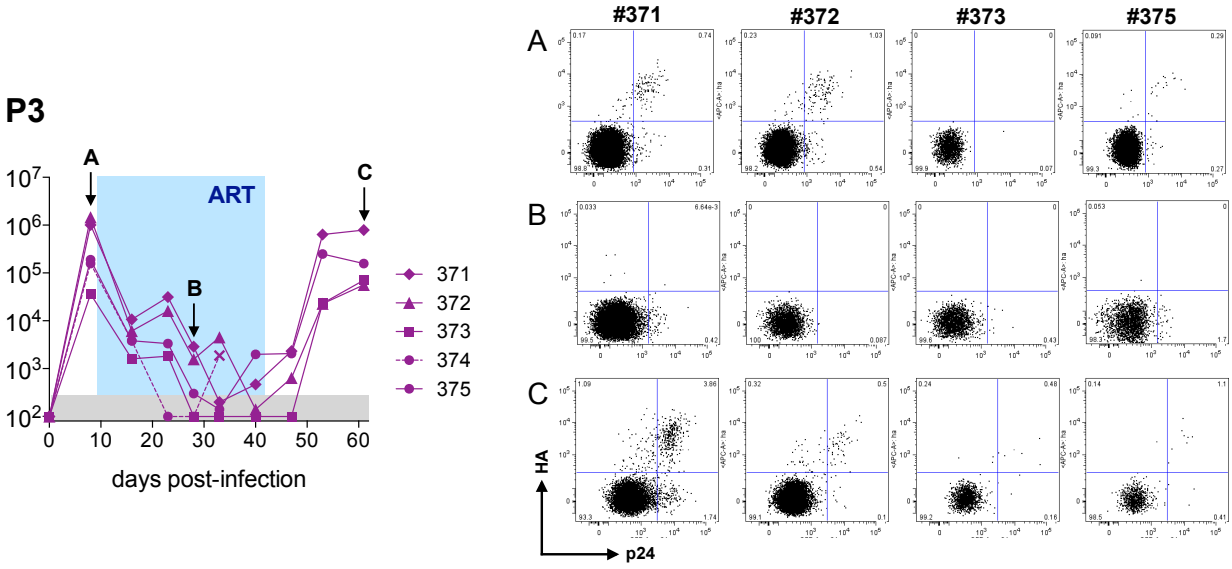

Figure 4.11: In vivo-adapted reporter virus demonstrates stability and latency in vivo.

Left, viral loads of P3 mice (Fig. 4.7D) treated with cART for 32 days (blue shading), then withdrawn from cART. *Right*, flow cytometry analysis of HA+/p24+ cells in PBMC of P3 mice at the indicated time points at left.

Most infected cells that do not express Env harbor defective HIV-1 genomes

The intended design of my recombinant HIV-1 latency reporter virus was to facilitate identification of LICs. However, HIV-1 infection is highly error-prone, and it is probable that a significant fraction of HA-expressing cells not expressing viral markers (such as Env) may, in fact, be defective rather than latent. To determine the extent of defective infection in the Env- subset of HA+ cells, I developed assays to quantitatively and qualitatively characterize HIV-1 genome integrity of single cells (Fig. 4.12). Cells were stained for Env using a combination of biotinylated bNAbs, 3BNC117 and 10-1074. By adapting a method for single-cell PCR(69), I sorted single cells from the spleen of ID#300 and cloned their *env* genes. Cells were lysed and reverse-transcribed first with a primer targeting the 3' LTR polyadenylation signal(70). I then performed quantitative PCR on 10% of the cell lysate (using a secondary RT-PCR step targeting either the HIV-1 *pol* region or the HA gene). This approach was designed to quantify total intracellular viral nucleic acids to determine the relative abundance of unspliced LTR-driven (*pol*-targeted) and IL16pro-driven (HA-targeted) transcripts. Whereas Env+ cells harbored significantly higher levels of LTR-driven viral nucleic acids than Env- cells, all HA+ cells exhibited relatively equal abundance of IL16pro-driven transcripts. All CD4+ cells that were HA-/Env- (assumed to be uninfected) had undetectable levels of either form of nucleic acids, validating that the assay was clean. These data suggested that Env- cells may have been Env- because of lower viral transcription levels, which might be indicative of cells in, or transitioning into, latency. To verify that these Env- cells were not simply harboring defective viral genomes (due to aberrations in *env*, e.g.), I next amplified the complete *env* region from the same single-cell RT lysate as I had used for

intracellular qRT-PCR (using 5% of total lysate). Of all cells, PCR bands were obtained for 35/40 Env+ cells and 20/40 Env- cells. No bands were obtained from HA-/Env- cells. PCR band recovery was linked to viral nucleic acid (vNA) abundance. Sequencing revealed that, while 17/18 Env+ cells harbored fully intact *env* ORFs, only 5/20 sequences from Env- cells were intact. These data suggested that the majority of infected, Env- cells among ID#300 splenocytes harbored defective virus, rather than being latently infected. However, these defective *env* genes were obtained from Env- cells expressing high enough levels of vNAs to yield a PCR band from 5% of lysate, and it remains to be seen whether a subset of the un-amplified cells (which expressed lower levels of pol-containing vNAs) comprises the latent fraction.

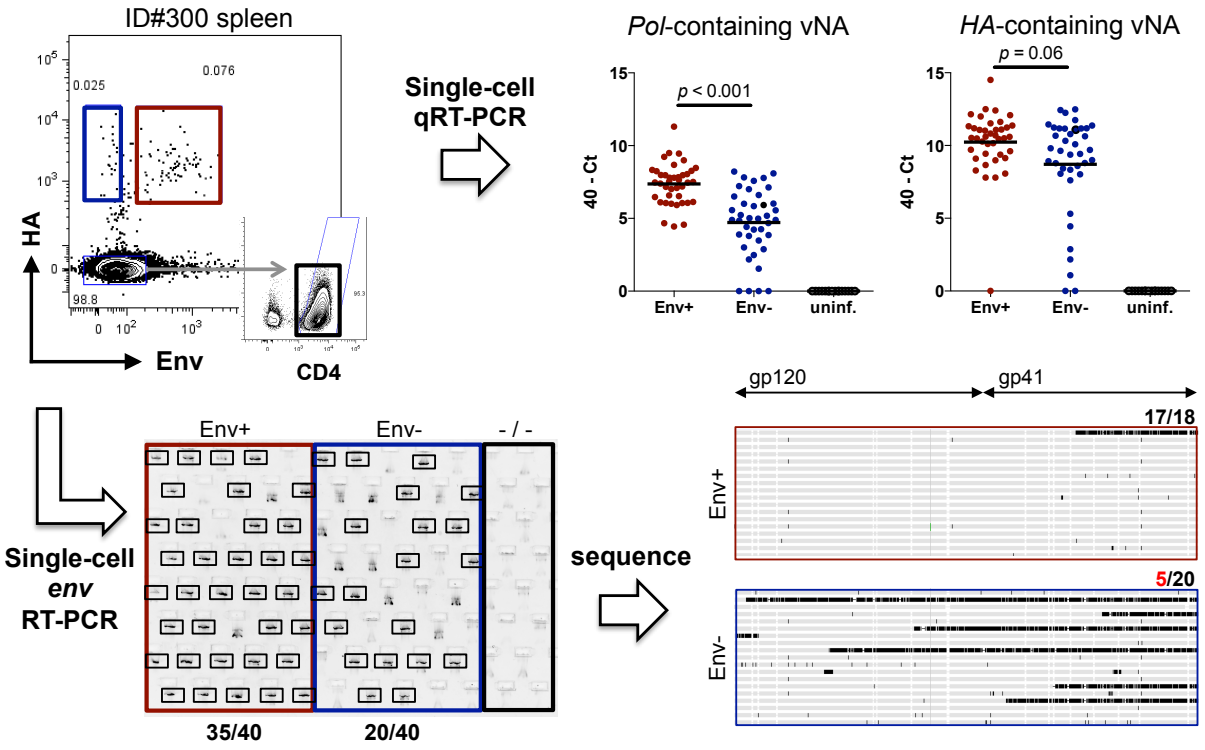

Figure 4.12: Single-cell analyses reveal that reporter virus-infected, Env- cells carry defective *env*.

Fluorescence-activated cell sorting of single cells from ID#300 (copied from Fig. 4.7B) for single cell analyses is shown. Cells were sorted into a single 96-well plate with the layout shown at bottom-left, then lysed and reverse-transcribed. A fraction of the RT reaction was used for quantitative PCR (with an additional target-specific RT step) to measure viral nucleic acids (vNA) containing the indicated targets, in two separate reactions, at top-right. Data are shown as 40 minus the cycle threshold (Ct) for each assay; wells for which no Ct was achieved were assigned a Ct value of 40. At bottom-left, another fraction of the original RT reaction was used for nested PCR targeting the complete *env* gene. PCR products were analyzed on an e-gel, with positive bands indicated by a small black box. 18 positive bands among Env+ cells and all 20 positive bands among Env- cells were sequenced (both by Sanger and Illumina methods) and analyzed for the presence of functional, intact *env* genes (alignments shown at bottom-right, black lines indicate mismatches with respect to the consensus *env* sequence).

A single-cell viral outgrowth assay to identify bona fide LICs

In order to determine whether HA+ cells that do not express Env indeed harbor functional viral genomes, it was critical to establish an assay that could report intact virus from within a single cell. As viral outgrowth is the only definitive assay for determining the presence of cells harboring functional viruses, I combined single-cell

sorting techniques with a classic viral outgrowth assay to establish a means of amplifying virus from individual cells. (For brevity, it shall suffice to state that significant adaptation was required in order to establish an assay that yielded an appreciable frequency of outgrowth.) The assay was performed as follows: two days prior to sorting, healthy donor PBMC were stimulated with 1ug/ml phytohaemagglutinin (PHA) in the presence of 100 IU/ml IL2. Separately, PHA-stimulated healthy donor PBMC were infected in vitro with HIV300. On the day of sorting, CD4+ T-cells were magnetically isolated from the PHA-stimulated, uninfected blasts, and seeded at $5x10^4$ cells per well in a 50ul volume into round-bottom 96-well plates. Single cells infected with HIV300 (Fig. 4.13A) were sorted on top of the CD4+ blasts, and media volume was increased to 150 ul/well with 100 IU/ml IL-2 and 5 ug/ml polybrene (Pb). To test whether various stimuli might be capable of enhancing outgrowth, replicate cultures were treated with either 100 IU/ml IL-2 or IL-2 plus the putative latency-reversing agent (pLRA) ingenol dibenzoate (Ing)(71). Three days after sorting, 100 ul media was removed, cells were resuspended in 100 ul fresh media containing IL-2 and Pb, and transferred to flat-bottom 96-well plates with $5x10^4$/well freshly stimulated CD4+ healthy donor blasts. Medium was changed every three days, and fresh CD4+ blasts were again added on day 10 of culture. On day 14, cells were assayed for the presence of p24 antigen in supernatant by ELISA (Lenti-X p24 rapid titer kit, Clontech). 10/20 cultures of Env+ cells and 8/20 cultures of Env- cells treated with IL-2 alone became positive, whereas only 4/20 Env+ cells and 0/20 Env- cells treated with IL-2 + Ing were positive (Fig. 4.13B). These data indicated that, while IL-2 treatment was sufficient to produce ~50% viral

outgrowth from Env+ cells, the addition of ingenol dibenzoate had deleterious effects on outgrowth [as had been found for other pLRAs, (70)].

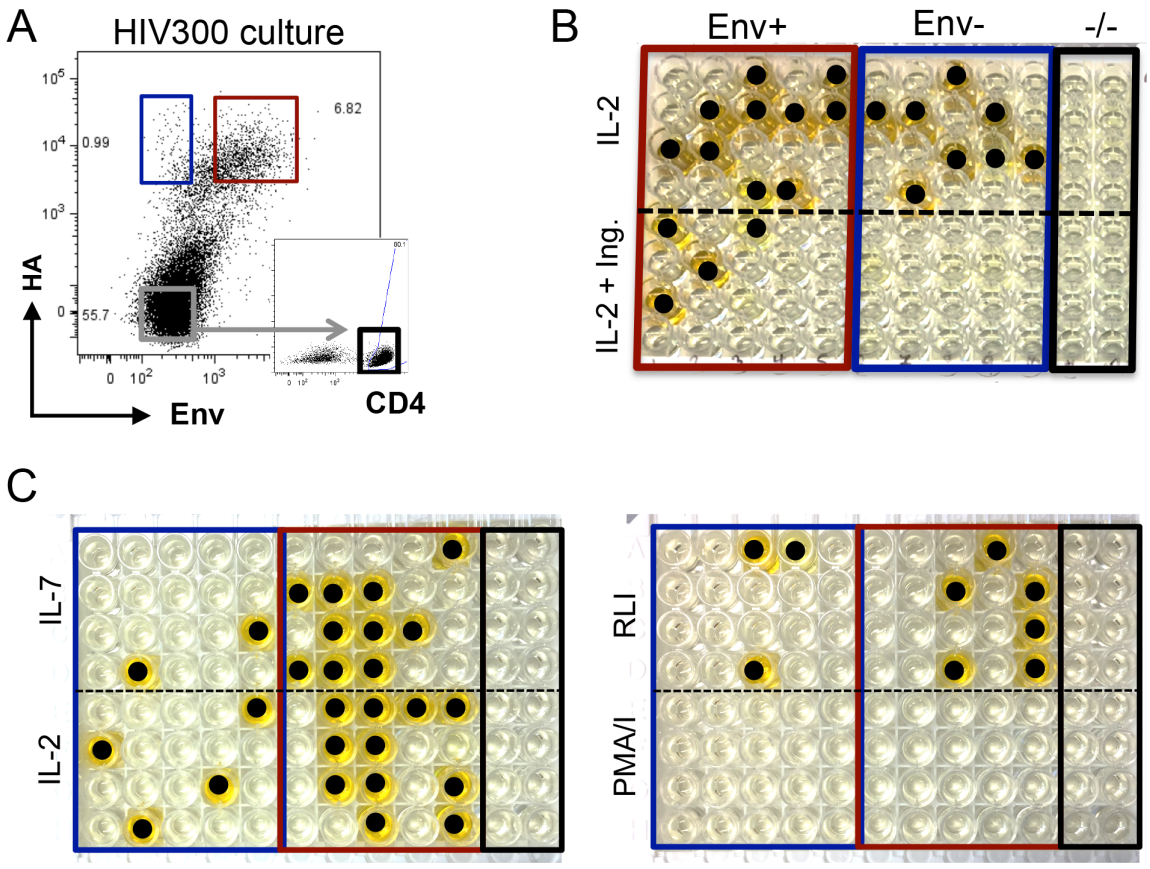

Figure 4.13: A single-cell viral outgrowth assay to detect cells harboring intact viral genomes.

A, FACS of infected (HA+) Env+ or Env-, or uninfected CD4 cells, from a healthy donor human PBMC culture infected with HIV300. *B*, Single cells sorted (from *A*) into viral outgrowth cultures with the indicated conditions. Results of a p24 ELISA with matching plate layout are shown, with positive wells marked by a solid black circle. *C,* Single cells sorted (as in *A*, from a separate infection with more stringent gating for Env- cells, not shown) into viral outgrowth cultures with the indicated conditions (as in *B*).

In a second experiment (Fig. 4.13C), I attempted the following additional conditions: 1 ng/ml IL-7, or 30 ng/ml RLI (IL-15/IL-15Ra superagonist), or 50 ng/ml PMA + 1 uM Ionomycin (PMA/I) instead of IL-2(44, 70, 72-74). Outgrowth cultures from Env+/HA+ cells were positive in 11/20 wells treated with IL-2, 10/20 wells treated with IL-7, 6/20 wells treated with RLI, and 0/20 wells treated with PMA/I (Fig. 4.13C). Env-/HA+ cells

uniformly grew out at far lower frequencies, at 4/20 wells treated with IL-2, 2/20 treated with IL-7, 3/20 treated with RLI, and 0/20 treated with PMA/I. None of the cultures into which CD4+/Env-/HA- cells were sorted produced a p24+ signal, indicating that the assay was clean. These results demonstrated that single Env+/HA+ cells could reliably spread virus to outgrowth cultures stimulated with IL-2, IL-7, or RLI. The dramatically lower rates of outgrowth observed for Env-/HA+ cells is unsurprising, given the aforementioned results obtained from single-cell analyses of genome integrity from ID#300 splenocytes. However, it was encouraging that some cells from this subset resulted in positive outgrowth cultures, possibly validating that LICs may be found within the HA+/Env- fraction.

In summary, through a combination of rational design and directed evolution approaches, I was able to generate an HA-expressing HIV-1 reporter virus that would robustly and faithfully replicate in hu-mice. Single-cell analyses revealed that significant differences exist between Env+ and Env- cells among HA+ (reporter virus-infected) cells: while Env+ cells harbored abundant viral transcripts and readily yielded positive outgrowth cultures, Env- cells harbored comparatively fewer viral transcripts, and rarely yielded positive outgrowth cultures. Significant follow-up work remains to determine the frequency of bona fide LICs among HA+/Env- cells, both in vitro and in vivo.

CHAPTER V: DISCUSSION

Antibodies as effective therapeutic agents in vivo

HIV-1 antibody research has seen a renaissance over the past decade, due in large part to the popularization of single-cell cloning techniques that facilitated antibody discovery(69). This development gave rise to improved understanding of the diverse range of B-cell responses to HIV-1 infection(20, 32, 75, 76), and as a result, several extremely potent bNAbs were identified targeting previously unknown sites of vulnerability on the viral spike [reviewed in (77)].

Though the utility of bNAbs as putative antiviral agents was proposed shortly after the discovery of neutralizing sera(78, 79), it was not until ten years later that members of the first generation of monoclonal bNAbs were shown to be protective against infection in animal models(22, 23). However, when tested in therapy experiments, the same antibodies were unable to control HIV-1 infection in either hu-mice or in humans(25-27). While the successful results of protection experiments lent hope to the idea that bNAbs could confer immunity if elicited by vaccination, the discouraging results of therapy experiments led to the notion that bNAbs could not comprise an effective antiviral regimen or a therapeutic vaccine.

The subsequent identification of highly somatically mutated bNAbs that were orders of magnitude more potent than first-generation bNAbs raised the possibility that better antibodies might succeed where the early generation had failed. The experiments I conducted (outlined in Chapter I of this thesis) were designed specifically to test that possibility. Those experiments showed that several second-generation bNAbs independently exerted selective pressure on established HIV-1 infection in hu-mice, and

when combined, could rapidly and durably suppress viral loads. These encouraging results were later recapitulated in SHIV-infected macaques(61, 62), and the ability of bNAbs to exert strong selective pressure on viral populations was recently confirmed in HIV-1-infected humans(60, 80).

The experiments I conducted with single bNAbs in viremic hu-mice revealed several striking differences in antibody effectiveness that could not have been predicted on the basis of the *in vitro* neutralizing potencies of the bNAbs tested. For example, 3BC176, a bNAb with *in vitro* potency against HIV-1_{YU2} equivalent to PG16, PGT128, or 10-1074, was unable to transiently reduce viral loads or select for resistance mutations in infected hu-mice despite having the longest half-life of the five bNAbs tested. PG16, which exhibited *in vitro* neutralizing potency equivalent to PGT128 and 10-1074, had the smallest effect on viral load of the four efficacious bNAbs tested. Additionally, 10-1074 was found to be dramatically more escape-restrictive than its highly similar counterpart, PGT128, despite equivalent *in vitro* neutralizing potencies.

These single-bNAb therapy experiments highlighted that *in vitro* neutralizing potency is merely one metric by which to assess bNAb effectiveness against HIV-1, and demonstrated the significant utility of the hu-mouse model for gleaning critical information about bNAb activity *in vivo* and their restrictiveness on viral escape pathways. However, significant caveats to this hu-mouse model must be acknowledged that limit the extrapolative capacity of these results. First, the hu-mouse model I employed is highly immune-compromised, with respect to both human and murine immune cell lineages. It is not outfitted with human thymus and liver implants [as for BLT mice, (56)], which are known to improve some adaptive cell-mediated and humoral

responses to pathogens, and the model is extremely deficient in myeloid lineages and natural killer cells. These adaptive and innate immune effector cells may play significant roles in the dynamics of viral infection in humans, and are largely absent in this hu-mouse model. It remains unclear whether such cells (or their murine counterparts) can direct bNAb-mediated ADCC in hu-mice, for example, which may be a critical factor in the activity of certain bNAbs against HIV-1 infection *in vivo*. The results of these studies, therefore, must be interpreted with the understanding that specific mechanisms outside direct virus neutralization have not been determined in assessing bNAb activity *in vivo*.

Another caveat of the hu-mouse model I have employed throughout this thesis is that all experiments in Chapters I and II were conducted using HIV-1_{YU2}, which is a clonal YU2 *env* chimera of a laboratory-adapted strain (NL4/3). The YU2 *env* was chosen because it is a clade B virus that is difficult to neutralize (Tier 2), but which is potently neutralized *in vitro* by the six bNAbs tested in the experiments in Chapters I and II. It remains to be determined whether similar results would be obtained with other viral *env*s against which the tested bNAbs are less potent, or with primary clinical isolates, against which bNAbs may exhibit different activities *in vivo*. Furthermore, these experiments were conducted following infection with a molecular clone, which was permitted to diversify for 2-4 weeks prior to treatment. The viral diversity that could be expected from such an acute infection in an animal three orders of magnitude smaller than a human is likely to be dwarfed by that of HIV-1-infected humans, who are often chronically infected for months to years and have far greater total body viral loads.

However, it should be noted that many of the general findings made in Chapters I and II with respect to bNAb activity against established HIV-1_{YU2} infection in hu-mice

have now been recapitulated in both SHIV-infected macaques and in humans, as discussed in Chapter III and in (60-62, 80). Nonetheless, the extreme diversity of HIV-1 strains should be factored into any attempt to extrapolate from the profiles of viral escape described for HIV-1_{YU2}, as pathways to bNAb resistance are likely to differ significantly between virus strains and in the context of chronic infection.

Reducing viral load improves bNAb effectiveness

The central finding outlined in Chapter II of this thesis holds that viral load suppression prior to bNAb therapy improves the likelihood of sustained viral control by bNAbs, directly implying a link between viral load and the propensity for viral escape. This result was obtained by reducing viral loads first with cART, then withdrawing cART in the presence of a single bNAb. Whereas treatment of viremic (non-suppressed) animals with a single bNAb uniformly resulted in rapid viral escape, pre-suppression of viral loads below the limit of detection permitted high rates of sustained virological control with the same bNAbs. Animals whose viral loads were not fully suppressed before initiation of bNAb monotherapy quickly escaped antibody pressure, as was expected from the bNAb monotherapy experiments in viremic animals (Chapter I). Similar results were obtained for multiple bNAbs, and when animals were administered the same bNAbs by either continuous injection of IgG1 protein or a single gene therapy treatment, demonstrating that the general effect observed was highly reproducible.

It shall be noted that the results obtained for PG16-treated animals, in which only one of five animals remained suppressed during bNAb monotherapy, should not be taken to signify that PG16 is an inferior bNAb. PG16-treated animals, in contrast to

those treated with the other three bNAbs (Fig. 2.4), were infected for an extra week prior to cART suppression, thereby permitting further viral diversification prior to treatment. In addition, only three of five animals were below detection at the time cART was stopped, of which one remained suppressed under PG16 monotherapy. These results rather imply that viral diversity is a key determinant of the effectiveness of bNAb monotherapy: the prevalence of bNAb escape variants in viral reservoirs is likely to increase with the duration of infection(81).

The general finding that pre-suppression improves rates of bNAb-mediated therapeutic control can be explained by two non-mutually exclusive possibilities: first, viral load suppression reduces total viral diversity, simply due to the fact that far fewer infected cells are present at low viral loads than at high viral loads (therefore, even if the *average* diversity between viruses among infected cells is the same at high and low viral loads, the *total* diversity is necessarily lower because the total number of infected cells is smaller); and second, viral resistance may arise either through selection of pre-existing variants, or as a result of creation *during* bNAb therapy and selection thereafter. In the latter scenario, a high viral load would be deleterious to effective therapy because of the possibility that ongoing viral replication may occur until viral loads are fully suppressed, creating an additional time window in which an escape variant may be generated. This would be possible if privileged zones exist in which bNAb penetrance is insufficient to block all new infections. In either case, it is logical that the likelihood of viral escape from bNAbs (or any therapeutic intervention) would be linked to viral load. Indeed, these results were largely confirmed in 3BNC117 clinical trials: whereas treatment of viremic individuals resulted in transient viral load reduction, followed by

rebound to pretreatment levels within 3-4 weeks and selection for 3BNC117 resistance, treatment of aviremic individuals with 3BNC117 (Chapter III) coincident with ATI resulted in sustained virological suppression for 5-9 weeks, with variable levels of selection for resistance.

An important caveat of the experiments in cART-suppressed animals in Chapter II is that the cART regimen used may have been inadequate to suppress viremia in all hu-mice. While a majority of animals treated with cART did become suppressed in the experiments in Chapter II, it was later evident from larger experiments involving hu-mice treated with cART alone for six weeks (data not shown) that bNAb co-administration with cART for the latter two weeks of cART treatment intensified suppressive therapy. Therefore, it is possible that bNAb monotherapy in these experiments was *less* effective than would be expected with a fully effective cART regimen. In later experiments (Chapter IV), an optimized cART regimen was used that fully suppresses viral loads in HIV-1_{YU2}-infected hu-mice(68).

An optimized bNAb cocktail suppresses viremia and lowers cell-associated DNA

Two additional findings were made regarding the dynamics of bNAb-mediated viral suppression in the experiments outlined in Chapter II. First, an optimized bNAb cocktail of only three bNAbs suppressed viral loads, an improvement over the five-bNAb cocktail described in Chapter I. Second, suppressive bNAb therapy with the optimized tri-mix reduced cell-associated viral DNA. The first finding is notable because it signifies that, much like HAART in humans, which is effective because it combines drugs that target different elements of the viral life cycle (or have distinct mechanisms that target the

same elements, such as NNRTIs and NRTIs), bNAb therapy is most effective when its components target distinct viral epitopes. While the removal of 3BC176 from the original penta-mix was obvious because it was sub-therapeutic in monotherapy experiments, removal of PGT128 was decided upon because it was the weaker of two bNAbs targeting the same epitope. The three bNAbs used in the optimized tri-mix, 3BNC117, PG16, and 10-1074, each target a distinct epitope on the viral spike and elicit distinct resistance mutations. The ability of this optimized tri-mix to suppress viral loads (where an original tri-mix comprised of 3BC176, PG16, and 45-46W had largely failed) is probably due to the requirement for three simultaneous escape mutations. The original tri-mix was ineffective because it only required two simultaneous mutations, to PG16 and 45-46W (since 3BC176 was sub-therapeutic). Therefore, viral suppression by bNAbs can be generally understood to depend upon the likelihood of generating simultaneous resistance mutations to all components of the regimen.

The finding that bNAb therapy reduced levels of cell-associated viral DNA is encouraging because of the comparative inability of HAART to lower this measurement in humans over short timescales. This result suggests that bNAbs may act to clear infected cells via an ADCC-like mechanism, which may more effectively reduce HIV-1 DNA than passively blocking new infections (as HAART does). However, these results should be interpreted with the caution that cART-treated control mice were not included in these experiments, so the reduction in cell-associated DNA due to blocking new infections in hu-mice remains unknown. Furthermore, hu-mice are not humans, and the myriad factors that influence cell-associated viral DNA levels may be substantially

different in humans. Therefore, it cannot be ruled out that the effects of bNAb therapy on HIV-1 DNA in hu-mice are limited to blocking new infections.

BNAb gene therapy durably sustains virological suppression

Two observations on the experiments from Chapter II must be made about the results with AAV-based gene therapy. First, these experiments are highly encouraging that a single-shot approach could be used to deploy bNAbs to durably suppress viral loads in humans. Such a therapy, if found to be safe and effective in humans, would permit a "functional cure" of HIV-1 infection by relieving an infected person of all subsequent interventions – notably, daily ART – for an extended period. However, it was found during the course of these experiments that the cART regimen used in hu-mice inhibited AAV transduction, which must be considered if such an approach (or any other gene therapy approach) is to be attempted in humans. Second, it is further encouraging that bNAb titers remained stable for a majority of the observation period in both AAV-3BNC117 and AAV-10-1074-treated animals. It has since been found in hu-mice and in humans that viral loads negatively impact antibody titers(60, 68). This is because a neutralizing event results in destruction of both a virus and the antibodies to which it is bound. Even under suppressive therapy, latently infected cells are constantly becoming reactivated and releasing viral particles that can exhaust antibody titers. This variable must be accounted for in assessing the stability of antibody expression by gene therapy in HIV-1-infected persons. It is possible that deleterious effects on antibody expression were not observed in these experiments because of the relatively short timescales in which these AAV experiments were conducted (on the order of weeks).

3BNC117 delays viral rebound during ATI

In Chapter III of this thesis, results of a clinical trial showed that two infusions of 3BNC117 concurrent with ATI yielded virological suppression for 5-9 weeks during ATI. Historically, rebound occurs within 2-3 weeks in most infected individuals following ATI(40). The early clinical studies using first-generation bNAbs in the setting of ATI also found that a majority of chronically infected individuals rebounded within this timeframe. These studies highlight the importance of antibody potency in therapeutic contexts: two of the bNAbs (2F5 and 4E10) in the early clinical trials were deemed sub-therapeutic, while the only antibody found to exert any selective pressure on patient viruses (2G12) was 2-3 orders of magnitude less potent than, and only a third as broad as, 3BNC117. The success of 3BNC117 in prolonging virological suppression during ATI likely reflects that this bNAb was sufficiently potent to prevent recrudescence of viremia.

Three observations were made during the course of this work that warrant further exploration. First, rebound was merely delayed for 3-6 weeks beyond historical controls; second, rebounding plasma viruses were less sensitive (on the whole) to 3BNC117 than pre-treatment viruses; and third, rebound occurred when serum antibody titers were 11-45 times greater than the IC_{50}s of the rebound outgrowth cultures. To address all three observations, follow-up studies are presently underway in which the frequency and number of 3BNC117 infusions given during ATI were increased. These studies should definitively reveal whether rebound during ATI in the experiments described in Chapter III was the result of viral escape from 3BNC117, or simply the result of viral outgrowth at sub-therapeutic antibody titers. If the primary mode of rebound is escape, rebound

should again occur between 5-9 weeks of ATI, even when antibody titers are high. If, however, the primary mode of rebound is outgrowth at sub-therapeutic antibody titers, rebound should occur later, at equivalent antibody titers as those described for patients receiving only two infusions in Chapter III. Importantly, even if rebound can be explained by outgrowth of resistant viruses, viral outgrowth cultures obtained after ATI was terminated and subjects resumed HAART revealed baseline-level sensitivities to 3BNC117, indicating that broad resistance had not been selected as a result of infusion.

To expand upon the latter two observations that rebound was associated with loss of sensitivity and occurred at detectable antibody concentrations, it bears mentioning that a single viral outgrowth culture was used to determine baseline viral sensitivity of each patient to 3BNC117. Such a method already suffers an extreme sampling bias on the basis of utilizing only five million subject CD4+ T-cells, which are but a tiny fraction of the T-cell repertoire in an infected person. Additionally, bulk outgrowth cultures are highly clonal due to rapid spread of the first (or fittest) viruses to become reactivated, as can be seen from the nearly absent diversity of gp160 sequences obtained from pre-ATI cultures for each subject (Fig. 3.5). The use of such a screening technique fails to capture any of the broad viral diversity that would be expected to exist within each subject's T-cell repertoire. A much more informative approach (underway in follow-up studies) would be to utilize a larger number of subject lymphocytes in a limiting-dilution viral outgrowth culture designed to reactivate only one infected cell per well. Such an approach should yield a far more diverse profile of viral sequences and culture virus sensitivities at baseline for each study subject. Moreover, virus profiling in this way should permit a far more meaningful comparison of plasma

viruses at rebound to the pre-treatment repertoire. It may be found, for example, that the moderate loss of 3BNC117 sensitivity found in viral outgrowth cultures (and anticipated from plasma sequences) at rebound merely reflects expansion of a pre-existing viral clone that is unable to be neutralized by the limiting serum antibody titers found at time of rebound.

Paradigms of bNAb-mediated HIV-1 therapy in vivo

The experiments described in Chapters I-III of this thesis explored the abilities of bNAbs to antagonize established HIV-1 viremia in animal models and in humans. In summary, this work demonstrated that several second-generation bNAbs could succeed where first-generation bNAbs had failed in controlling HIV-1 viremia *in vivo*.

I found that second-generation bNAbs were extremely active as single reagents in exerting selective pressure on viral populations, often sufficient to transiently depress viral loads by more than a log. Combining multiple bNAbs severely limited the likelihood of viral escape, resulting in prolonged virological suppression in a majority of cases. Withdrawal of suppressive bNAb therapy resulted in viral rebound coincident with antibody washout, demonstrating that suppression was indeed maintained by the bNAbs. Viruses rebounding after prolonged suppression by bNAbs did not harbor resistance mutations, further confirming that the bNAbs had prevented viral escape.

As is true of HAART in humans, successful bNAb therapy was contingent upon the ability of the regimen to tightly restrict pathways for viral escape. Three bNAbs requiring two simultaneous mutations yielded minimal rates of control, while five antibodies requiring three simultaneous mutations yielded complete control in all

animals. Optimization of this regimen to comprise three bNAbs, each requiring a distinct resistance mutation, recapitulated the results seen for treatment with all five bNAbs.

Whereas several bNAbs were required to suppress established viremia when viral loads were high, I found that pre-suppression of viral loads with cART enabled bNAbs to sustain virological suppression as monotherapeutics after cART withdrawal. This effect was observed for all four bNAbs tested, and was most successful when viral loads were below detection at the time cART was withdrawn. These results were initially obtained by repeated administration of bNAb protein, but were completely recapitulated by gene therapy experiments deploying bNAb-expressing AAVs, for which only a single shot was required to maintain durable virological control. In light of the lifelong and daily burden faced by HIV-1 infected individuals undergoing HAART, these results provide proof-of-concept support for the hypothesis that bNAbs might one day comprise an effective alternative to ART drugs. It should be noted, however, that there may be impaired antibody penetrance into lymphoid tissues and the brain, where high local concentrations of bNAbs may be needed to maintain antiviral activity.

The findings made in hu-mice that individual bNAbs could delay viral rebound in an ATI-like setting were later confirmed in humans in a phase IIa clinical trial. Two infusions of the bNAb 3BNC117, which was already shown to be safe in humans(60), significantly delayed viral rebound during ATI without selecting for broad viral resistance. In addition to validating the exceptional utility of the hu-mouse model as a preclinical platform for evaluating putative HIV-1 therapeutics, the results of this trial are extremely encouraging and demonstrate that bNAbs can be potent antiviral agents against HIV-1 infection in humans.

A common thread through the findings of Chapters I-III is that the propensity for viral reservoirs to harbor bNAb-resistant clones was a key determinant of the success of bNAb therapy. Suppression of viral loads dramatically reduced the likelihood for viral escape, signifying that viral reservoir size and total diversity are smaller when viral loads are low. However, viral reservoirs indeed persisted despite prolonged suppression by bNAbs, as both hu-mice and humans rebounded after bNAb therapy when serum antibody levels were low. Re-emergent viruses in mice did not carry signature resistance mutations, while rebounding viruses in 3BNC117-treated humans during ATI revealed only moderate loss of neutralizing sensitivity. (In contrast, non-suppressive bNAb therapy in both hu-mice and in humans resulted in strong selection for viral resistance to bNAbs.) These results highlighted that, not only did the hu-mouse model harbor reservoirs of latently infected cells, those cells were also refractory to bNAb therapy.

Subsequent work(68) not described here revealed that reservoirs of latently infected cells in hu-mice were somewhat labile, and could be disrupted by interventions aimed at reactivating latently infected cells in the presence of bNAbs. However, significant questions remained as to the mechanisms by which those interventions, and concurrent bNAb administration, succeeded in disrupting latent reservoirs in hu-mice. Those questions, being important to the development of means to eradicate HIV-1 infection, required answers for which tools by and large did not yet exist: latently infected cells cannot yet be distinguished from uninfected cells by any known means, precluding their purification and study. I therefore pursued the goal of developing a means to identify latently infected cells using the hu-mouse model of HIV-1 infection.

A replication-competent reporter virus designed to identify latently infected cells

Many attempts have been made to study supposed latently infected cells *in vitro*(45, 82-85). Many such platforms have employed recombinant viral genomes harboring reporter genes to facilitate identification of latently infected cells, either in real time or post-reactivation. However, such viruses suffer numerous critical weaknesses that preclude their ability to identify bona fide latently infected cells. In two models(82, 83), two-color reporter viruses were designed for single-round infection *in vitro*. These viruses lack functional *env* genes, and therefore cannot spread. This property limits any ability to determine whether the cells identified as “latent” harbor functional viruses, because such cells cannot spread their virus. Furthermore, the determination of latency is made on the basis of cells expressing a “constitutive” marker driven by a promoter de-coupled from the viral LTR, but not an LTR-driven marker. While cells can be readily identified which satisfy that criterion, one such platform (45) found that the EF-1a promoter utilized for constitutive marker expression became quickly disabled in infected primary CD4+ T-cells when those cells were reverted to a resting phenotype. A second platform (82) utilized a CMV promoter for constitutive marker expression, which is highly dependent upon NF-kB, a factor also critical for LTR-driven expression(86). Both models, therefore, are unlikely to be capable of identifying latently infected cells *in vitro*, and cannot be used to identify bona fide latently infected cells that arise through the natural spread of HIV-1 infection *in vivo*.

To overcome the limitations of previous models, I set out to design a replication-competent HIV-1 reporter virus that would enable the identification and study of latently infected cells at single-cell resolution *ex vivo*. This virus was intended to constitutively express a surface marker on all infected cells, thereby facilitating the identification of latently infected cells as those lacking viral gene markers such as Env or p24. An important criterion was that cells putatively identified as latent should be recoverable as live cells for downstream analyses, permitting proof that they were, indeed, latently infected. As described at length in Chapter IV of this thesis, the road to a reporter virus that stably replicated *in vivo* was long, but ultimately successful. Through repeated re-design and gradual refinement, a reporter virus was developed that replicated with wild-type kinetics in a human CD4+ T-cell line *in vitro*. That virus, HIV-1_{IL16HA}, was then passaged in hu-mice to select for adaptive mutations that would confer additional replicative fitness *in vivo*. The adapted virus (HIV300) reproducibly yielded high viral loads, demonstrated the capacity to form latently infected cells, and exhibited stable reporter retention during the course of infection in hu-mice. An infectious molecular clone derived from the sequence of that strain was constructed (HIVivo$_{HA}$), yielding high viral loads in hu-mice and recapitulating the features of the adapted primary isolate.

Single-cell assays to facilitate dissection of HIV-1 latency

In order to prove that cells identified as “latent” did, in fact, harbor functional proviruses that can become reactivated to spread infection, it was necessary to design assays that would determine the functionality of proviruses contained within individual sorted cells. Therefore, I established staining protocols to permit single-cell sorting of cells on the

basis of a recombinant marker (HA) and a viral marker (Env). I subsequently developed three separate assays to facilitate characterization of putative latently infected cells after single-cell sorting: a quantitative intracellular viral nucleic acid assay to detect the relative abundance of viral (LTR-driven) and recombinant (IL16pro-driven) transcripts, which was intended to distinguish latently infected cells from actively infected cells; an *env* RT-PCR assay to determine whether individual Env- cells harbored intact *env* genes; and a viral outgrowth assay to determine whether individual, putative latently infected cells could be reactivated to spread infection.

Further proof is required to determine whether HIVivo$_{HA}$ can identify latency

The experiments outlined in Chapter IV of this thesis differ significantly from those of Chapters I-III in that the primary focus of Chapter IV was the design and development of a tool, the *in vivo*-adapted latency reporter virus HIVivo$_{HA}$, rather than the pursuit of experimental findings. Hence, the discussion of Chapter IV shall be primarily concerned with the characteristics and caveats of the reporter virus I designed, as well as identifying further experiments required to assess its utility for studying bona fide latently infected cells.

One of the key realizations made while characterizing the *in vivo*-adapted latency reporter virus was that HA+ cells that were Env- predominantly contained defective *env* genes. This result should not be surprising, in light of the fact that HIV-1 infection is highly error-prone. It has been long understood that sizeable pools of HIV-1 DNA exist that harbor defective viruses(12). These pools can easily confound the study of latency *ex vivo*, and extreme care must be taken to separate defective from intact infections

insofar as that is possible. Whereas two groups recently identified pools of clonal integrations within cancer genes as a major component of the viable HIV-1 latent reservoir(87, 88), it was later found that the vast majority (or all) of clonal integrations, in fact, harbored defective (yet integrated) proviruses(89). An elegant and exhaustive study (13) revealed that, while the pool of HIV-1 DNA in cells is orders of magnitude greater than the pool of cells that can be reactivated to produce virus by outgrowth assays *in vitro*, a substantial population of cells fails to reactivate that appear to harbor intact proviruses. In that study, roughly 12% of non-induced proviruses appeared intact by near-full length genome sequencing of cell DNA, while the rest were defective.

Any number and manner of aberrations can result in a defective provirus. With respect to the reporter virus I have designed, the recombinant cassette (IL16pro-HA) is only 5% of the size of the viral genome. This makes it highly likely that cells infected with such a virus can suffer aberrations that render the viral genome defective, yet leave the IL16pro-HA cassette intact. Thus, infected cells can be identified on the basis of HA expression (and absent Env expression, e.g.) that reflect dysfunctional infected cells, rather than latently infected cells, as was found for ID#300 splenocytes in the single-cell experiments outlined in Chapter IV. It is also important to note that these single-cell experiments were conducted on cells from a viremic animal, rather than a cART-suppressed one. Bona fide latently infected cells, almost by definition, are cells harboring intact proviruses that can persist for extended periods of time *in vivo*. It therefore remains critical to determine whether, indeed, any of the HA+ cells that persist after suppressive therapy in HIVivo$_{HA}$-infected hu-mice harbor intact proviruses that can be reactivated. Should such experiments confirm that a subset of such HA+ cells

harbors intact virus, they would definitively prove that the HIVivo$_{HA}$ reporter virus can identify bona fide latently infected cells – a feat not yet possible by any known means. However, even if a subset of HA+ cells are found to harbor latency, extensive further research must still be conducted to determine what, if any, unique features describe latently infected cells harboring intact proviruses, as opposed to those harboring defective ones.

In sum, the experiments conducted in Chapter IV of this thesis describe a new tool that may be useful in characterizing latent infection. Further work is required to determine whether the reporter virus described can, indeed, identify bona fide latently infected cells. Despite that important uncertainty, HIVivo$_{HA}$ should nonetheless prove to be a valuable tool for future experimentation, as it is the first known recombinant HIV-1 reporter virus capable of stably replicating at high viral loads *in vivo*.

REFERENCES

1. Klatzmann D, Champagne E, Chamaret S, Gruest J, Guetard D, Hercend T, Gluckman JC, & Montagnier L (1984) T-lymphocyte T4 molecule behaves as the receptor for human retrovirus LAV. *Nature* 312(5996):767-768.
2. Dalgleish AG, Beverley PC, Clapham PR, Crawford DH, Greaves MF, & Weiss RA (1984) The CD4 (T4) antigen is an essential component of the receptor for the AIDS retrovirus. *Nature* 312(5996):763-767.
3. Sattentau QJ & Weiss RA (1988) The CD4 antigen: physiological ligand and HIV receptor. *Cell* 52(5):631-633.
4. Roberts JD, Bebenek K, & Kunkel TA (1988) The accuracy of reverse transcriptase from HIV-1. *Science* 242(4882):1171-1173.
5. Preston BD, Poiesz BJ, & Loeb LA (1988) Fidelity of HIV-1 reverse transcriptase. *Science* 242(4882):1168-1171.
6. Bukrinsky MI, Sharova N, Dempsey MP, Stanwick TL, Bukrinskaya AG, Haggerty S, & Stevenson M (1992) Active nuclear import of human immunodeficiency virus type 1 preintegration complexes. *Proc Natl Acad Sci U S A* 89(14):6580-6584.
7. McCune JM, Rabin LB, Feinberg MB, Lieberman M, Kosek JC, Reyes GR, & Weissman IL (1988) Endoproteolytic cleavage of gp160 is required for the activation of human immunodeficiency virus. *Cell* 53(1):55-67.
8. Chun TW, Carruth L, Finzi D, Shen X, DiGiuseppe JA, Taylor H, Hermankova M, Chadwick K, Margolick J, Quinn TC, Kuo YH, Brookmeyer R, Zeiger MA, Barditch-Crovo P, & Siliciano RF (1997) Quantification of latent tissue reservoirs and total body viral load in HIV-1 infection. *Nature* 387(6629):183-188.
9. Rouet F, Ekouevi DK, Chaix ML, Burgard M, Inwoley A, Tony TD, Danel C, Anglaret X, Leroy V, Msellati P, Dabis F, & Rouzioux C (2005) Transfer and evaluation of an automated, low-cost real-time reverse transcription-PCR test for diagnosis and monitoring of human immunodeficiency virus type 1 infection in a West African resource-limited setting. *J Clin Microbiol* 43(6):2709-2717.
10. Butler SL, Johnson EP, & Bushman FD (2002) Human immunodeficiency virus cDNA metabolism: notable stability of two-long terminal repeat circles. *J Virol* 76(8):3739-3747.
11. Pierson TC, Kieffer TL, Ruff CT, Buck C, Gange SJ, & Siliciano RF (2002) Intrinsic stability of episomal circles formed during human immunodeficiency virus type 1 replication. *J Virol* 76(8):4138-4144.
12. Eriksson S, Graf EH, Dahl V, Strain MC, Yukl SA, Lysenko ES, Bosch RJ, Lai J, Chioma S, Emad F, Abdel-Mohsen M, Hoh R, Hecht F, Hunt P, Somsouk M, Wong J, Johnston R, Siliciano RF, Richman DD, O'Doherty U, Palmer S, Deeks SG, & Siliciano JD (2013) Comparative analysis of measures of viral reservoirs in HIV-1 eradication studies. *PLoS Pathog* 9(2):e1003174.
13. Ho YC, Shan L, Hosmane NN, Wang J, Laskey SB, Rosenbloom DI, Lai J, Blankson JN, Siliciano JD, & Siliciano RF (2013) Replication-competent noninduced proviruses in the latent reservoir increase barrier to HIV-1 cure. *Cell* 155(3):540-551.
14. Molina JM, Andrade-Villanueva J, Echevarria J, Chetchotisakd P, Corral J, David N, Moyle G, Mancini M, Percival L, Yang R, Wirtz V, Lataillade M, Absalon J,

McGrath D, & Team CS (2010) Once-daily atazanavir/ritonavir compared with twice-daily lopinavir/ritonavir, each in combination with tenofovir and emtricitabine, for management of antiretroviral-naive HIV-1-infected patients: 96-week efficacy and safety results of the CASTLE study. *J Acquir Immune Defic Syndr* 53(3):323-332.

15. Perelson AS, Neumann AU, Markowitz M, Leonard JM, & Ho DD (1996) HIV-1 dynamics in vivo: virion clearance rate, infected cell life-span, and viral generation time. *Science* 271(5255):1582-1586.
16. Cooper A, Garcia M, Petrovas C, Yamamoto T, Koup RA, & Nabel GJ (2013) HIV-1 causes CD4 cell death through DNA-dependent protein kinase during viral integration. *Nature* 498(7454):376-379.
17. Doitsh G, Galloway NL, Geng X, Yang Z, Monroe KM, Zepeda O, Hunt PW, Hatano H, Sowinski S, Munoz-Arias I, & Greene WC (2014) Cell death by pyroptosis drives CD4 T-cell depletion in HIV-1 infection. *Nature* 505(7484):509-514.
18. Klein MR & Miedema F (1995) Long-term survivors of HIV-1 infection. *Trends Microbiol* 3(10):386-391.
19. Doria-Rose NA, Klein RM, Daniels MG, O'Dell S, Nason M, Lapedes A, Bhattacharya T, Migueles SA, Wyatt RT, Korber BT, Mascola JR, & Connors M (2010) Breadth of human immunodeficiency virus-specific neutralizing activity in sera: clustering analysis and association with clinical variables. *J Virol* 84(3):1631-1636.
20. Liao HX, Lynch R, Zhou T, Gao F, Alam SM, Boyd SD, Fire AZ, Roskin KM, Schramm CA, Zhang Z, Zhu J, Shapiro L, Program NCS, Mullikin JC, Gnanakaran S, Hraber P, Wiehe K, Kelsoe G, Yang G, Xia SM, Montefiori DC, Parks R, Lloyd KE, Scearce RM, Soderberg KA, Cohen M, Kamanga G, Louder MK, Tran LM, Chen Y, Cai F, Chen S, Moquin S, Du X, Joyce MG, Srivatsan S, Zhang B, Zheng A, Shaw GM, Hahn BH, Kepler TB, Korber BT, Kwong PD, Mascola JR, & Haynes BF (2013) Co-evolution of a broadly neutralizing HIV-1 antibody and founder virus. *Nature* 496(7446):469-476.
21. Doria-Rose NA, Schramm CA, Gorman J, Moore PL, Bhiman JN, DeKosky BJ, Ernandes MJ, Georgiev IS, Kim HJ, Pancera M, Staupe RP, Altae-Tran HR, Bailer RT, Crooks ET, Cupo A, Druz A, Garrett NJ, Hoi KH, Kong R, Louder MK, Longo NS, McKee K, Nonyane M, O'Dell S, Roark RS, Rudicell RS, Schmidt SD, Sheward DJ, Soto C, Wibmer CK, Yang Y, Zhang Z, Program NCS, Mullikin JC, Binley JM, Sanders RW, Wilson IA, Moore JP, Ward AB, Georgiou G, Williamson C, Abdool Karim SS, Morris L, Kwong PD, Shapiro L, & Mascola JR (2014) Developmental pathway for potent V1V2-directed HIV-neutralizing antibodies. *Nature* 509(7498):55-62.
22. Mascola JR, Lewis MG, Stiegler G, Harris D, VanCott TC, Hayes D, Louder MK, Brown CR, Sapan CV, Frankel SS, Lu Y, Robb ML, Katinger H, & Birx DL (1999) Protection of Macaques against pathogenic simian/human immunodeficiency virus 89.6PD by passive transfer of neutralizing antibodies. *J Virol* 73(5):4009-4018.
23. Mascola JR, Stiegler G, VanCott TC, Katinger H, Carpenter CB, Hanson CE, Beary H, Hayes D, Frankel SS, Birx DL, & Lewis MG (2000) Protection of

macaques against vaginal transmission of a pathogenic HIV-1/SIV chimeric virus by passive infusion of neutralizing antibodies. *Nat Med* 6(2):207-210.
24. Balazs AB, Chen J, Hong CM, Rao DS, Yang L, & Baltimore D (2012) Antibody-based protection against HIV infection by vectored immunoprophylaxis. *Nature* 481(7379):81-84.
25. Poignard P, Sabbe R, Picchio GR, Wang M, Gulizia RJ, Katinger H, Parren PW, Mosier DE, & Burton DR (1999) Neutralizing antibodies have limited effects on the control of established HIV-1 infection in vivo. *Immunity* 10(4):431-438.
26. Trkola A, Kuster H, Rusert P, Joos B, Fischer M, Leemann C, Manrique A, Huber M, Rehr M, Oxenius A, Weber R, Stiegler G, Vcelar B, Katinger H, Aceto L, & Gunthard HF (2005) Delay of HIV-1 rebound after cessation of antiretroviral therapy through passive transfer of human neutralizing antibodies. *Nat Med* 11(6):615-622.
27. Mehandru S, Vcelar B, Wrin T, Stiegler G, Joos B, Mohri H, Boden D, Galovich J, Tenner-Racz K, Racz P, Carrington M, Petropoulos C, Katinger H, & Markowitz M (2007) Adjunctive passive immunotherapy in human immunodeficiency virus type 1-infected individuals treated with antiviral therapy during acute and early infection. *J Virol* 81(20):11016-11031.
28. Purtscher M, Trkola A, Gruber G, Buchacher A, Predl R, Steindl F, Tauer C, Berger R, Barrett N, Jungbauer A, & et al. (1994) A broadly neutralizing human monoclonal antibody against gp41 of human immunodeficiency virus type 1. *AIDS Res Hum Retroviruses* 10(12):1651-1658.
29. Buchacher A, Predl R, Strutzenberger K, Steinfellner W, Trkola A, Purtscher M, Gruber G, Tauer C, Steindl F, Jungbauer A, & et al. (1994) Generation of human monoclonal antibodies against HIV-1 proteins; electrofusion and Epstein-Barr virus transformation for peripheral blood lymphocyte immortalization. *AIDS Res Hum Retroviruses* 10(4):359-369.
30. Trkola A, Purtscher M, Muster T, Ballaun C, Buchacher A, Sullivan N, Srinivasan K, Sodroski J, Moore JP, & Katinger H (1996) Human monoclonal antibody 2G12 defines a distinctive neutralization epitope on the gp120 glycoprotein of human immunodeficiency virus type 1. *J Virol* 70(2):1100-1108.
31. Burton DR, Pyati J, Koduri R, Sharp SJ, Thornton GB, Parren PW, Sawyer LS, Hendry RM, Dunlop N, Nara PL, & et al. (1994) Efficient neutralization of primary isolates of HIV-1 by a recombinant human monoclonal antibody. *Science* 266(5187):1024-1027.
32. Scheid JF, Mouquet H, Ueberheide B, Diskin R, Klein F, Oliveira TY, Pietzsch J, Fenyo D, Abadir A, Velinzon K, Hurley A, Myung S, Boulad F, Poignard P, Burton DR, Pereyra F, Ho DD, Walker BD, Seaman MS, Bjorkman PJ, Chait BT, & Nussenzweig MC (2011) Sequence and structural convergence of broad and potent HIV antibodies that mimic CD4 binding. *Science* 333(6049):1633-1637.
33. Mouquet H, Scharf L, Euler Z, Liu Y, Eden C, Scheid JF, Halper-Stromberg A, Gnanapragasam PN, Spencer DI, Seaman MS, Schuitemaker H, Feizi T, Nussenzweig MC, & Bjorkman PJ (2012) Complex-type N-glycan recognition by potent broadly neutralizing HIV antibodies. *Proc Natl Acad Sci U S A* 109(47):E3268-3277.

34. Klein F, Gaebler C, Mouquet H, Sather DN, Lehmann C, Scheid JF, Kraft Z, Liu Y, Pietzsch J, Hurley A, Poignard P, Feizi T, Morris L, Walker BD, Fatkenheuer G, Seaman MS, Stamatatos L, & Nussenzweig MC (2012) Broad neutralization by a combination of antibodies recognizing the CD4 binding site and a new conformational epitope on the HIV-1 envelope protein. *J Exp Med* 209(8):1469-1479.
35. Wege AK, Melkus MW, Denton PW, Estes JD, & Garcia JV (2008) Functional and phenotypic characterization of the humanized BLT mouse model. *Curr Top Microbiol Immunol* 324:149-165.
36. Billerbeck E, Horwitz JA, Labitt RN, Donovan BM, Vega K, Budell WC, Koo GC, Rice CM, & Ploss A (2013) Characterization of human antiviral adaptive immune responses during hepatotropic virus infection in HLA-transgenic human immune system mice. *J Immunol* 191(4):1753-1764.
37. Pantaleo G, Graziosi C, Demarest JF, Butini L, Montroni M, Fox CH, Orenstein JM, Kotler DP, & Fauci AS (1993) HIV infection is active and progressive in lymphoid tissue during the clinically latent stage of disease. *Nature* 362(6418):355-358.
38. Siliciano JD, Kajdas J, Finzi D, Quinn TC, Chadwick K, Margolick JB, Kovacs C, Gange SJ, & Siliciano RF (2003) Long-term follow-up studies confirm the stability of the latent reservoir for HIV-1 in resting CD4+ T cells. *Nat Med* 9(6):727-728.
39. Palmer S, Wiegand AP, Maldarelli F, Bazmi H, Mican JM, Polis M, Dewar RL, Planta A, Liu S, Metcalf JA, Mellors JW, & Coffin JM (2003) New real-time reverse transcriptase-initiated PCR assay with single-copy sensitivity for human immunodeficiency virus type 1 RNA in plasma. *J Clin Microbiol* 41(10):4531-4536.
40. Rothenberger MK, Keele BF, Wietgrefe SW, Fletcher CV, Beilman GJ, Chipman JG, Khoruts A, Estes JD, Anderson J, Callisto SP, Schmidt TE, Thorkelson A, Reilly C, Perkey K, Reimann TG, Utay NS, Nganou Makamdop K, Stevenson M, Douek DC, Haase AT, & Schacker TW (2015) Large number of rebounding/founder HIV variants emerge from multifocal infection in lymphatic tissues after treatment interruption. *Proc Natl Acad Sci U S A* 112(10):E1126-1134.
41. Folks TM, Powell D, Lightfoote M, Koenig S, Fauci AS, Benn S, Rabson A, Daugherty D, Gendelman HE, Hoggan MD, & et al. (1986) Biological and biochemical characterization of a cloned Leu-3- cell surviving infection with the acquired immune deficiency syndrome retrovirus. *J Exp Med* 164(1):280-290.
42. Lassen K, Han Y, Zhou Y, Siliciano J, & Siliciano RF (2004) The multifactorial nature of HIV-1 latency. *Trends Mol Med* 10(11):525-531.
43. Chun TW, Finzi D, Margolick J, Chadwick K, Schwartz D, & Siliciano RF (1995) In vivo fate of HIV-1-infected T cells: quantitative analysis of the transition to stable latency. *Nat Med* 1(12):1284-1290.
44. Chomont N, El-Far M, Ancuta P, Trautmann L, Procopio FA, Yassine-Diab B, Boucher G, Boulassel MR, Ghattas G, Brenchley JM, Schacker TW, Hill BJ, Douek DC, Routy JP, Haddad EK, & Sekaly RP (2009) HIV reservoir size and persistence are driven by T cell survival and homeostatic proliferation. *Nat Med* 15(8):893-900.

45. Chavez L, Calvanese V, & Verdin E (2015) HIV Latency Is Established Directly and Early in Both Resting and Activated Primary CD4 T Cells. *PLoS Pathog* 11(6):e1004955.
46. Zack JA, Arrigo SJ, Weitsman SR, Go AS, Haislip A, & Chen IS (1990) HIV-1 entry into quiescent primary lymphocytes: molecular analysis reveals a labile, latent viral structure. *Cell* 61(2):213-222.
47. Spina CA, Guatelli JC, & Richman DD (1995) Establishment of a stable, inducible form of human immunodeficiency virus type 1 DNA in quiescent CD4 lymphocytes in vitro. *J Virol* 69(5):2977-2988.
48. Gowda SD, Stein BS, Mohagheghpour N, Benike CJ, & Engleman EG (1989) Evidence that T cell activation is required for HIV-1 entry in CD4+ lymphocytes. *J Immunol* 142(3):773-780.
49. Walker LM, Phogat SK, Chan-Hui PY, Wagner D, Phung P, Goss JL, Wrin T, Simek MD, Fling S, Mitcham JL, Lehrman JK, Priddy FH, Olsen OA, Frey SM, Hammond PW, Protocol GPI, Kaminsky S, Zamb T, Moyle M, Koff WC, Poignard P, & Burton DR (2009) Broad and potent neutralizing antibodies from an African donor reveal a new HIV-1 vaccine target. *Science* 326(5950):285-289.
50. Pejchal R, Doores KJ, Walker LM, Khayat R, Huang PS, Wang SK, Stanfield RL, Julien JP, Ramos A, Crispin M, Depetris R, Katpally U, Marozsan A, Cupo A, Maloveste S, Liu Y, McBride R, Ito Y, Sanders RW, Ogohara C, Paulson JC, Feizi T, Scanlan CN, Wong CH, Moore JP, Olson WC, Ward AB, Poignard P, Schief WR, Burton DR, & Wilson IA (2011) A potent and broad neutralizing antibody recognizes and penetrates the HIV glycan shield. *Science* 334(6059):1097-1103.
51. Diskin R, Scheid JF, Marcovecchio PM, West AP, Jr., Klein F, Gao H, Gnanapragasam PN, Abadir A, Seaman MS, Nussenzweig MC, & Bjorkman PJ (2011) Increasing the potency and breadth of an HIV antibody by using structure-based rational design. *Science* 334(6060):1289-1293.
52. Klein F, Halper-Stromberg A, Horwitz JA, Gruell H, Scheid JF, Bournazos S, Mouquet H, Spatz LA, Diskin R, Abadir A, Zang T, Dorner M, Billerbeck E, Labitt RN, Gaebler C, Marcovecchio PM, Incesu RB, Eisenreich TR, Bieniasz PD, Seaman MS, Bjorkman PJ, Ravetch JV, Ploss A, & Nussenzweig MC (2012) HIV therapy by a combination of broadly neutralizing antibodies in humanized mice. *Nature* 492(7427):118-122.
53. Montefiori DC (2005) Evaluating neutralizing antibodies against HIV, SIV, and SHIV in luciferase reporter gene assays. *Curr Protoc Immunol* Chapter 12:Unit 12 11.
54. Ostrowski M, Benko E, Yue FY, Kim CJ, Huibner S, Lee T, Singer J, Pankovich J, Laeyendecker O, Kaul R, Kandel G, & Kovacs C (2015) Intensifying Antiretroviral Therapy With Raltegravir and Maraviroc During Early Human Immunodeficiency Virus (HIV) Infection Does Not Accelerate HIV Reservoir Reduction. *Open Forum Infect Dis* 2(4):ofv138.
55. Choudhary SK, Rezk NL, Ince WL, Cheema M, Zhang L, Su L, Swanstrom R, Kashuba AD, & Margolis DM (2009) Suppression of human immunodeficiency virus type 1 (HIV-1) viremia with reverse transcriptase and integrase inhibitors, CD4+ T-cell recovery, and viral rebound upon interruption of therapy in a new

model for HIV treatment in the humanized Rag2-/-{gamma}c-/- mouse. *J Virol* 83(16):8254-8258.
56. Denton PW, Olesen R, Choudhary SK, Archin NM, Wahl A, Swanson MD, Chateau M, Nochi T, Krisko JF, Spagnuolo RA, Margolis DM, & Garcia JV (2012) Generation of HIV latency in humanized BLT mice. *J Virol* 86(1):630-634.
57. Ruiz L, Martinez-Picado J, Romeu J, Paredes R, Zayat MK, Marfil S, Negredo E, Sirera G, Tural C, & Clotet B (2000) Structured treatment interruption in chronically HIV-1 infected patients after long-term viral suppression. *AIDS* 14(4):397-403.
58. Fang J, Yi S, Simmons A, Tu GH, Nguyen M, Harding TC, VanRoey M, & Jooss K (2007) An antibody delivery system for regulated expression of therapeutic levels of monoclonal antibodies in vivo. *Mol Ther* 15(6):1153-1159.
59. Herzog RW (2007) Immune responses to AAV capsid: are mice not humans after all? *Mol Ther* 15(4):649-650.
60. Caskey M, Klein F, Lorenzi JC, Seaman MS, West AP, Jr., Buckley N, Kremer G, Nogueira L, Braunschweig M, Scheid JF, Horwitz JA, Shimeliovich I, Ben-Avraham S, Witmer-Pack M, Platten M, Lehmann C, Burke LA, Hawthorne T, Gorelick RJ, Walker BD, Keler T, Gulick RM, Fatkenheuer G, Schlesinger SJ, & Nussenzweig MC (2015) Viraemia suppressed in HIV-1-infected humans by broadly neutralizing antibody 3BNC117. *Nature* 522(7557):487-491.
61. Barouch DH, Whitney JB, Moldt B, Klein F, Oliveira TY, Liu J, Stephenson KE, Chang HW, Shekhar K, Gupta S, Nkolola JP, Seaman MS, Smith KM, Borducchi EN, Cabral C, Smith JY, Blackmore S, Sanisetty S, Perry JR, Beck M, Lewis MG, Rinaldi W, Chakraborty AK, Poignard P, Nussenzweig MC, & Burton DR (2013) Therapeutic efficacy of potent neutralizing HIV-1-specific monoclonal antibodies in SHIV-infected rhesus monkeys. *Nature* 503(7475):224-228.
62. Shingai M, Nishimura Y, Klein F, Mouquet H, Donau OK, Plishka R, Buckler-White A, Seaman M, Piatak M, Jr., Lifson JD, Dimitrov DS, Nussenzweig MC, & Martin MA (2013) Antibody-mediated immunotherapy of macaques chronically infected with SHIV suppresses viraemia. *Nature* 503(7475):277-280.
63. Salazar-Gonzalez JF, Bailes E, Pham KT, Salazar MG, Guffey MB, Keele BF, Derdeyn CA, Farmer P, Hunter E, Allen S, Manigart O, Mulenga J, Anderson JA, Swanstrom R, Haynes BF, Athreya GS, Korber BT, Sharp PM, Shaw GM, & Hahn BH (2008) Deciphering human immunodeficiency virus type 1 transmission and early envelope diversification by single-genome amplification and sequencing. *J Virol* 82(8):3952-3970.
64. Ali A & Yang OO (2006) A novel small reporter gene and HIV-1 fitness assay. *J Virol Methods* 133(1):41-47.
65. Lindwasser OW, Smith WJ, Chaudhuri R, Yang P, Hurley JH, & Bonifacino JS (2008) A diacidic motif in human immunodeficiency virus type 1 Nef is a novel determinant of binding to AP-2. *J Virol* 82(3):1166-1174.
66. Willey RL, Maldarelli F, Martin MA, & Strebel K (1992) Human immunodeficiency virus type 1 Vpu protein induces rapid degradation of CD4. *J Virol* 66(12):7193-7200.

67. Bour S, Schubert U, & Strebel K (1995) The human immunodeficiency virus type 1 Vpu protein specifically binds to the cytoplasmic domain of CD4: implications for the mechanism of degradation. *J Virol* 69(3):1510-1520.
68. Halper-Stromberg A, Lu CL, Klein F, Horwitz JA, Bournazos S, Nogueira L, Eisenreich TR, Liu C, Gazumyan A, Schaefer U, Furze RC, Seaman MS, Prinjha R, Tarakhovsky A, Ravetch JV, & Nussenzweig MC (2014) Broadly neutralizing antibodies and viral inducers decrease rebound from HIV-1 latent reservoirs in humanized mice. *Cell* 158(5):989-999.
69. Wardemann H, Yurasov S, Schaefer A, Young JW, Meffre E, & Nussenzweig MC (2003) Predominant autoantibody production by early human B cell precursors. *Science* 301(5638):1374-1377.
70. Bullen CK, Laird GM, Durand CM, Siliciano JD, & Siliciano RF (2014) New ex vivo approaches distinguish effective and ineffective single agents for reversing HIV-1 latency in vivo. *Nat Med* 20(4):425-429.
71. Fujiwara M, Okamoto M, Ijichi K, Tokuhisa K, Hanasaki Y, Katsuura K, Uemura D, Shigeta S, Konno K, Yokota T, & Baba M (1998) Upregulation of HIV-1 replication in chronically infected cells by ingenol derivatives. *Arch Virol* 143(10):2003-2010.
72. Lehrman G, Ylisastigui L, Bosch RJ, & Margolis DM (2004) Interleukin-7 induces HIV type 1 outgrowth from peripheral resting CD4+ T cells. *J Acquir Immune Defic Syndr* 36(5):1103-1104.
73. Al-Harthi L, Roebuck KA, & Landay A (1998) Induction of HIV-1 replication by type 1-like cytokines, interleukin (IL)-12 and IL-15: effect on viral transcriptional activation, cellular proliferation, and endogenous cytokine production. *J Clin Immunol* 18(2):124-131.
74. Mortier E, Quemener A, Vusio P, Lorenzen I, Boublik Y, Grotzinger J, Plet A, & Jacques Y (2006) Soluble interleukin-15 receptor alpha (IL-15R alpha)-sushi as a selective and potent agonist of IL-15 action through IL-15R beta/gamma. Hyperagonist IL-15 x IL-15R alpha fusion proteins. *J Biol Chem* 281(3):1612-1619.
75. Scheid JF, Mouquet H, Feldhahn N, Seaman MS, Velinzon K, Pietzsch J, Ott RG, Anthony RM, Zebroski H, Hurley A, Phogat A, Chakrabarti B, Li Y, Connors M, Pereyra F, Walker BD, Wardemann H, Ho D, Wyatt RT, Mascola JR, Ravetch JV, & Nussenzweig MC (2009) Broad diversity of neutralizing antibodies isolated from memory B cells in HIV-infected individuals. *Nature* 458(7238):636-640.
76. Mouquet H, Scheid JF, Zoller MJ, Krogsgaard M, Ott RG, Shukair S, Artyomov MN, Pietzsch J, Connors M, Pereyra F, Walker BD, Ho DD, Wilson PC, Seaman MS, Eisen HN, Chakraborty AK, Hope TJ, Ravetch JV, Wardemann H, & Nussenzweig MC (2010) Polyreactivity increases the apparent affinity of anti-HIV antibodies by heteroligation. *Nature* 467(7315):591-595.
77. West AP, Jr., Scharf L, Scheid JF, Klein F, Bjorkman PJ, & Nussenzweig MC (2014) Structural insights on the role of antibodies in HIV-1 vaccine and therapy. *Cell* 156(4):633-648.
78. Albert J, Abrahamsson B, Nagy K, Aurelius E, Gaines H, Nystrom G, & Fenyo EM (1990) Rapid development of isolate-specific neutralizing antibodies after

primary HIV-1 infection and consequent emergence of virus variants which resist neutralization by autologous sera. *AIDS* 4(2):107-112.
79. Prince AM, Reesink H, Pascual D, Horowitz B, Hewlett I, Murthy KK, Cobb KE, & Eichberg JW (1991) Prevention of HIV infection by passive immunization with HIV immunoglobulin. *AIDS Res Hum Retroviruses* 7(12):971-973.
80. Lynch RM, Boritz E, Coates EE, DeZure A, Madden P, Costner P, Enama ME, Plummer S, Holman L, Hendel CS, Gordon I, Casazza J, Conan-Cibotti M, Migueles SA, Tressler R, Bailer RT, McDermott A, Narpala S, O'Dell S, Wolf G, Lifson JD, Freemire BA, Gorelick RJ, Pandey JP, Mohan S, Chomont N, Fromentin R, Chun TW, Fauci AS, Schwartz RM, Koup RA, Douek DC, Hu Z, Capparelli E, Graham BS, Mascola JR, Ledgerwood JE, & Team VRCS (2015) Virologic effects of broadly neutralizing antibody VRC01 administration during chronic HIV-1 infection. *Sci Transl Med* 7(319):319ra206.
81. Keele BF, Giorgi EE, Salazar-Gonzalez JF, Decker JM, Pham KT, Salazar MG, Sun C, Grayson T, Wang S, Li H, Wei X, Jiang C, Kirchherr JL, Gao F, Anderson JA, Ping LH, Swanstrom R, Tomaras GD, Blattner WA, Goepfert PA, Kilby JM, Saag MS, Delwart EL, Busch MP, Cohen MS, Montefiori DC, Haynes BF, Gaschen B, Athreya GS, Lee HY, Wood N, Seoighe C, Perelson AS, Bhattacharya T, Korber BT, Hahn BH, & Shaw GM (2008) Identification and characterization of transmitted and early founder virus envelopes in primary HIV-1 infection. *Proc Natl Acad Sci U S A* 105(21):7552-7557.
82. Dahabieh MS, Ooms M, Simon V, & Sadowski I (2013) A doubly fluorescent HIV-1 reporter shows that the majority of integrated HIV-1 is latent shortly after infection. *J Virol* 87(8):4716-4727.
83. Calvanese V, Chavez L, Laurent T, Ding S, & Verdin E (2013) Dual-color HIV reporters trace a population of latently infected cells and enable their purification. *Virology* 446(1-2):283-292.
84. Shan L, Deng K, Shroff NS, Durand CM, Rabi SA, Yang HC, Zhang H, Margolick JB, Blankson JN, & Siliciano RF (2012) Stimulation of HIV-1-specific cytolytic T lymphocytes facilitates elimination of latent viral reservoir after virus reactivation. *Immunity* 36(3):491-501.
85. Spina CA, Anderson J, Archin NM, Bosque A, Chan J, Famiglietti M, Greene WC, Kashuba A, Lewin SR, Margolis DM, Mau M, Ruelas D, Saleh S, Shirakawa K, Siliciano RF, Singhania A, Soto PC, Terry VH, Verdin E, Woelk C, Wooden S, Xing S, & Planelles V (2013) An in-depth comparison of latent HIV-1 reactivation in multiple cell model systems and resting CD4+ T cells from aviremic patients. *PLoS Pathog* 9(12):e1003834.
86. Nabel G & Baltimore D (1987) An inducible transcription factor activates expression of human immunodeficiency virus in T cells. *Nature* 326(6114):711-713.
87. Maldarelli F, Wu X, Su L, Simonetti FR, Shao W, Hill S, Spindler J, Ferris AL, Mellors JW, Kearney MF, Coffin JM, & Hughes SH (2014) HIV latency. Specific HIV integration sites are linked to clonal expansion and persistence of infected cells. *Science* 345(6193):179-183.
88. Wagner TA, McLaughlin S, Garg K, Cheung CY, Larsen BB, Styrchak S, Huang HC, Edlefsen PT, Mullins JI, & Frenkel LM (2014) HIV latency. Proliferation of

cells with HIV integrated into cancer genes contributes to persistent infection. *Science* 345(6196):570-573.

89. Cohn LB, Silva IT, Oliveira TY, Rosales RA, Parrish EH, Learn GH, Hahn BH, Czartoski JL, McElrath MJ, Lehmann C, Klein F, Caskey M, Walker BD, Siliciano JD, Siliciano RF, Jankovic M, & Nussenzweig MC (2015) HIV-1 integration landscape during latent and active infection. *Cell* 160(3):420-432.